

19930092835

ARR Jan. 1943

NATIONAL ADVISORY COMMITTEE FOR AERONAUTICS

WARTIME REPORT

ORIGINALLY ISSUED
January 1943 as
Advance ~~Report~~ Report

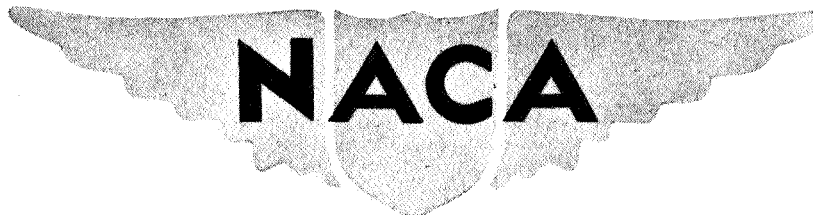
AERODYNAMIC CHARACTERISTICS AND FLAP LOADS

OF PERFORATED DOUBLE SPLIT FLAPS ON A

RECTANGULAR NACA 23012 AIRFOIL

By Paul E. Purser and Thomas R. Turner

Langley Memorial Aeronautical Laboratory
Langley Field, Va.



WASHINGTON

NACA WARTIME REPORTS are reprints of papers originally issued to provide rapid distribution of advance research results to an authorized group requiring them for the war effort. They were previously held under a security status but are now unclassified. Some of these reports were not technically edited. All have been reproduced without change in order to expedite general distribution.

NATIONAL ADVISORY COMMITTEE FOR AERONAUTICS

ADVANCE XXXXXXXXXX REPORT

AERODYNAMIC CHARACTERISTICS AND FLAP LOADS
OF PERFORATED DOUBLE SPLIT FLAPS ON A
RECTANGULAR NACA 23012 AIRFOIL

By Paul E. Purser and Thomas R. Turner

SUMMARY

At the request of the Bureau of Aeronautics, Navy Department, tests have been made in the LMAL 7- by 1.0-foot tunnel to determine flap loads and additional aerodynamic characteristics of perforated double split flaps on a rectangular NACA 23012 airfoil. Flap loads were measured at two spanwise sections on full-span flaps. The effects of differential flap deflection, flap span, perforation shape, location and amount of perforation, and presence of a fuselage on the flap loads at one spanwise section were also determined. The data are presented in standard coefficient form and include lift, drag, and pitching moment for the airfoil and for the complete model and the normal force, hinge moment, and center of pressure for the flaps.

In general, the drag coefficient and the flap loads decreased as the amount of perforation was increased and as one row of perforations was moved from the flap leading edge to the flap trailing edge. The variation of drag coefficient and flap loads with lift coefficient also decreased as the amount of perforation was increased. The shape of the perforations had little effect on the flap loads.

The presence of an elliptical fuselage reduced the flap loads and the drag coefficient available with 60-percent-span perforated double split flaps. With the double split flaps retracted or with only the lower flap deflected (as for landing), the presence of circular perforations that removed 33.1 percent of the original area in the upper and lower flaps reduced the slope of the lift curve by about 5 percent and the maximum lift coefficient by about 10 percent.

INTRODUCTION

In connection with the development of dive- and fighter-brake devices the Bureau of Aeronautics requested data concerning the loads to be expected on perforated split flaps and concerning the effects on these loads of perforation shape, amount, and location. In accordance with the request of the Bureau of Aeronautics, load tests of perforated flaps were included in the NACA investigation of dive- and fighter-brake devices. The results of the load tests and some additional aerodynamic characteristics of perforated double split flaps on a rectangular NACA 23012 airfoil are given in the present report.

APPARATUS AND METHODS

Models

The airfoil model used (fig. 1) was of laminated mahogany built to the NACA 23012 profile. The model was rectangular in plan form and had an aspect ratio of 6.0 (10-in. chord and 60-in. span). The perforated split flaps were made of 1/16-inch sheet steel and had chords of 2 inches (20 percent of the airfoil chord). The perforations in the flaps were symmetrically spaced circular, triangular, square, or rectangular holes (see flap details, figs. 1 and 2) and removed 33.1 percent of the original flap area. In order to facilitate partial-span-flap tests each flap was made in 10 equal segments, each segment having a span of 20 percent of the airfoil semispan. The segments on each semispan were numbered from 1 to 5 progressively from the plane of symmetry outboard to the airfoil tip. Flap deflections were measured with respect to the airfoil, surface at the flap hinge point and the gap between the airfoil and the flap was sealed with modeling clay except at the flap segments that were mounted on the strain-gage units. For all tests, the trailing-edge portion of the airfoil was removed over the part of the span covered by the flaps.

The elliptical fuselage used in the tests (figs. 3 and 4) was that used in previous wing-fuselage interference investigations (reference 1) and was of laminated mahogany built to the dimensions given in table I. The horizontal tail was tapered approximately 3:1 in plan form,

had a straight trailing edge, and was of laminated mahogany built to the NACA 0009 profile. When changes in horizontal tail setting were made, the tail was pivoted about the 50-percent-root-chord station.

Test Installation

The tests were made in the closed-throat LMAL 7- by 10-foot tunnel described in references 2 and 3. The flap loads were measured by two-component electrical strain-gage units and readings were taken from a control panel located outside the tunnel. Because of the small size of the model, loads could be measured on only one upper or one lower flap segment at any one spanwise location. The strain-gage unit for the upper flap was located in the right semispan of the model and that for the lower flap was in the left semispan. With the strain-gage units in place, the flaps could not be set at deflections smaller than about 12° . A view of the strain-gage unit installed in the model is shown in figure 5. During the tests the units were protected from the airstream by thin metal cover plates.

Test Conditions

All the tests were made at a dynamic pressure of 16.37 pounds per square foot which corresponds to a velocity of about 60 miles per hour and to a test Reynolds number of about 609,000 based on the chord of the model (10 in.). The effective Reynolds number of the tests was about 974,000 based on a turbulence factor of 1.6 for the LMAL 7- by 10-foot tunnel.

RESULTS AND DISCUSSION

Coefficients and Corrections

The coefficients used in the presentation of the results are:

C_L lift coefficient of airfoil or of complete model (L/qS)

C_D drag coefficient of airfoil or of complete model (D/qS)

- $C_{m_c}/4$ pitching-moment coefficient about quarter-chord point of airfoil chord of airfoil or of the complete model (M/qcS)
 C_{N_f} flap normal-force coefficient (N_f/qS_f)
 C_{h_f} flap hinge-moment coefficient about flap loading edge (H_f/qS_fc_f)
 $(C.P.)_f$ flap center of pressure in percentage of flap chord from flap leading edge $[-(C_{h_f}/C_{N_f}) \times 100]$

where

- L lift of airfoil-flap combination or of complete model
 D drag of airfoil-flap combination or of complete model
 M pitching moment of airfoil-flap combination or of complete model
 N_f normal force on one flap segment
 H_f hinge moment of one flap segment
 q dynamic pressure of airstream $\left(\frac{1}{2}\rho V^2\right)$
 S airfoil area
 S_f area of one flap segment
 c airfoil chord
 c_f flap chord
 and
 α angle of attack
 δ_f flap deflection from neutral
 i_t horizontal tail setting with respect to fuselage center line; positive when trailing edge is down

The subscripts U and L refer to the upper and lower flaps, respectively.

Because the support-strut interference and tare were relatively small, these corrections were applied only to the plain airfoil data. The standard jet-boundary corrections, which were applied to all the airfoil and complete-model data, are:

$$\Delta\alpha_i = \delta \frac{S}{C} C_L (57.3)$$

$$\Delta C_{D_i} = \delta \frac{S}{C} C_L^2$$

where $\Delta\alpha_i$ is measured in degrees, δ is the jet-boundary correction factor, and C is the jet cross-sectional area. A value of $\delta = 0.112$ for the closed-throat wind tunnel was used in correcting the results. No account was taken of the different span load distributions with different airfoil-flap combinations and no corrections of any kind were applied to the flap-load data or to the pitching-moment coefficients.

Aerodynamic Characteristics

~~Airfoil~~-- The characteristics of the airfoil with various spans and deflections of perforated double split flaps are shown in figures 6 to 14. The effects of flap span on the airfoil drag coefficient at zero lift for various flap deflections are summarized in figure 15, which is a cross plot of the data from figures 6, 10, and 14. The airfoil characteristics are discussed in reference 4 and it is felt that no further discussion is necessary. The principal differences between the results presented herein and those of reference 4 are that, in the present tests, a more complete range of flap deflections was investigated and, for all the subject tests, the trailing-edge portion of the airfoil was removed from the part of the span covered by the flaps,

The effects on the airfoil characteristics of varying the number and location of the perforations in full-span double split flaps with equal upper and lower deflections of 30° and 90° are shown in figures 16 and 17, respectively. Perforations of 33.1 percent reduced the

increment in drag coefficient at zero lift by about 15 percent with flaps deflected 30° and by about 19 percent with flaps deflected 90° . With flaps deflected 90° , the same ratio of reduction of drag coefficient at zero lift to reduction of area held fairly well when the perforations were symmetrically distributed along both the flap leading and trailing edges but did not hold: when only one row of perforations was used along the flap Leading edge, midchord, or trailing edge. With flaps deflected 90° , the drag coefficient at zero lift decreased about 17 percent as one row of perforations was moved from the flap leading edge to the flap trailing edge,

Complete model.— The characteristics of the complete model with stabilizer settings of 0° and -4.4° are shown in figure 18 for solid and perforated 60-percent-span double split flaps with the upper flap retracted and with the lower flap deflected 0° , 30° , and 60° . Figure 19 shows the characteristics of the same model with equal upper and lower deflections of the perforated flaps. With the upper flap retracted, the perforations in the upper and lower flaps reduced the slope of the lift curve $\partial C_L / \partial \alpha$ by about 5 percent and reduced the maximum lift coefficients by about 10 percent. The effects of the perforations on the slope of the pitching-moment curve $\partial C_m / \partial C_L$ and on the tail effectiveness $\partial C_m / \partial i_t$ were small and inconsistent (fig. 18). Deflecting perforated double split flaps (fig. 19) produced marked changes in both $\partial C_m / \partial C_L$ and $\partial C_m / \partial i_t$. Near zero lift, $\partial C_m / \partial C_L$ changed from -0.12 to 0.05 when the flaps were deflected 90° , and the value was positive for deflections larger than about 30° . The value of $\partial C_m / \partial i_t$ changed from -0.020 to -0.001 when the flaps were deflected 90° at zero Lift.. The values of dynamic pressure at the tail computed from $\partial C_m / \partial i_t$ agreed reasonably well with the values measured in the tests of reference 4. According to the results of reference 4, the tail would have to be raised about $0.75c$ in order to clear the wake.

The results of tests made of the airfoil and the 60-percent-span flaps with a cut-out the width of the elliptical fuselage at the flap midspan are shown in figure 20. Figure 21 presents cross plots of the increments of drag coefficient at zero Lift due to deflecting the flaps for various arrangements of perforated double split flaps. The results (fig. 21) show that the increment in drag

coefficient due to deflecting perforated double split flaps on a midwing monoplane not only does not carry across the fuselage but is actually reduced by the wing-fuselage interference to a value slightly less than that obtained from an equal flap area on the plain airfoil, (See also references 1 and 5.)

Flap Loads

Effect of flap span and location.— Flap loads for equal upper- and lower-flap deflections are presented in figures 6, 10, and 14 for the flap segment extending from $0.20\ b/2$ to $0.40\ b/2$ on full-span, 60-percent-span, and 40-percent-span flaps and for the tip segment of full-span flaps. Figure 22 is a summary of the data of figures 6, 10, and 14 in the form of flap normal-force and hinge-moment coefficients plotted against flap deflection at lift coefficients of 0 and 0.9. At constant flap deflection the upper-flap loads showed less variation with lift coefficient when the segment under consideration was at the flap tip than when the segment was not at the flap tip. For the lower-flap loads, the trend previously noted was reversed for the full-span flaps and was small and inconsistent for the partial-span flaps. At constant lift coefficients of 0 and 0.9, the loads on the $0.20\ b/2$ to $0.40\ b/2$ upper-flap segment generally became smaller as the flap span was reduced and the comparable lower-flap loads generally became larger. At zero lift, the upper-flap loads were smaller for the tip segment but, at a lift coefficient of 0.9, the upper-flap loads were smaller when the segment under consideration was not at the tip. For the lower flap, the tip-segment loads were larger at lift Coefficients of both 0 and 0.9.

Effect of lower flap on upper-flap loads.— The effects on the upper-flap loads caused by deflecting the lower flap are shown in figures 7 to 9 for full-span flaps and in figures 11 to 13 for 60-percent-span flaps. For both full-span and partial-span flaps, increasing the lower-flap deflection usually increased the upper-flap normal-force and hinge-moment coefficients but the numerical values were inconsistent. Deflecting the lower flap had little effect on the variation of upper-flap loads with lift coefficient.

Effect of upper flap on lower-flap loads.— The effects on the lower-flap loads caused by deflecting the

upper flap may be determined from comparisons of figures 7 to 9 for full-span flaps and figures 11 to 13 for 60-percent-span flaps. In general, the effects of the upper flap on the lower-flap loads follow the same trend previously noted for the effects of the lower flap on the upper-flap loads; that is, increasing the upper-flap deflections increased the loads on the lower flap.

Effect of varying number and location of perforations.— The effects on the flap loads of varying the number and location of the perforations in full-span double split flaps are shown in figures 16 and 17 for equal upper- and lower-flap deflections of 30° and 90° , respectively. The effects on the flap loads of varying the number and the location of the perforations were rather inconsistent but showed the same trends noted previously in the discussion of drag; that is, the flap loads generally became smaller as the amount of perforation was increased and as the location of one row of perforations was changed from the flap leading edge to the flap trailing edge. Decreasing the amount of perforation generally increased the variation of flap loads with lift coefficient.

Effect of perforation shape on upper-flap loads.— The loads on the upper-flap segment extending from $0.20 b/2$ to $0.40 b/2$ for 30° and 90° deflections of full-span double split flaps with circular, triangular, square, and rectangular perforations are shown in figure 23. At flap deflections of 30° , the flap with circular perforations had the largest loads. Changing the perforations to squares reduced the flap loads and moved the flap center of pressure nearer the trailing edge; triangular and rectangular perforations also reduced the flap loads but moved the flap center of pressure nearer the leading edge. The circular perforations gave the smallest variation of flap loads with lift coefficient. With the flaps deflected 90° , there was no consistent variation of flap loads with perforation shape.

Effect of fuselage on upper-flap loads.— The effects of the presence of the fuselage on the upper-flap loads for equal upper- and lower-flap deflections are shown in figure 24. The principal effects of the fuselage were to reduce the flap normal-force coefficients and to move the flap center of pressure nearer the flap trailing edge with the result that little effect was apparent on the flap hinge-moment coefficients. In general, the presence of the

fuselage slightly reduced the variation of flap normal-force coefficient with angle of attack.

Application of Data

The application of data on perforated split flaps to the design of dive brakes and fighter brakes has been discussed in references 4, 6, and 7. As an aid to such applications, a part of the aerodynamic data presented in this report has been summarized in figures 25 and 26. Figure 25 presents contours of angle of attack, drag coefficient, and pitching-moment coefficient at zero lift for full-span and 60-percent-span perforated double split flaps. Contours of lift, drag, and pitching-moment coefficients at zero angle of attack are given in figure 26. The contours at zero lift can be used in dive-brake design, the contours at zero angle of attack can be used in fighter-brake design, and the cross plots in figures 15 and 21 should be useful as guides for interpolation in applying the data of figures 25 and 26 to the design of flaps other than full-span or 60-percent-span flaps.

CONCLUSIONS

The results of the tests of double split flaps on a 10- by 60-inch rectangular NACA 23012 airfoil indicate that the effects of perforations on the flap characteristics may be summarized as follows: In general, the drag coefficient and the flap loads decreased as the amount of perforation was increased and as one row of perforations was moved from the flap leading edge to the flap trailing edge. The variation of drag coefficient and flap loads with lift Coefficient also decreased as the amount of perforation was increased. The shape of the perforations had little effect on the flap loads..

The presence of an elliptical fuselage reduced the loads on and the drag coefficient available with 60-percent-span perforated double split flaps. With the double split flaps retracted or with only the lower flap deflected (as for landing) the presence of circular perforations that removed 33.1 percent of the original area in the upper and lower flaps reduced the slope of the lift curve by about

5 percent and reduced the maximum lift coefficient by about 10 percent.

Langley Memorial Aeronautical Laboratory,
National Advisory Committee for Aeronautics,
Langley Field, Va.

REFERENCES

1. House, Rufus O., and Wallace, Arthur R.: Wind-Tunnel Investigation of Effect of Interference on Lateral-Stability Characteristics of Four NACA 23012 Wings, an Elliptical and a Circular Fuselage, and Vertical Fins. Rep. No. 705, NACA, 1941.
2. Harris, Thomas A.: The 7 by 10 Foot Wind Tunnel of the National Advisory Committee for Aeronautics. Rep. No. 412, NACA, 1931.
3. Wenzinger, Carl J., and Harris, Thomas A.: Wind-Tunnel Investigation of an N.A.C.A. 23012 Airfoil with Various Arrangements of Slotted Flaps. Rep. No. 664, NACA, 1939.
4. Purser, Paul E., and Turner, Thomas R.: Wind-Tunnel Investigation of Perforated Split Flaps for Use as Dive Brakes on a Rectangular NACA 23012 Airfoil. NACA A.C.R., July 1941.
5. Jacobs, Eastman N., and Ward, Kenneth E.: Interference of Wing and Fuselage from Tests of 209 Combinations in the N.A.C.A. Variable-Density Tunnel. Rep. No. 540, NACA, 1935.
6. Purser, Paul E., and Turner, Thomas R.: Wind-Tunnel Investigation of Perforated Split Flaps for Use as Dive Brakes on a Tapered NACA 23012 Airfoil. NACA A.C.R., Nov. 1941.
7. Purser, Paul E.: A Study of the Application of Data on Various Types of Flap to the Design of Fighter Brakes. NACA A.C.R., June 1942.

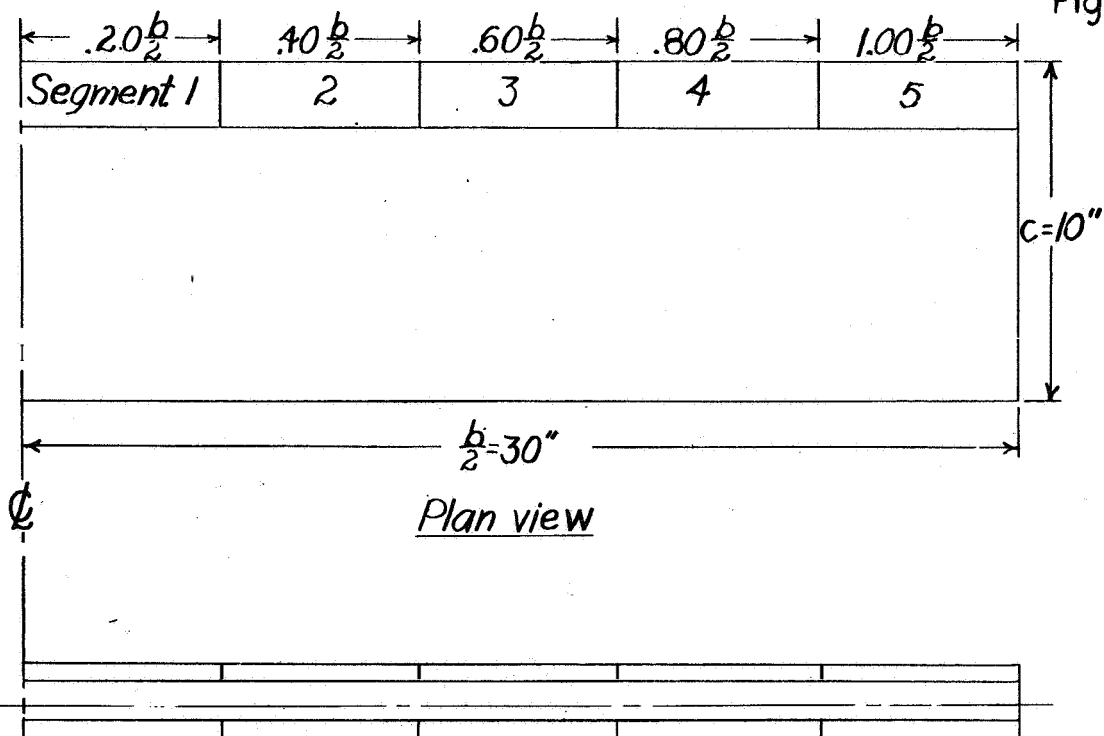
TABLE I
DIMENSIONS OF ELLIPTICAL FUSELAGE

Station (in.)	Major axis (in.)	Minor axis (in.)
0	0	0
.312	2.044	1.168
.812	3.286	1.878
1.312	4.158	2.376
2.312	5.408	3.090
4.312	7.010	4.006
6.312	8.564	4.894
12.312	9.020	5.154
16.312	9.100	5.200
20.312	9.010	5.148
24.312	8.646	4.940
28.312	7.910	4.520
32.312	6.658	3.804
34.312	5.740	3.280
36.312	4.494	2.568
38.312	2.646	1.512
39.312	1.450	.828
40.312	0	0

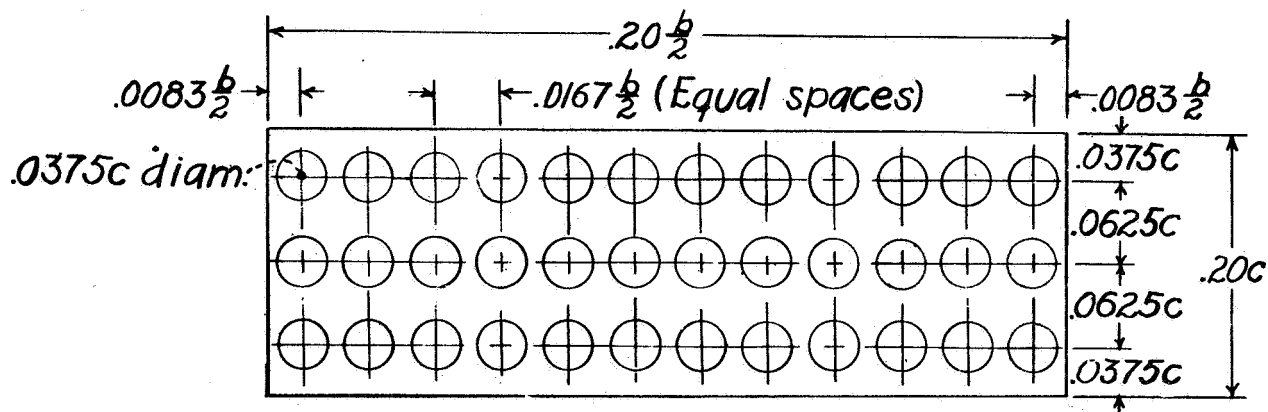
I-415

NACA

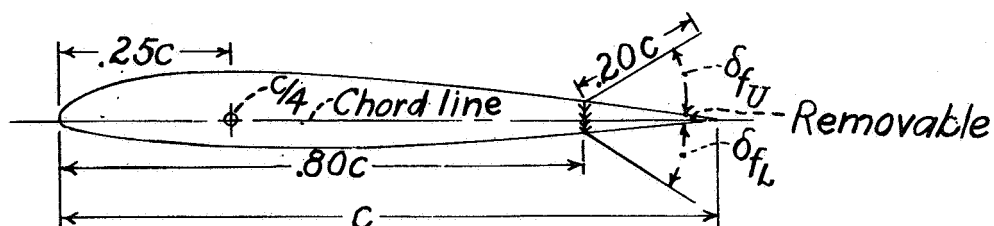
Fig-1



Plan view

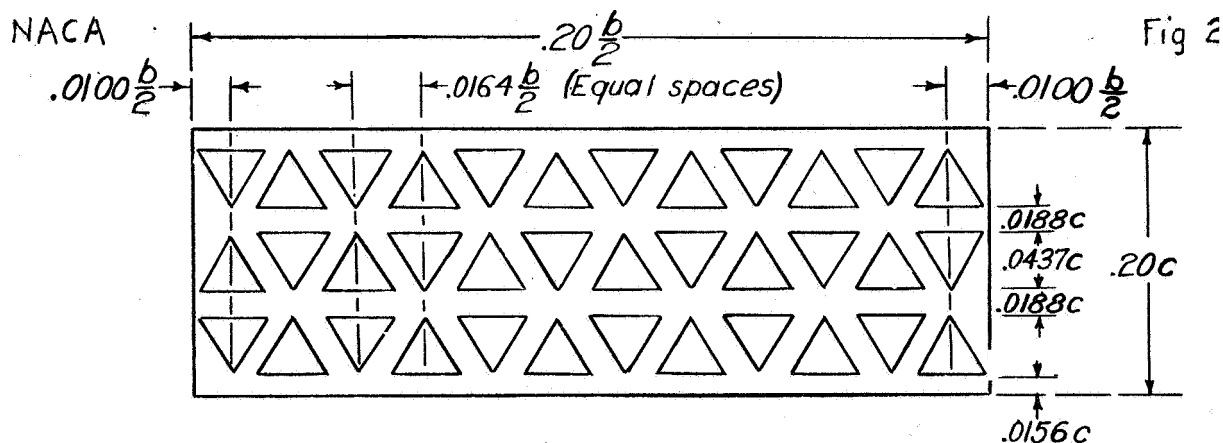


Front view

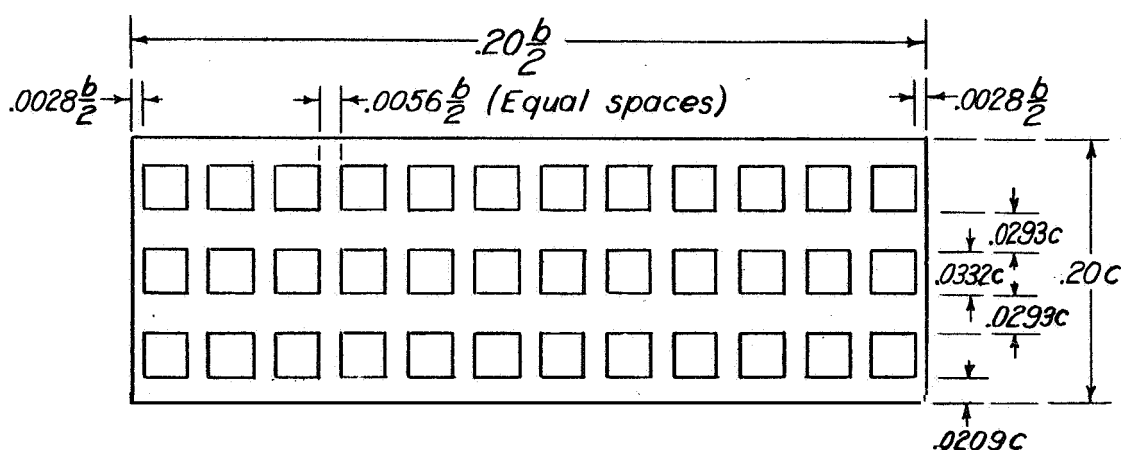


Flap detail

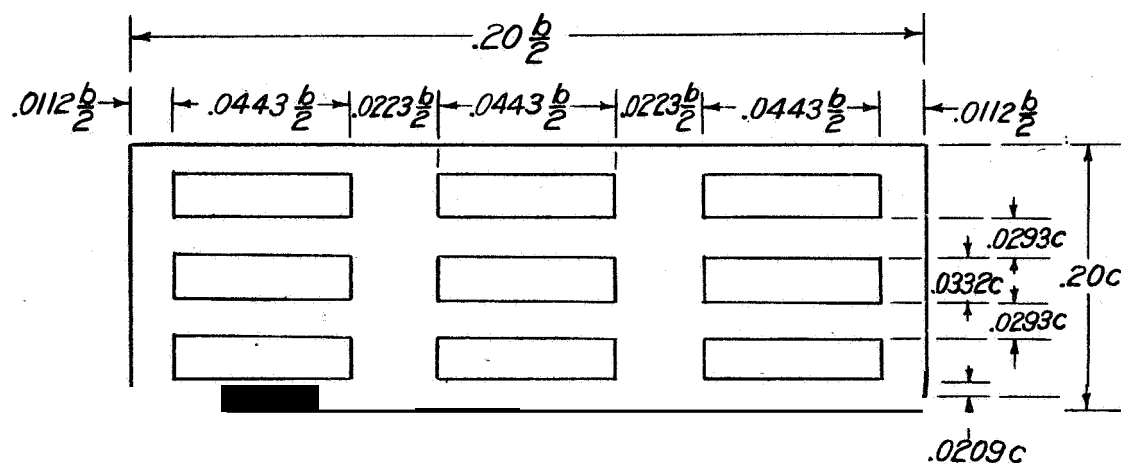
Figure 1.- The 10-by 60-inch rectangular NACA 23012 airfoil with $0.20c$ perforated double split flaps. Perforations remove 33.1 percent of the original flap area.



(a) Equilateral triangles.



(b) Squares.



(c) Rectangles.

Figure 2.-Details of the $0.20c$ by $0.20 \frac{b}{2}$ perforated split flap segments tested on the 10-by-60-inch rectangular NACA 23012 airfoil. Perforations remove 33.1 percent of original flap area.

NACA

Fig 3

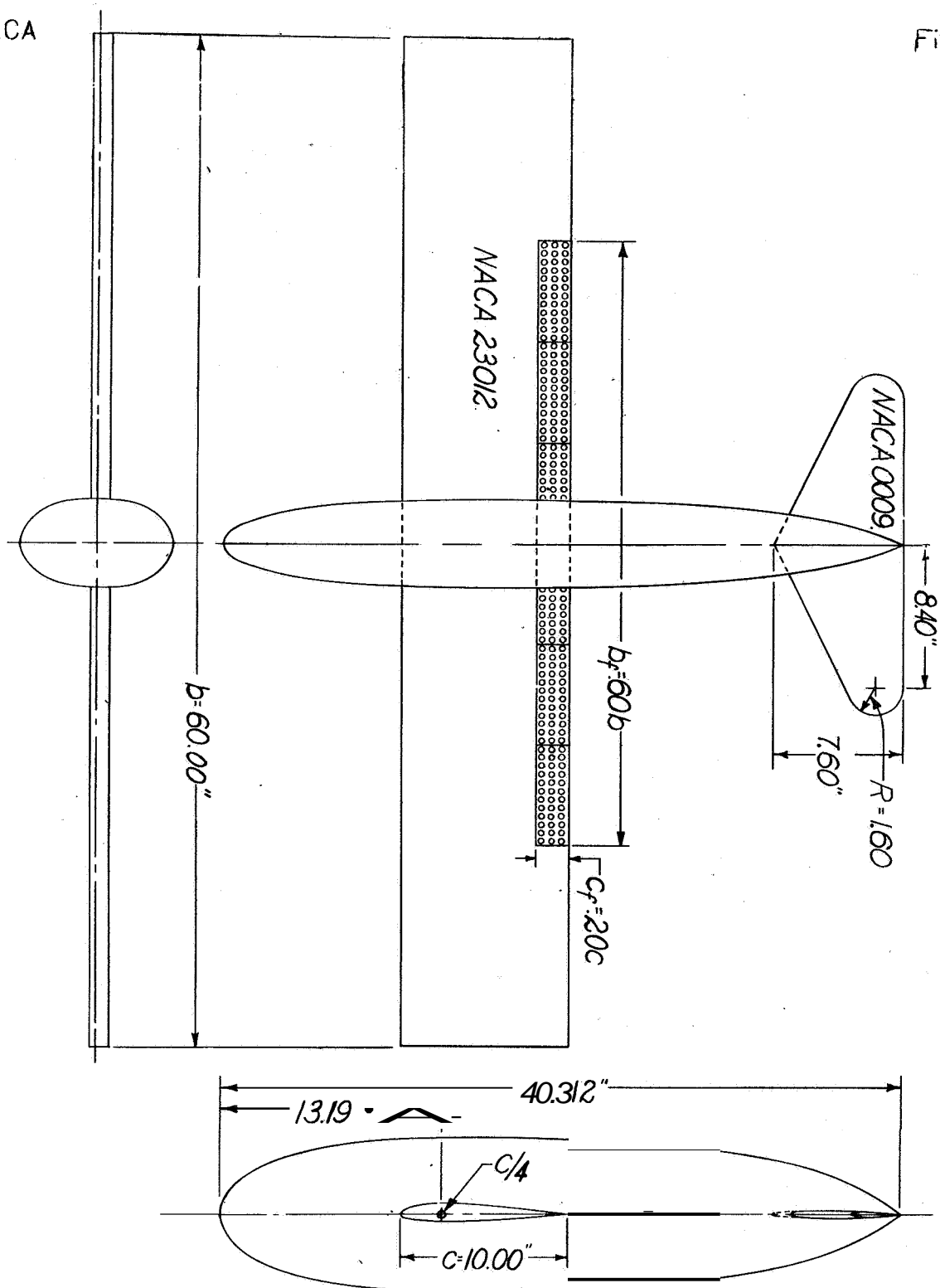
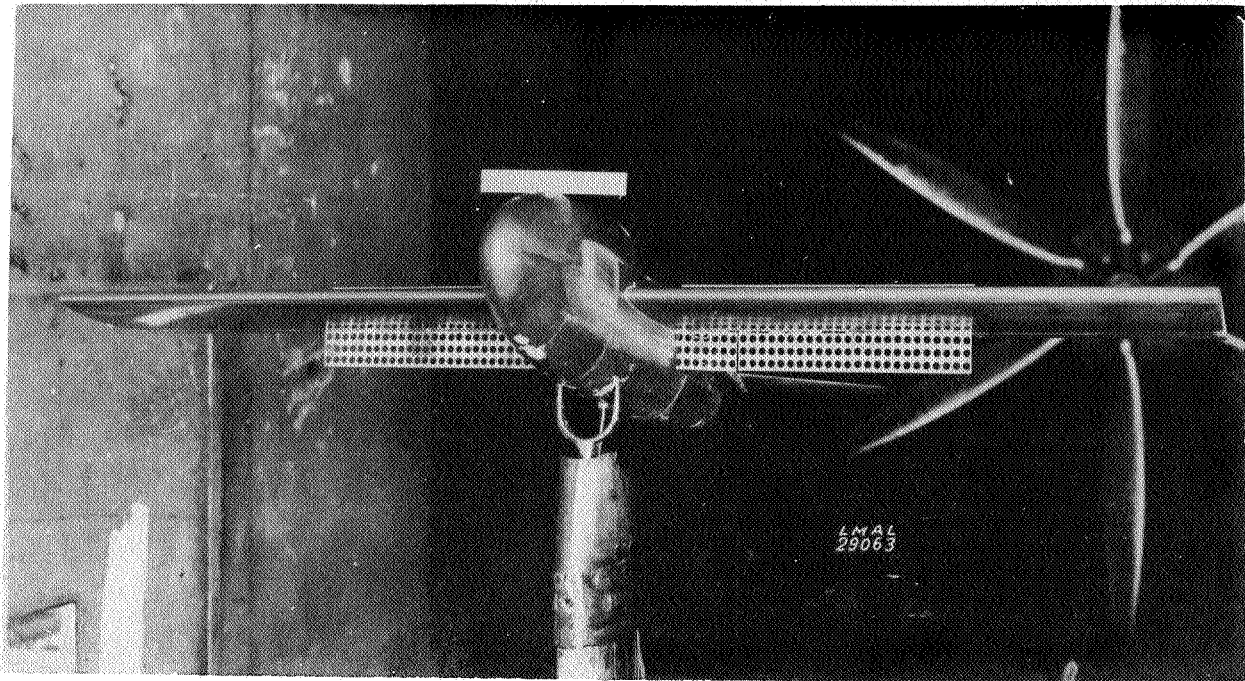
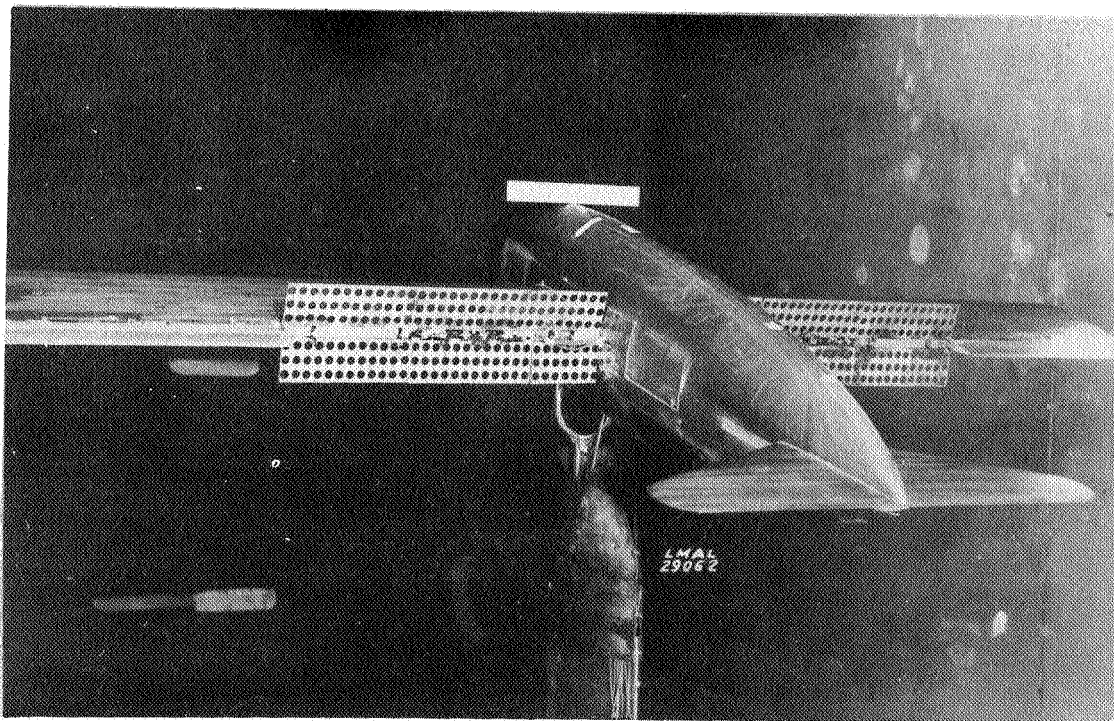


Figure 3.- The 10-by-60-inch rectangular NACA 23012 airfoil with 0.20c by 0.606 perforated double split flaps in combination with the elliptical fuselage and horizontal tail.



(a) Three-quarter front view.



(b) Three-quarter rear view.

Figure 4.- The 10-by 60-inch rectangular NACA 23012 airfoil with 0.20c by 0.60b perforated.. double split flaps in combination with the elliptical fuselage and horizontal tail mounted in the LMAL 7-by 10-foot tunnel.

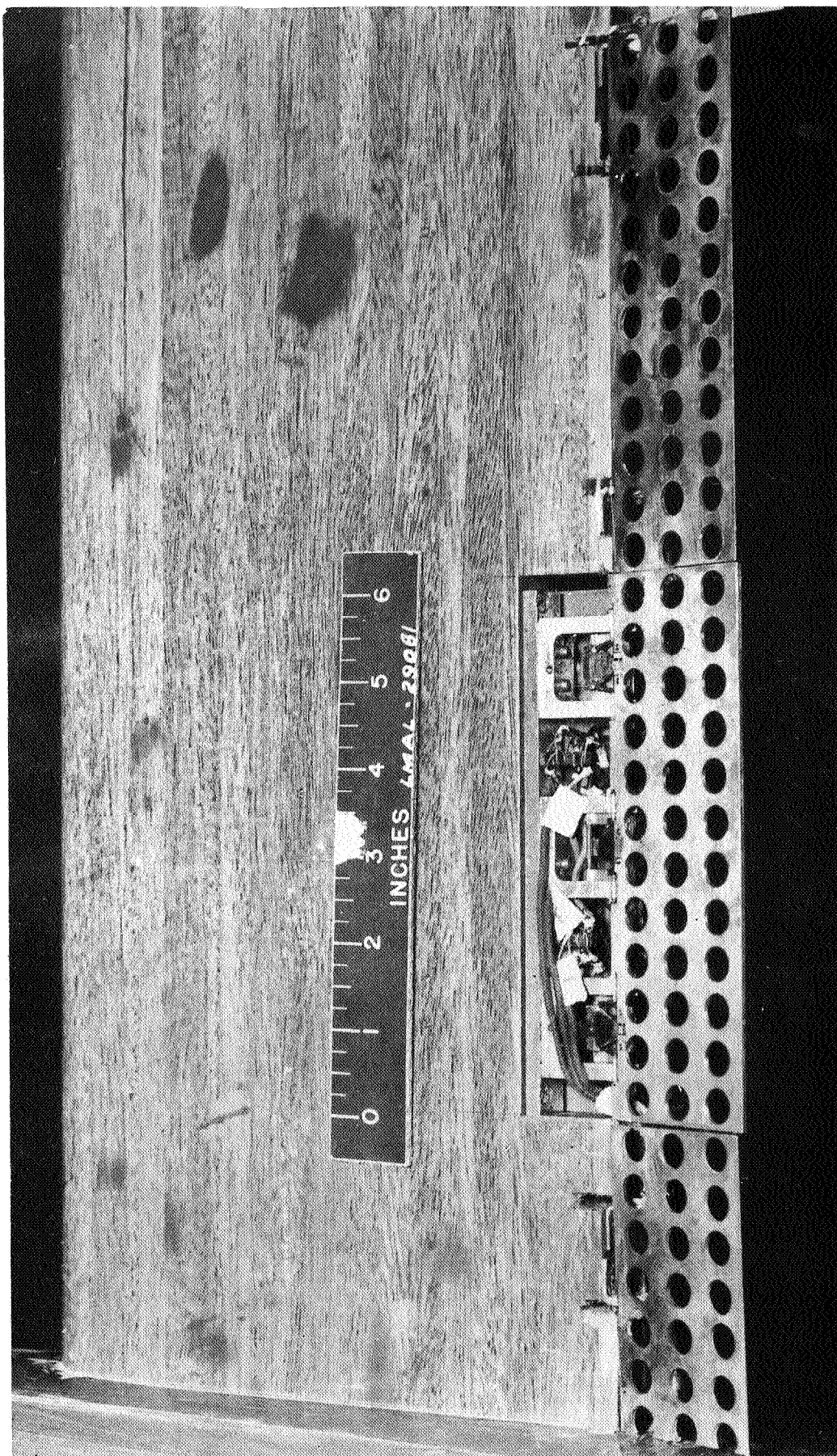
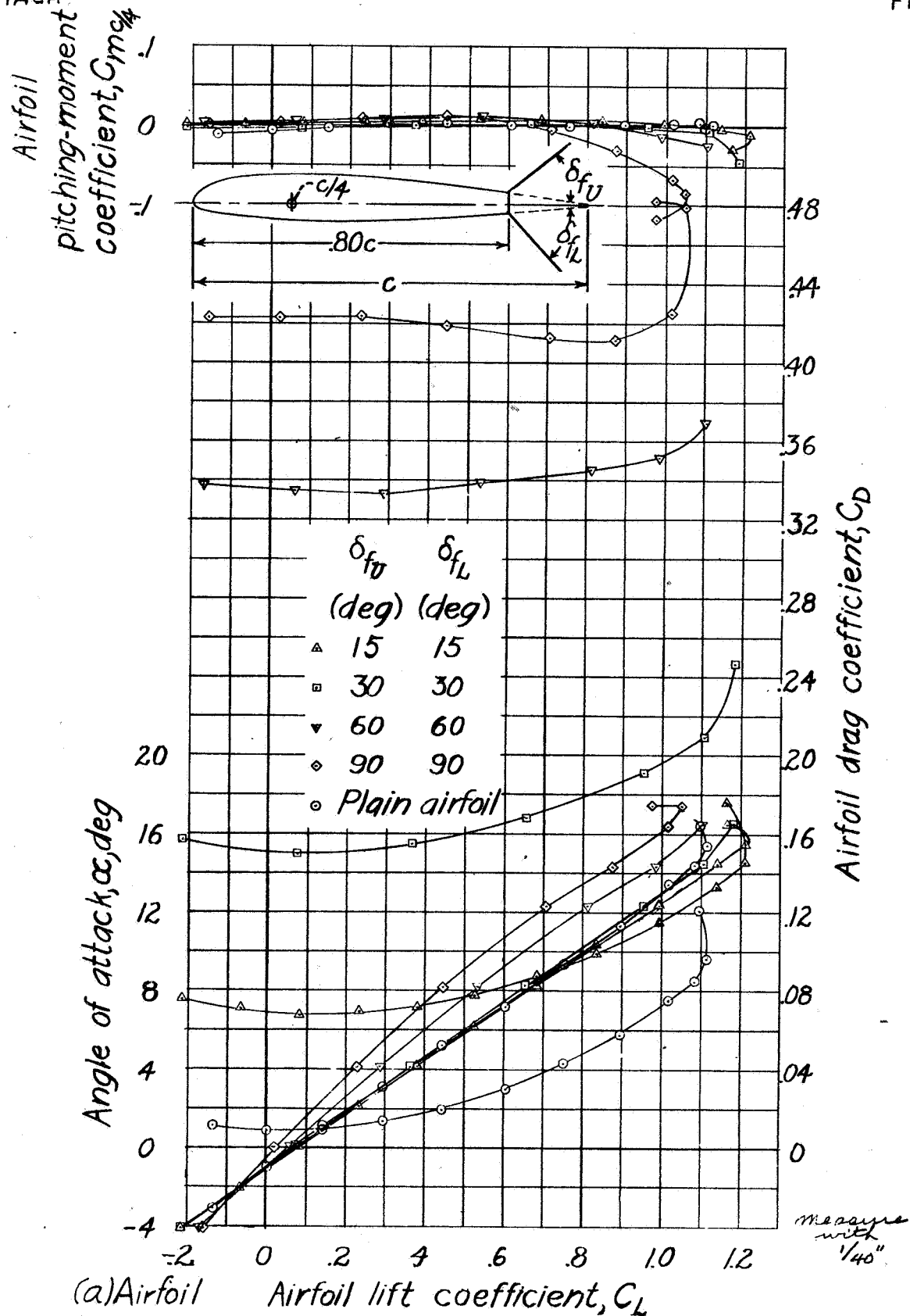


Figure 5.- Close-up view of the strain-gage unit used for measuring flap loads. Hinge reaction is measured by end gages and hinge moment is measured by center gage.



(a) Airfoil lift coefficient, C_L
 Figure 6.- Characteristics of the rectangular NACA 23012 airfoil with 0.20c full-span perforated double split flaps. Circular perforations remove 33.1 percent of original flap area. Equal upper and lower flap deflection.

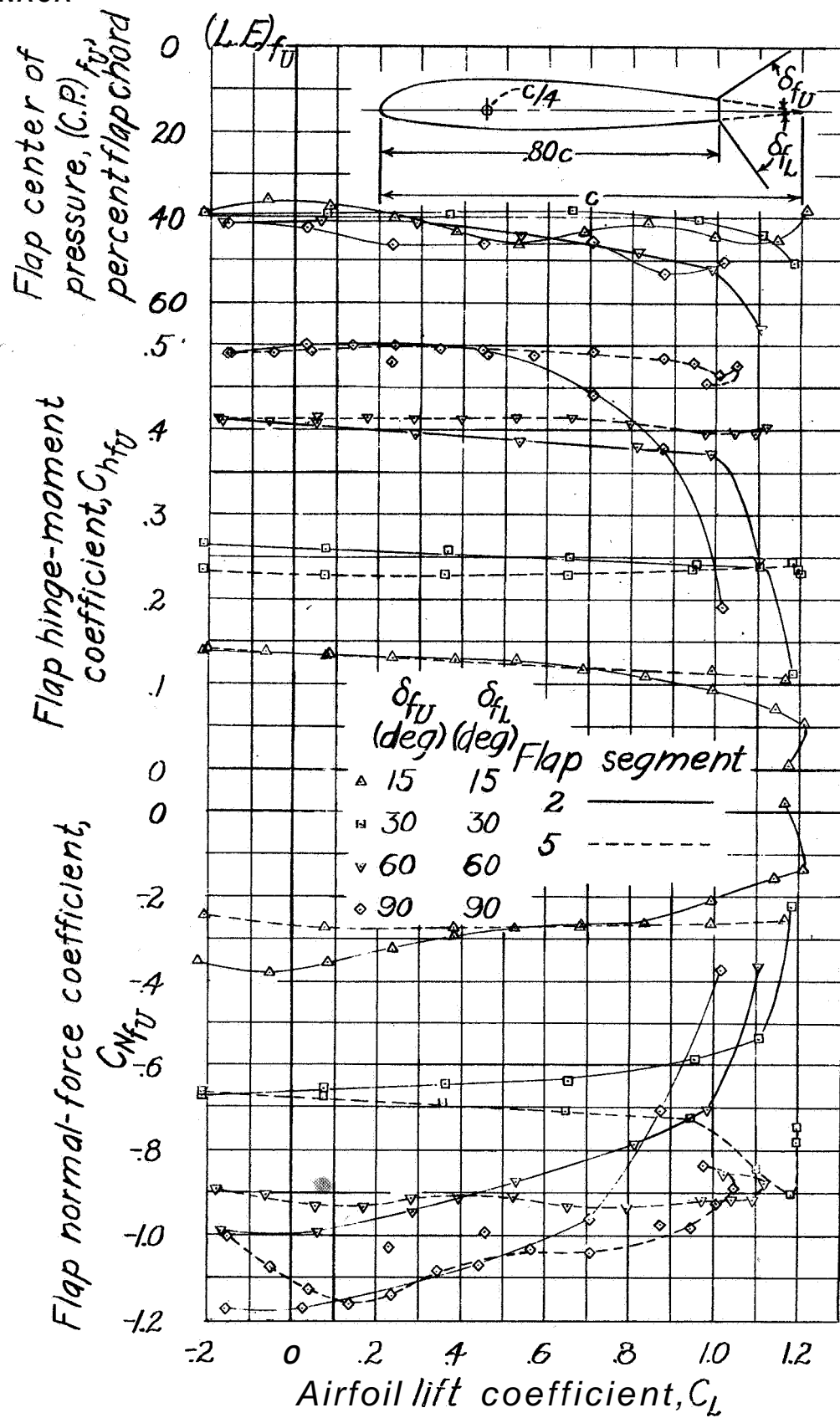
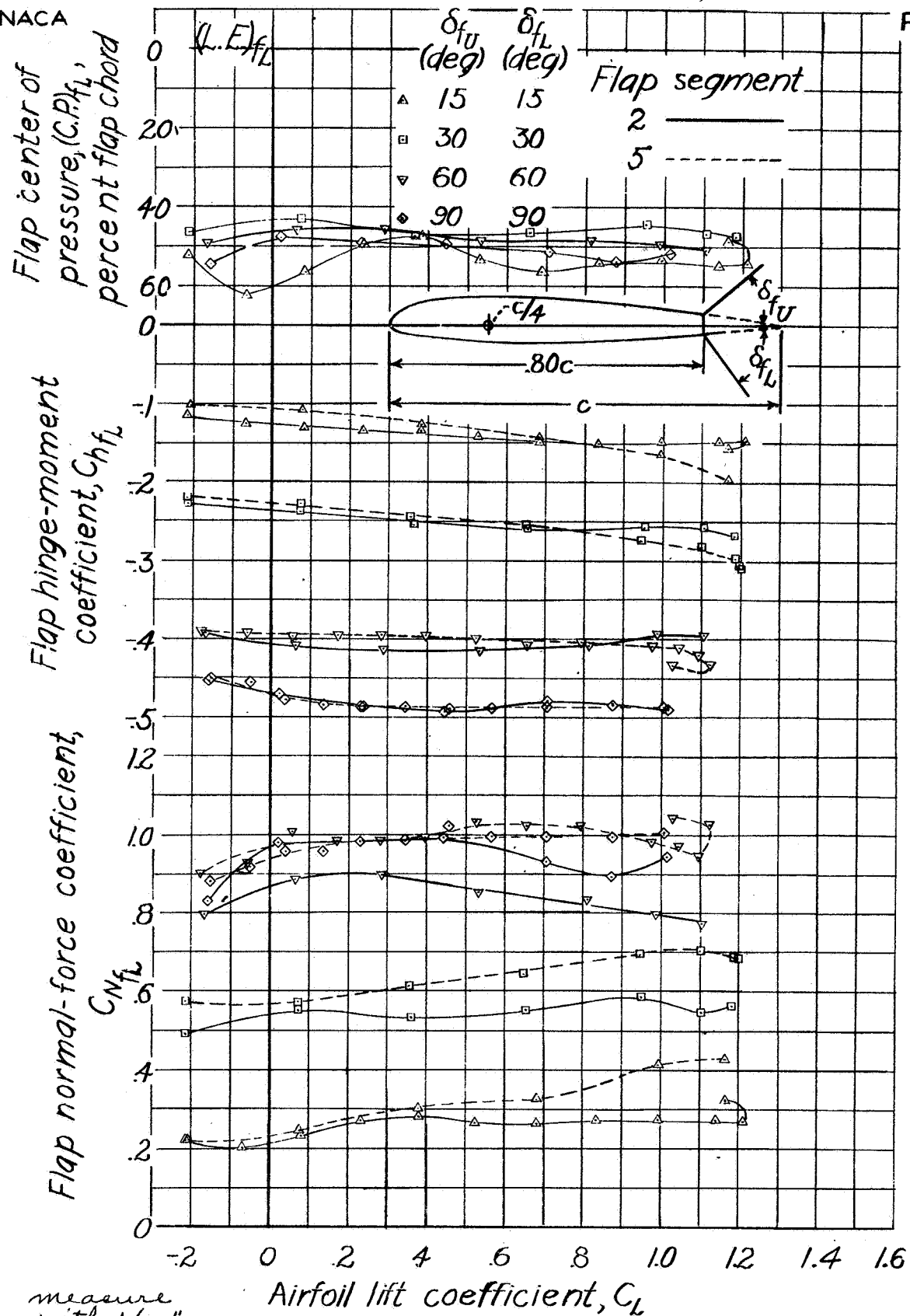


figure 6.-Continued.

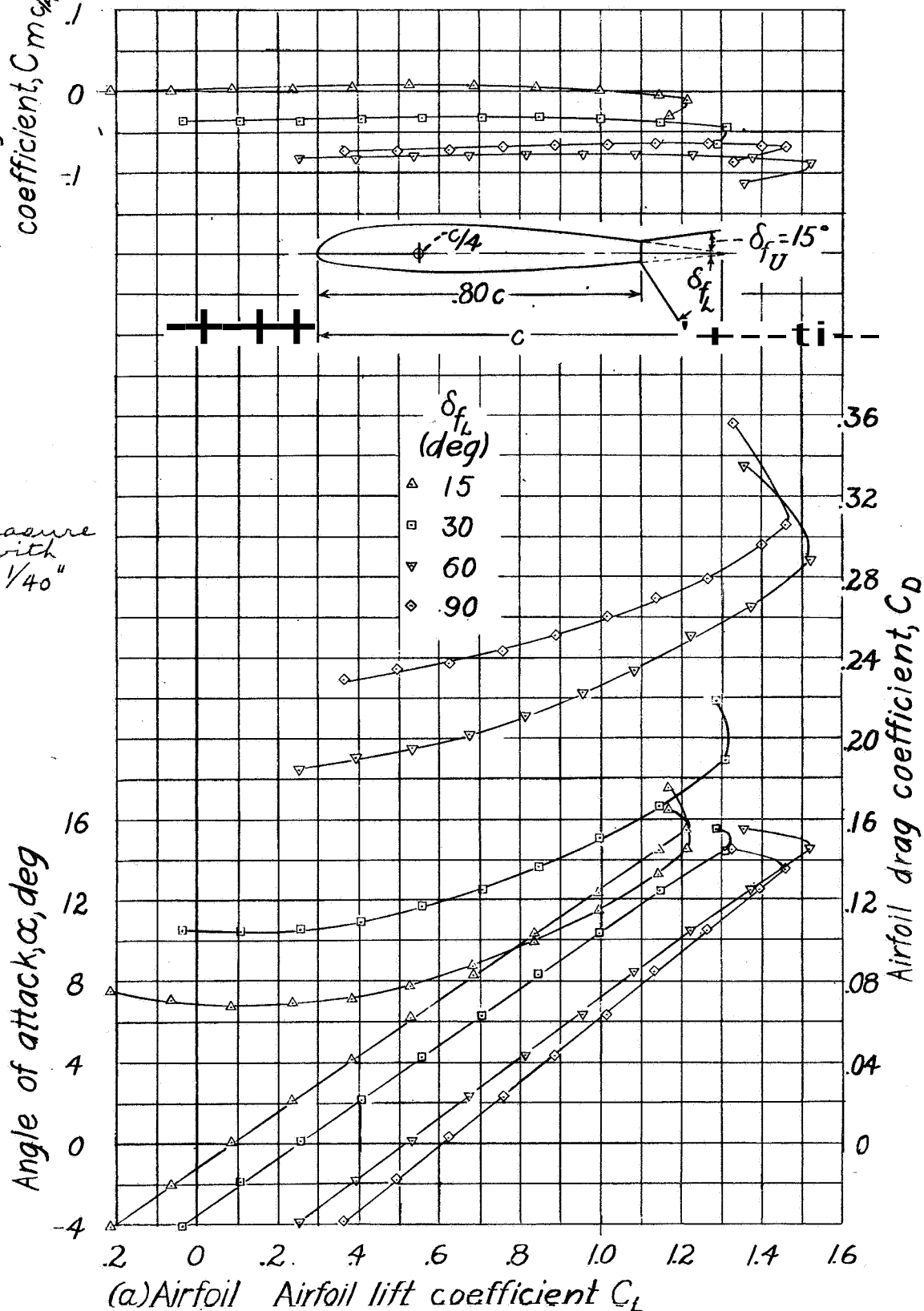
NACA

Fig 6c



NACA

Fig. 7a

Airfoil
pitching-moment
coefficient, $C_{m_{c/4}}$ measure
with
1/40"

(a) Airfoil Airfoil lift coefficient C_L
 Figure 7.-Characteristics of the rectangular NACA 23012 airfoil with 0.20c full-span perforated double split flaps. Circular perforations remove 33.1 percent of original flap area Flap loads on segment 2. $\delta_{fU}, 15^\circ$

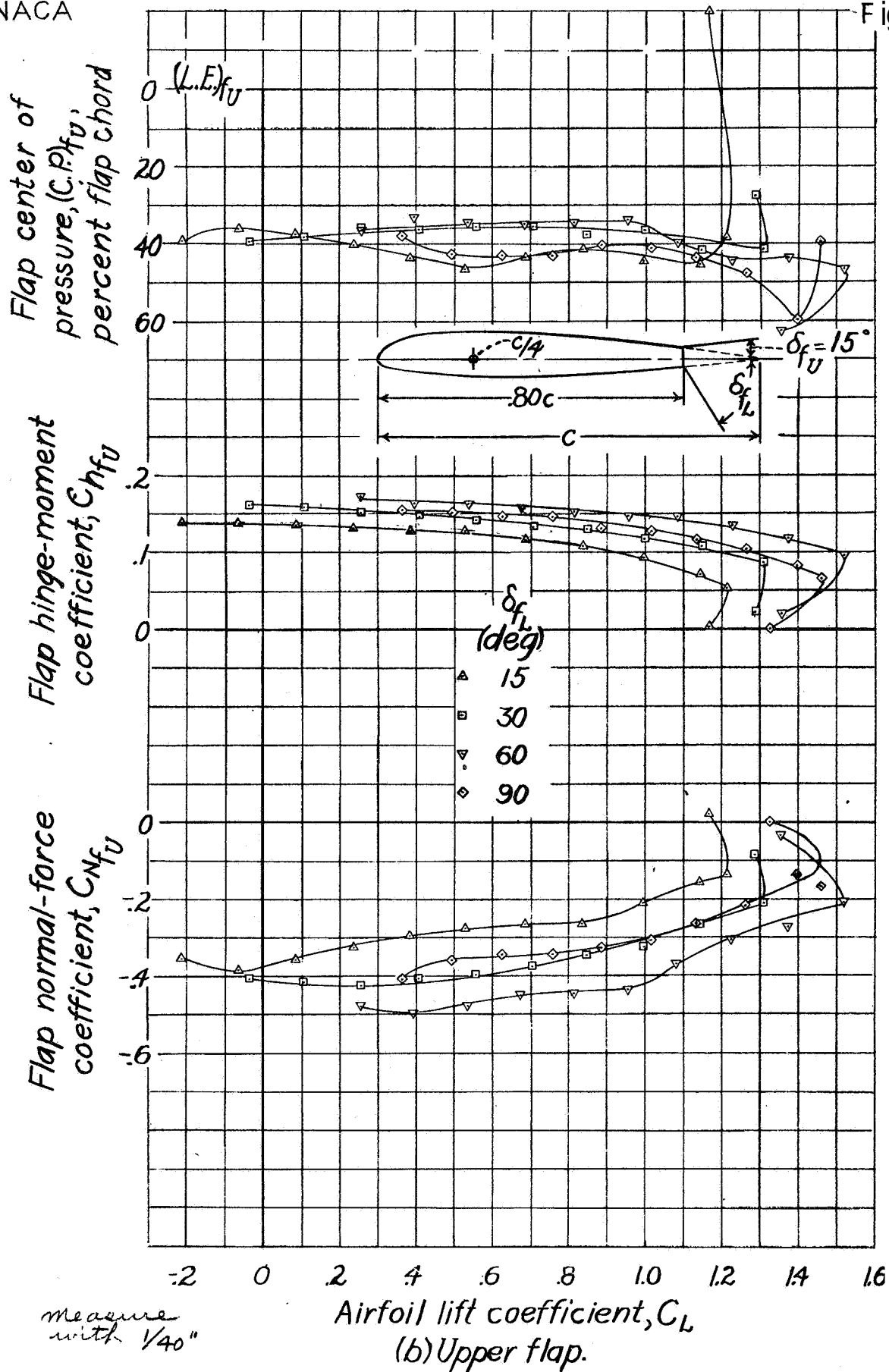


figure 7-Continued.

L-415

NACA

Flap center of pressure, $(C.P.)_{fL}$, percent flap chord

Flap hinge-moment coefficient, C_{hfL}

Flap normal-force coefficient, C_{NfL}

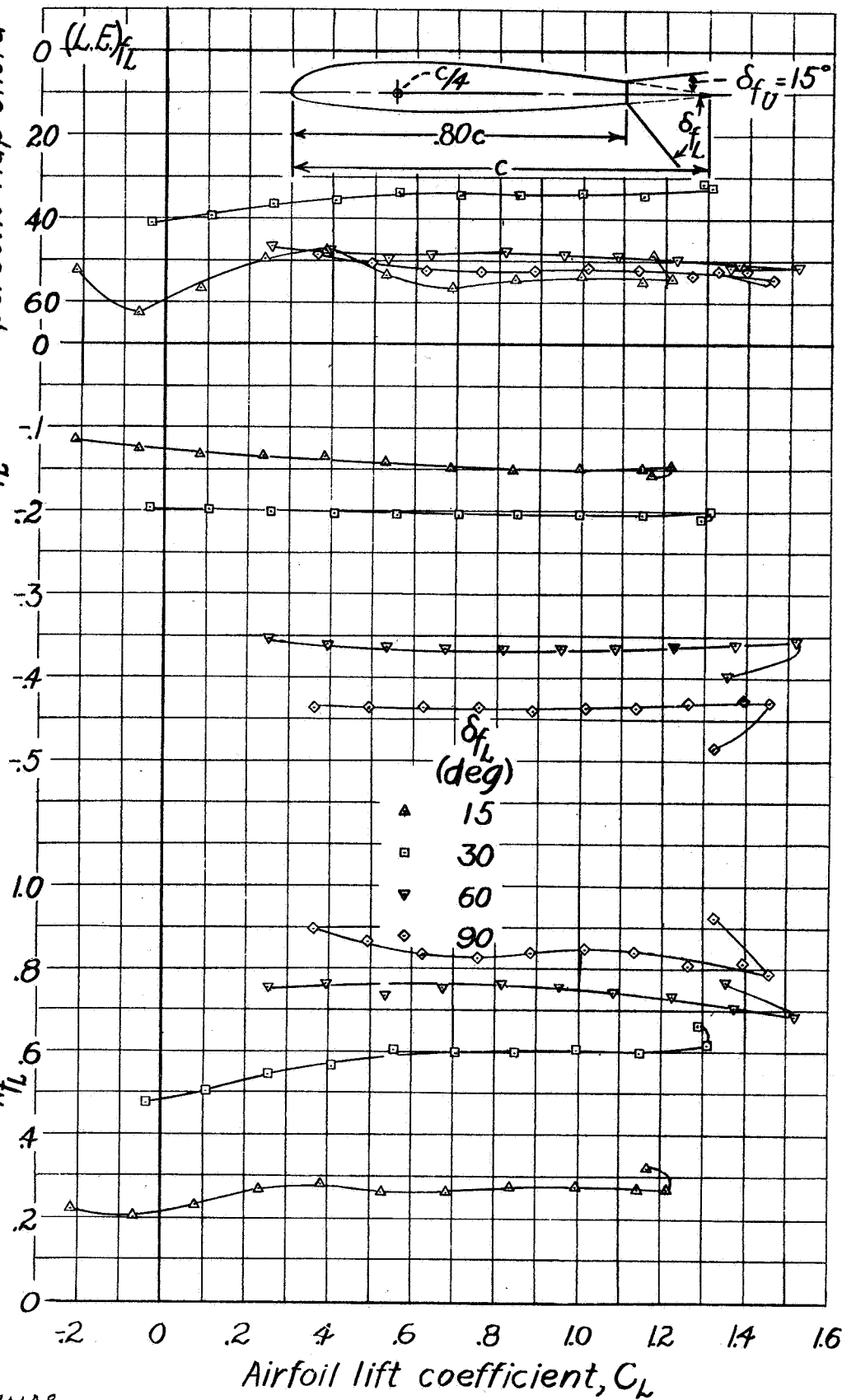


Fig. 7c

measured with $1/40^\circ$

(c) Lower flap.

Figure 7.-Concluded.

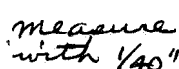


Figure 8.-Characteristics of the rectangular NACA 23012 airfoil with 0.20c full-span perforated double split flaps. Circular perforations remove 33.1 percent of original flap area. Flap loads on segment 2, δ_{f11} , 30°

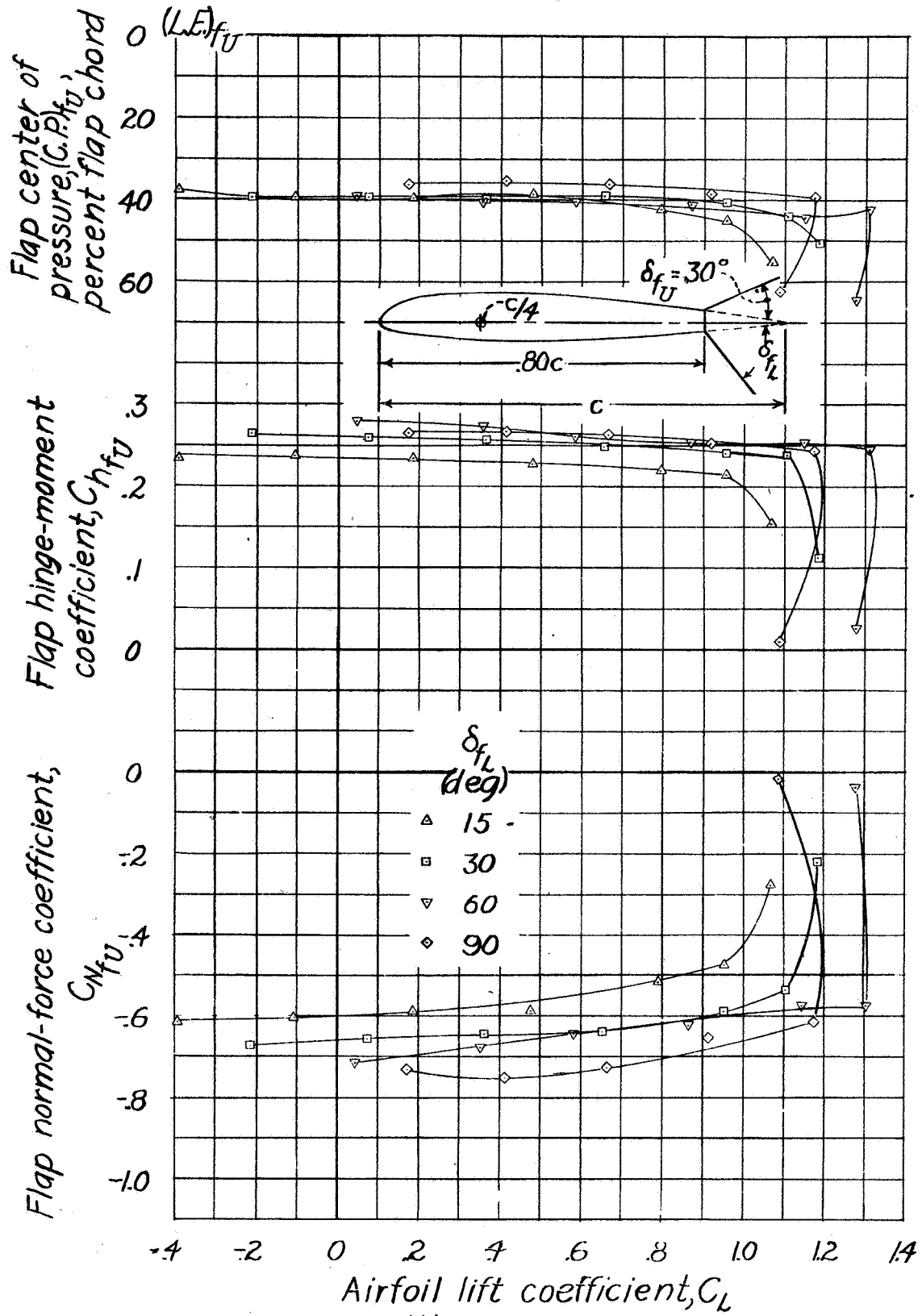


Figure 8.-Continued.

Fig. 8c

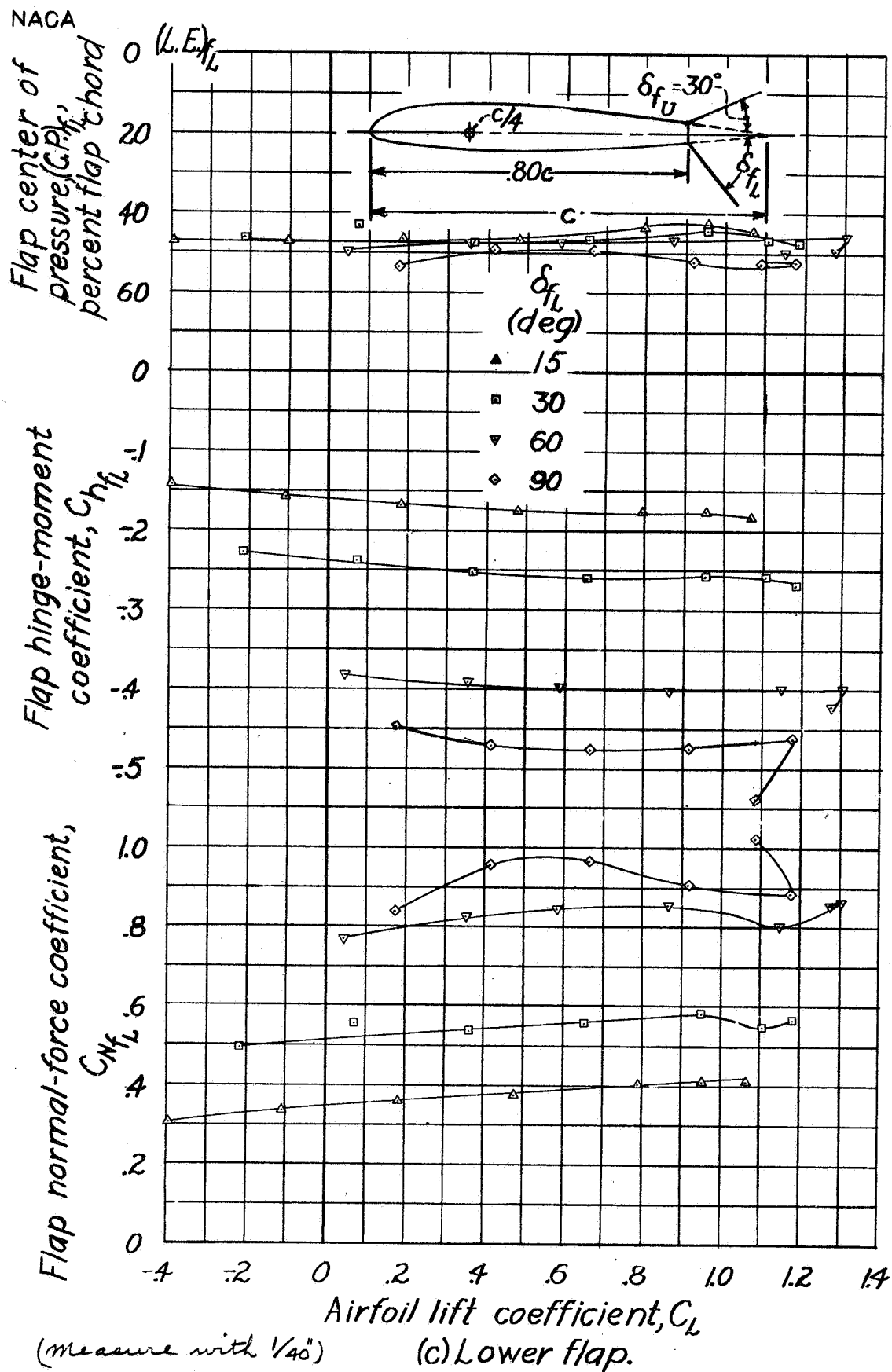


Figure 8.- Concluded.

NACA

Fig. 9a

Airfoil
pitching-moment
coefficient,
 $C_{m_{c/4}}$ Angle of attack, α , degmeasure
with
 $\frac{1}{40}$ "Airfoil lift coefficient, C_L

(a) Airfoil.

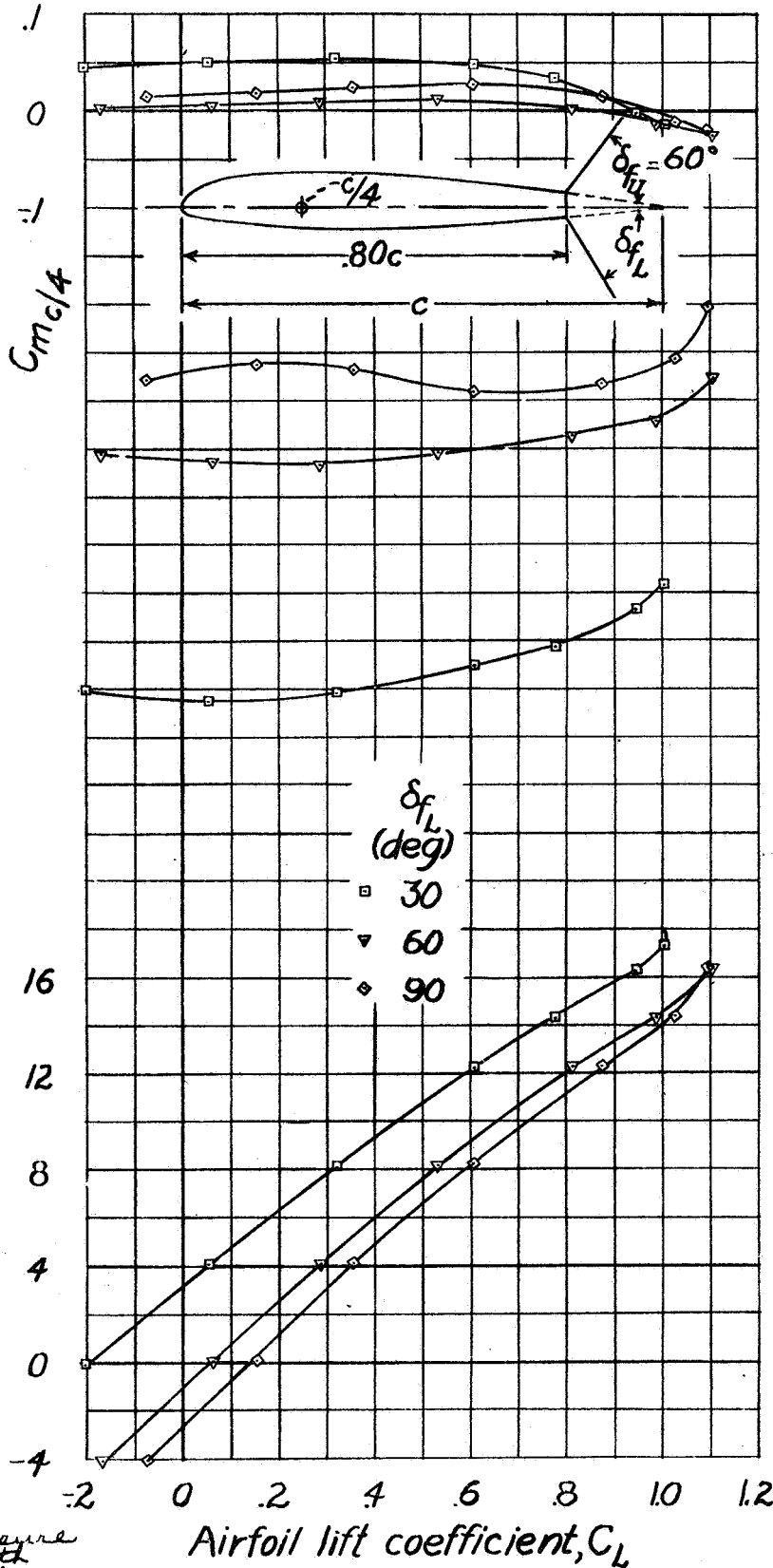


Figure 9.-Characteristics of the rectangular NACA 23012 airfoil with 0.20c full-span perforated double split flaps. Circular perforations remove 33.1 percent of original flap area. Flap loads on segment 2. δ_{f_U} , 60° .

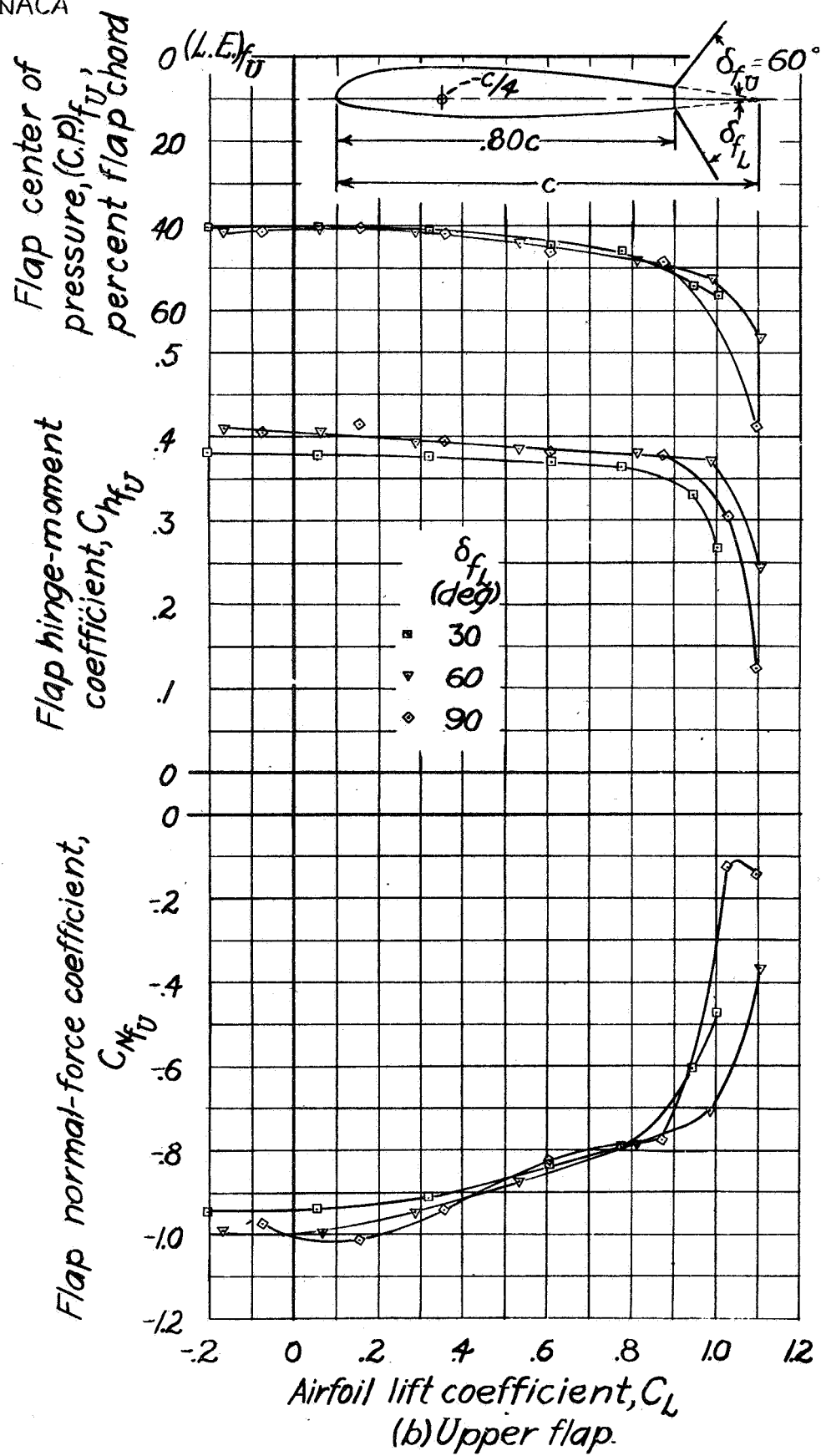


Figure 9.-Continued.

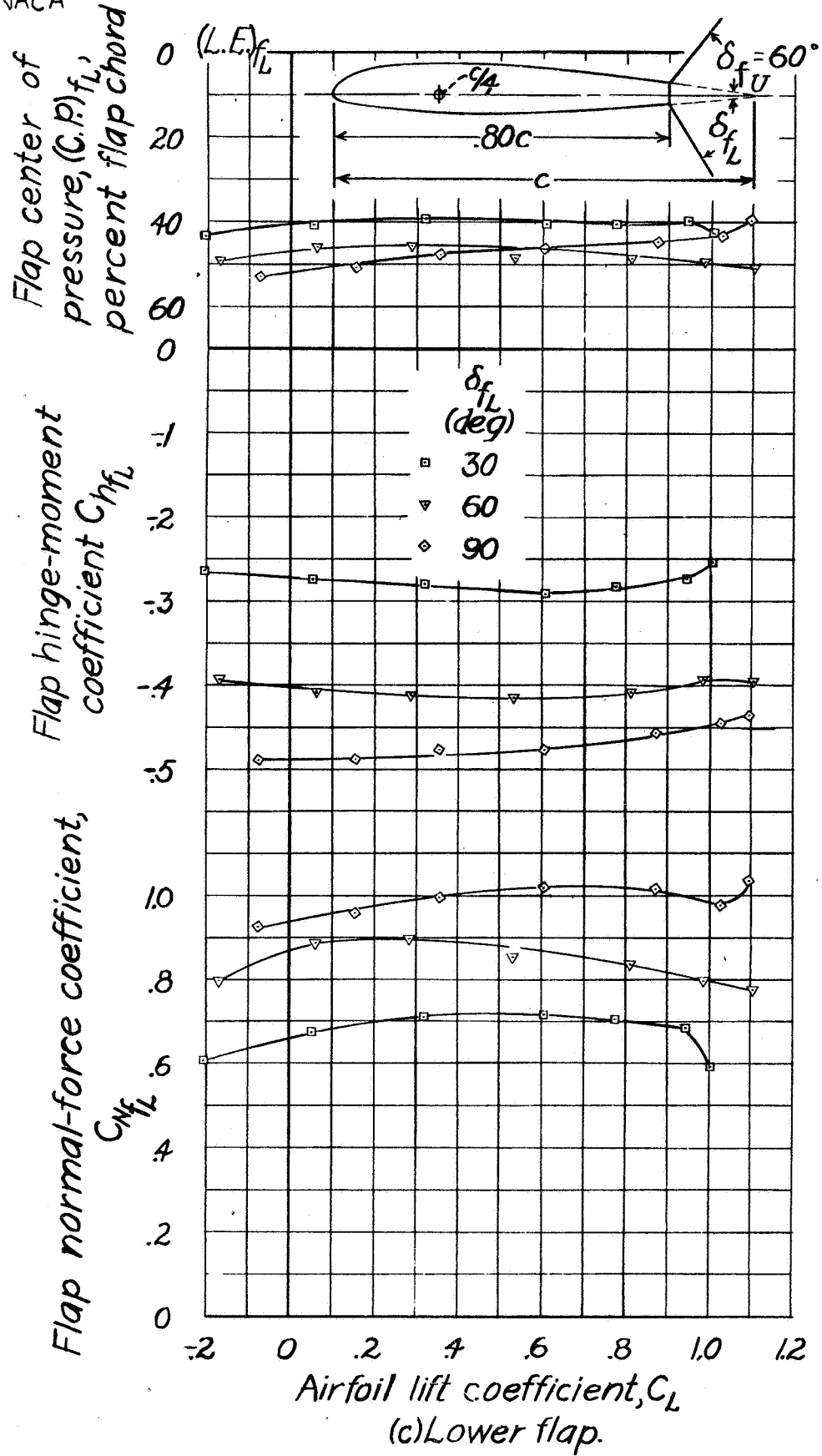


Figure 9.-Concluded.

NACA

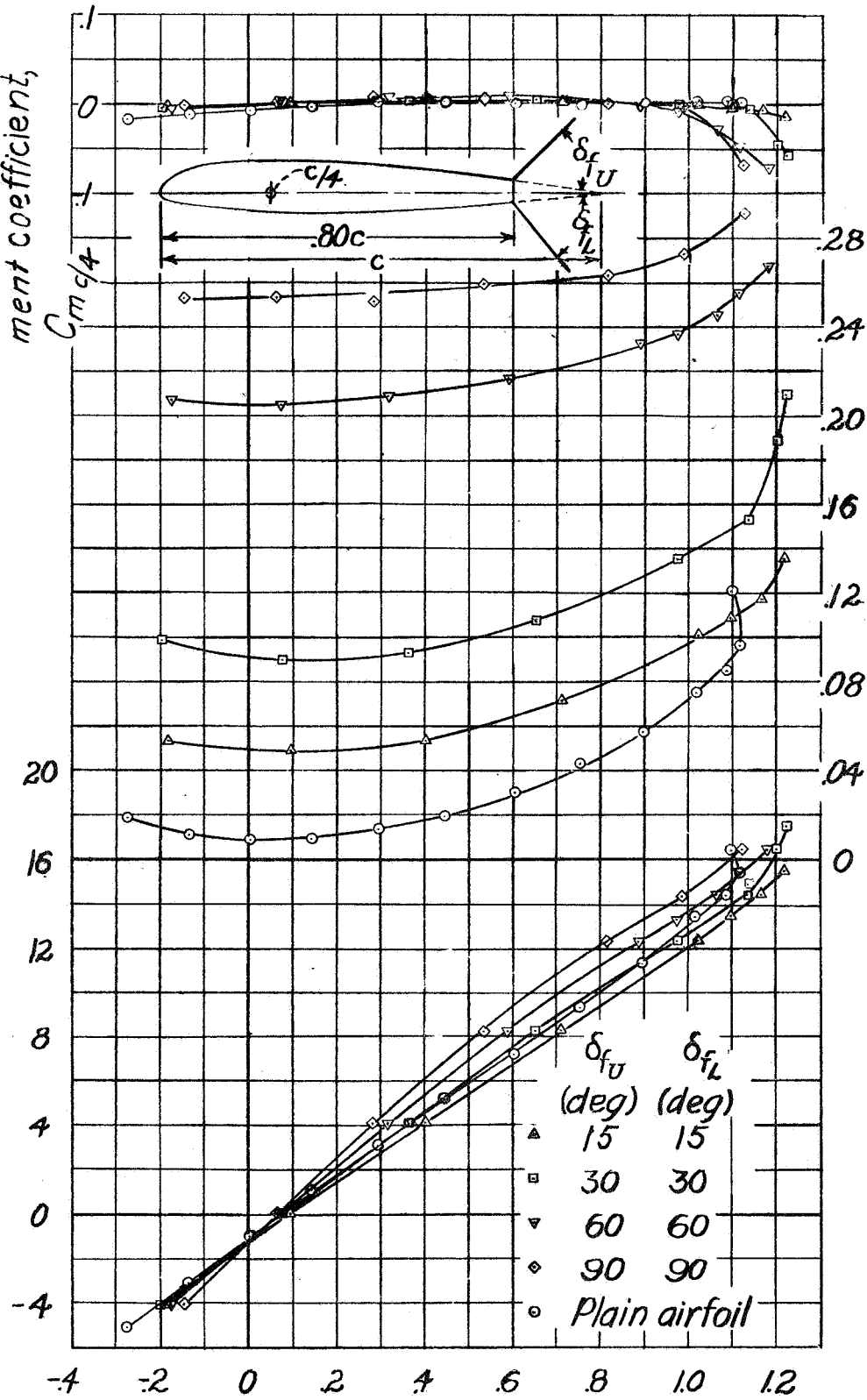
Fig. 10a

Airfoil pitching-moment coefficient, $C_{m_{c/4}}$

Angle of attack, α , deg

Airfoil lift coefficient, C_L

Airfoil drag coefficient, C_D



measure with 1/40"

(a) Airfoil

Figure 10 - Characteristics of the rectangular NACA 23012 airfoil with 0.20c by 0.60b perforated double split flaps. Circular perforations remove 33.1 percent of original flap area. Flap loads on segment 2. Equal upper and lower flap deflection.

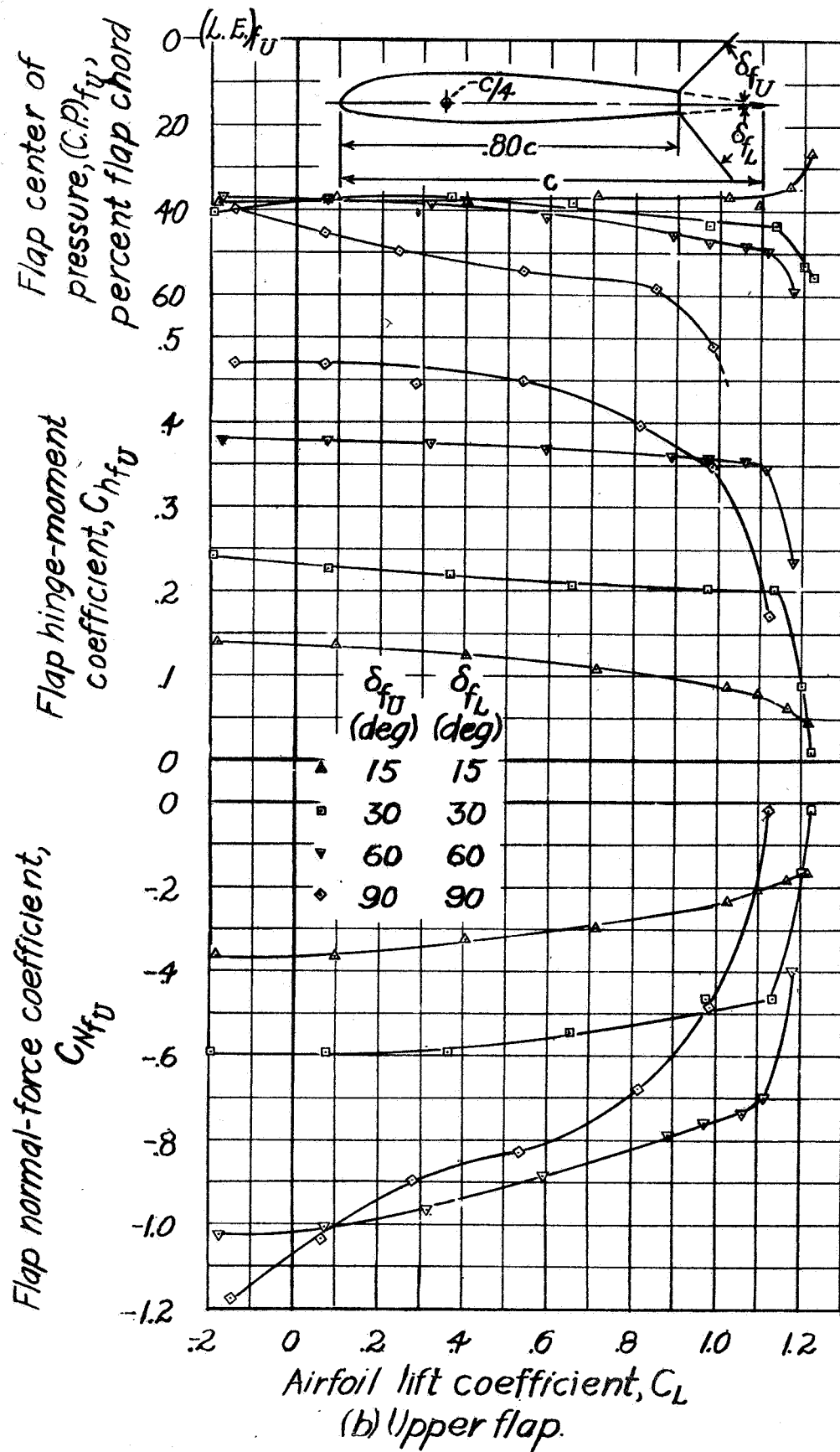


Figure 10.-Continued.

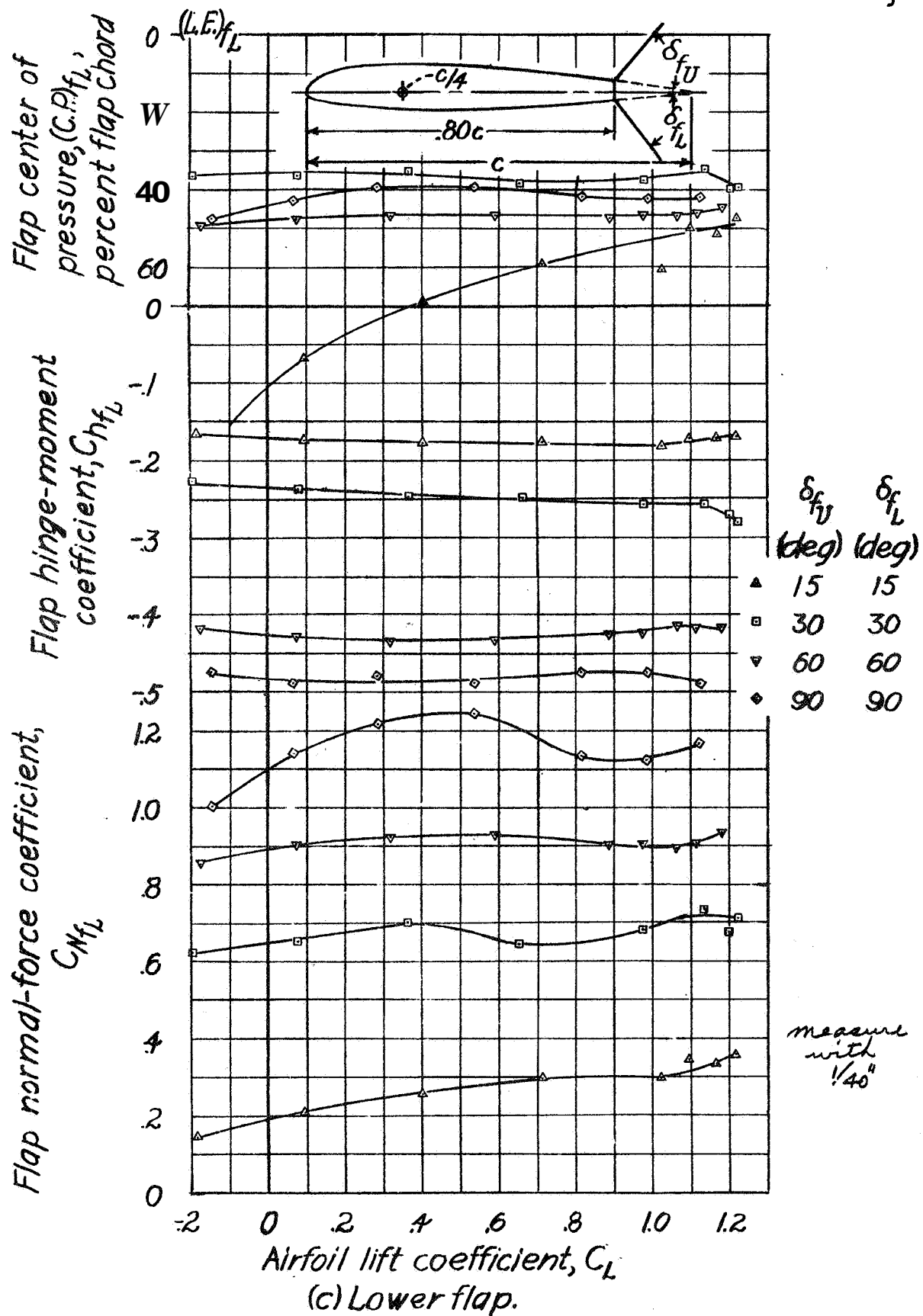
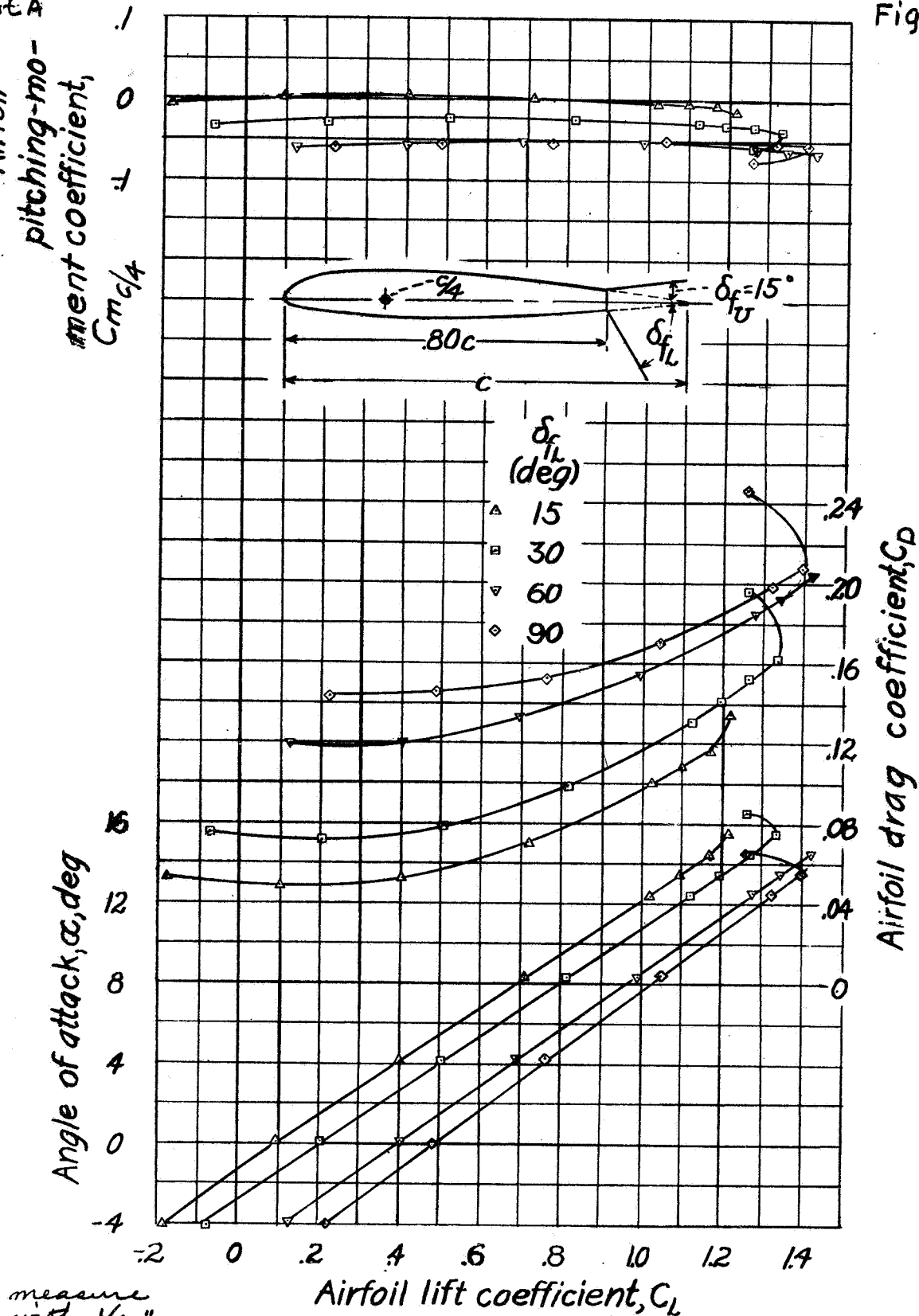


Figure 10.- Concluded.

NACA

Airfoil
pitching-mo-
ment coefficient,
 $C_{m_{c/4}}$

Fig. 11a



(a) Airfoil.

Figure 11 - Characteristics of the rectangular NACA 23012 airfoil with 0.20c by 0.60b perforated double split flaps. Circular perforations remove 33.1 percent of original flap area. flap loads on segment 2. $\delta_{fL} 15^\circ$.

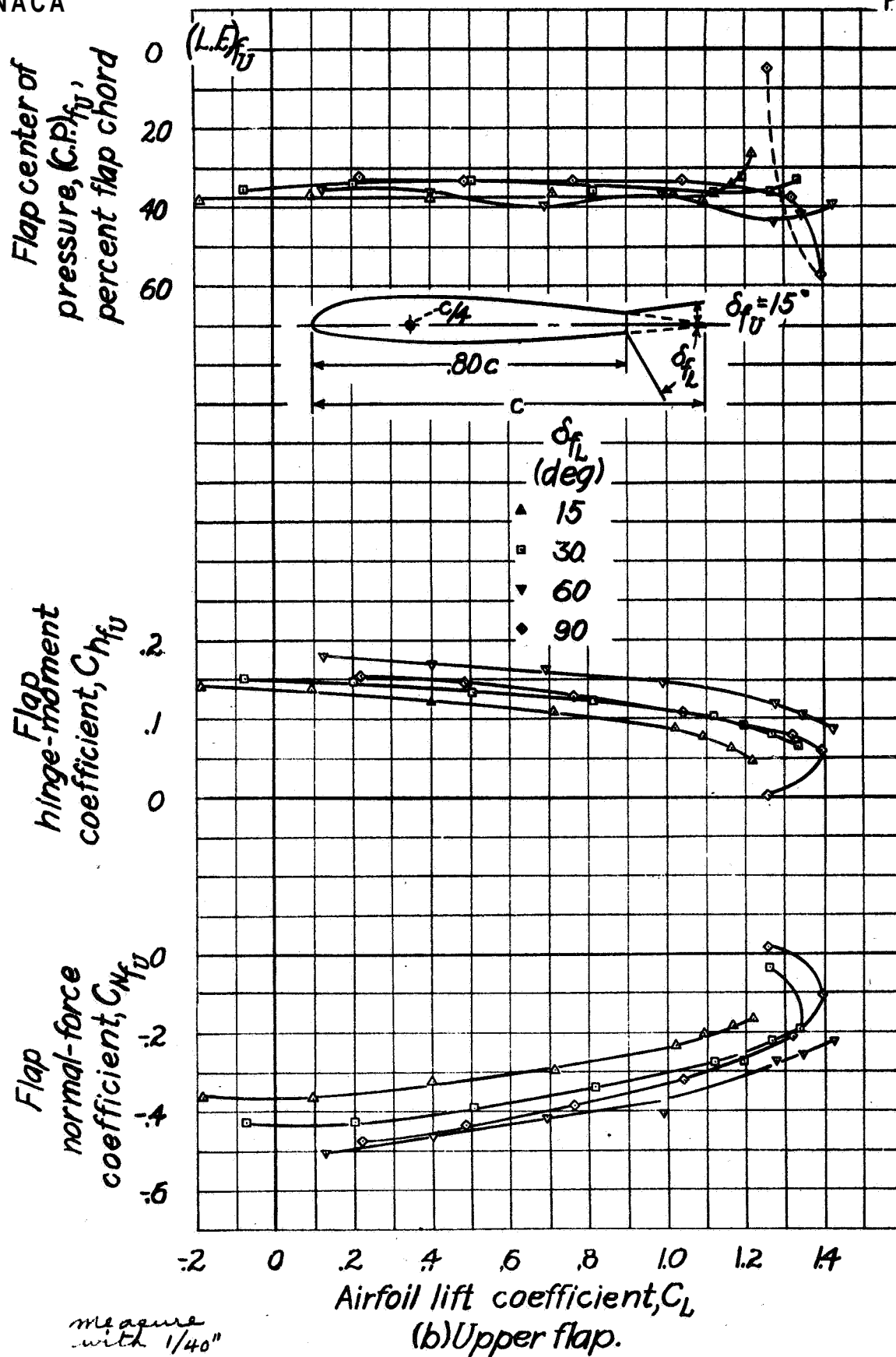


Figure 11 - Continued.

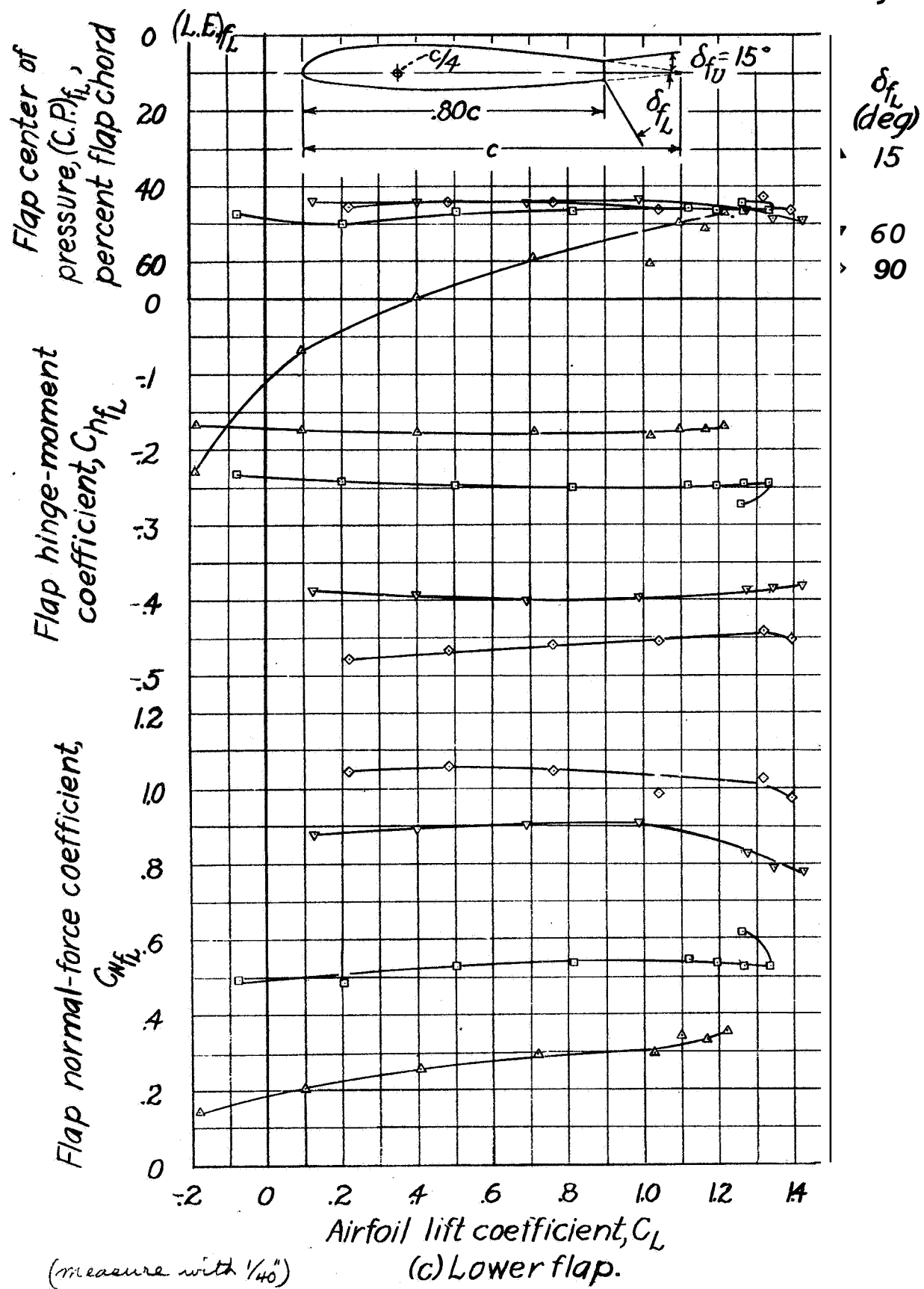


Figure 11.-Concluded.

NACA

Airfoil
pitching-mo-
ment coefficient,
 $C_{m_{c/4}}$

Fig. 12a

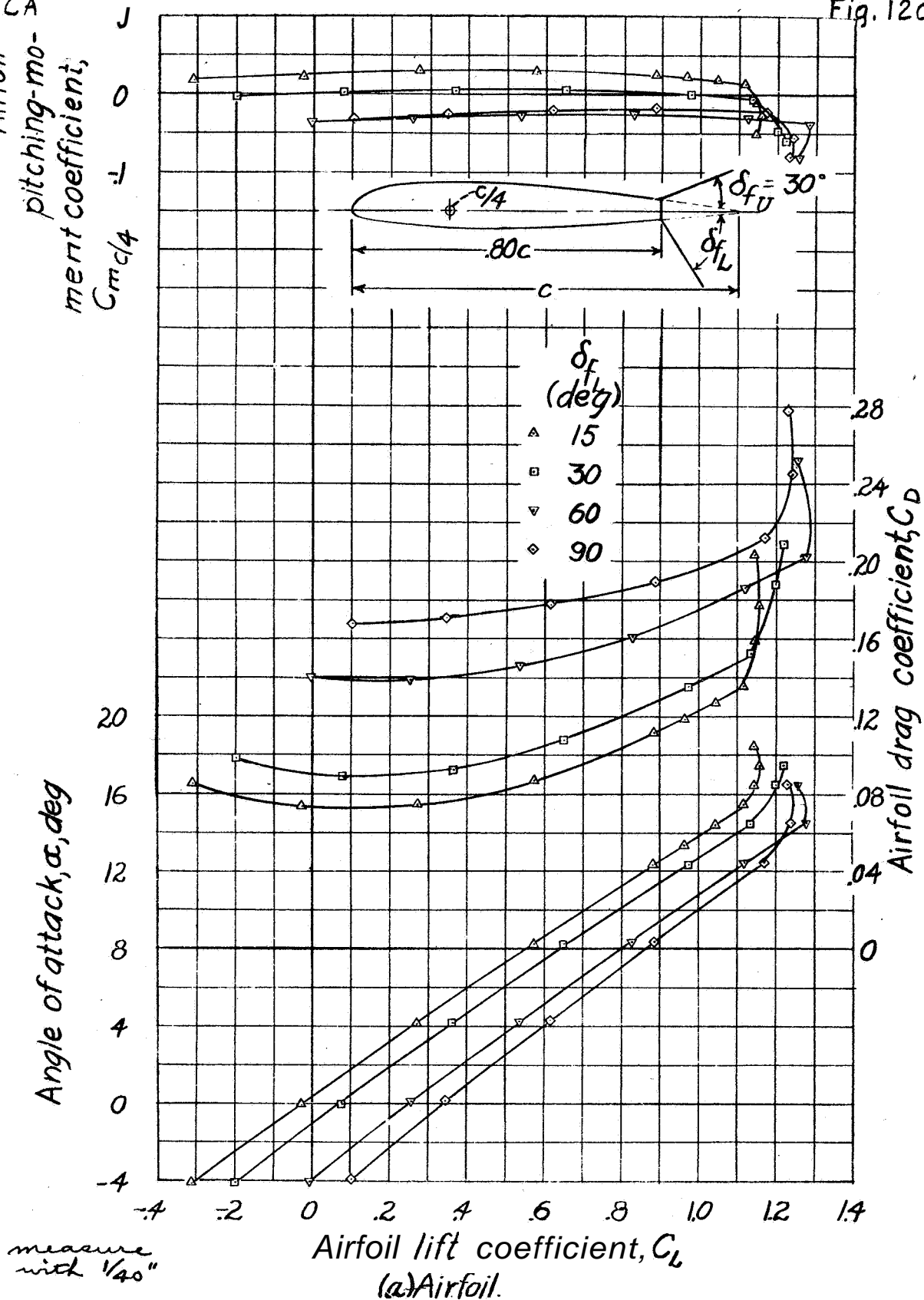
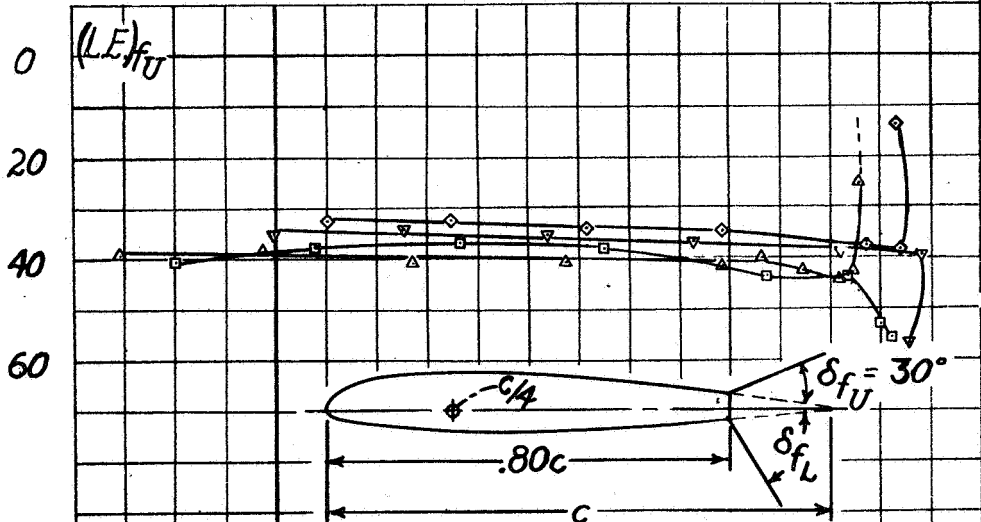


figure 12 - Characteristics of the rectangular NACA 23012 airfoil with 0.20c by 0.60b perforated double split flaps. Circular perforations remove 33.1 percent of original flap area. Flap loads on segment 2. $\delta_{f_u}, 30^\circ$.

NACA

Fig 12b

Flap center of pressure, $(C.P.)_{f_U}$, percent flap chord



δ_{f_L} (deg)

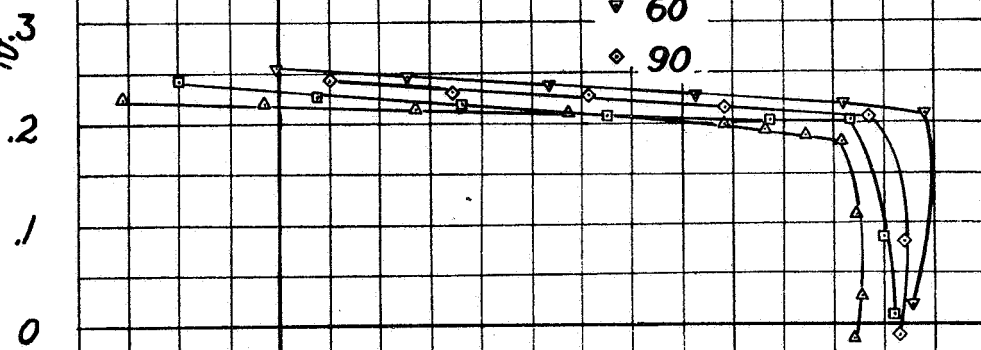
▲ 15

◻ 30

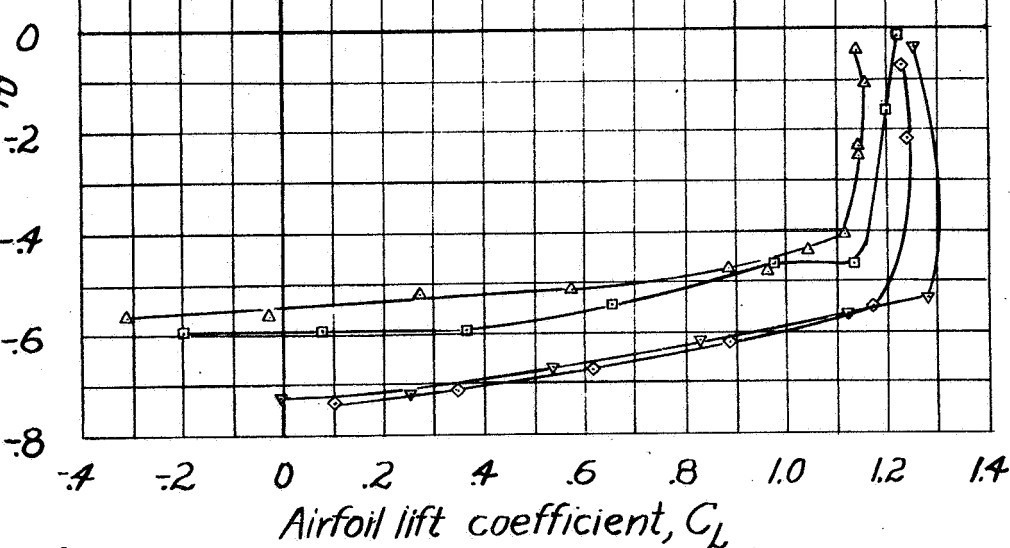
▼ 60

◆ 90

Flap hinge-moment coefficient, $C_{h_{f_U}}$



Flap normal-force coefficient, $C_{N_{f_U}}$



measured with 1/40"

(b) Upper flap.

Figure 12.-Continued.

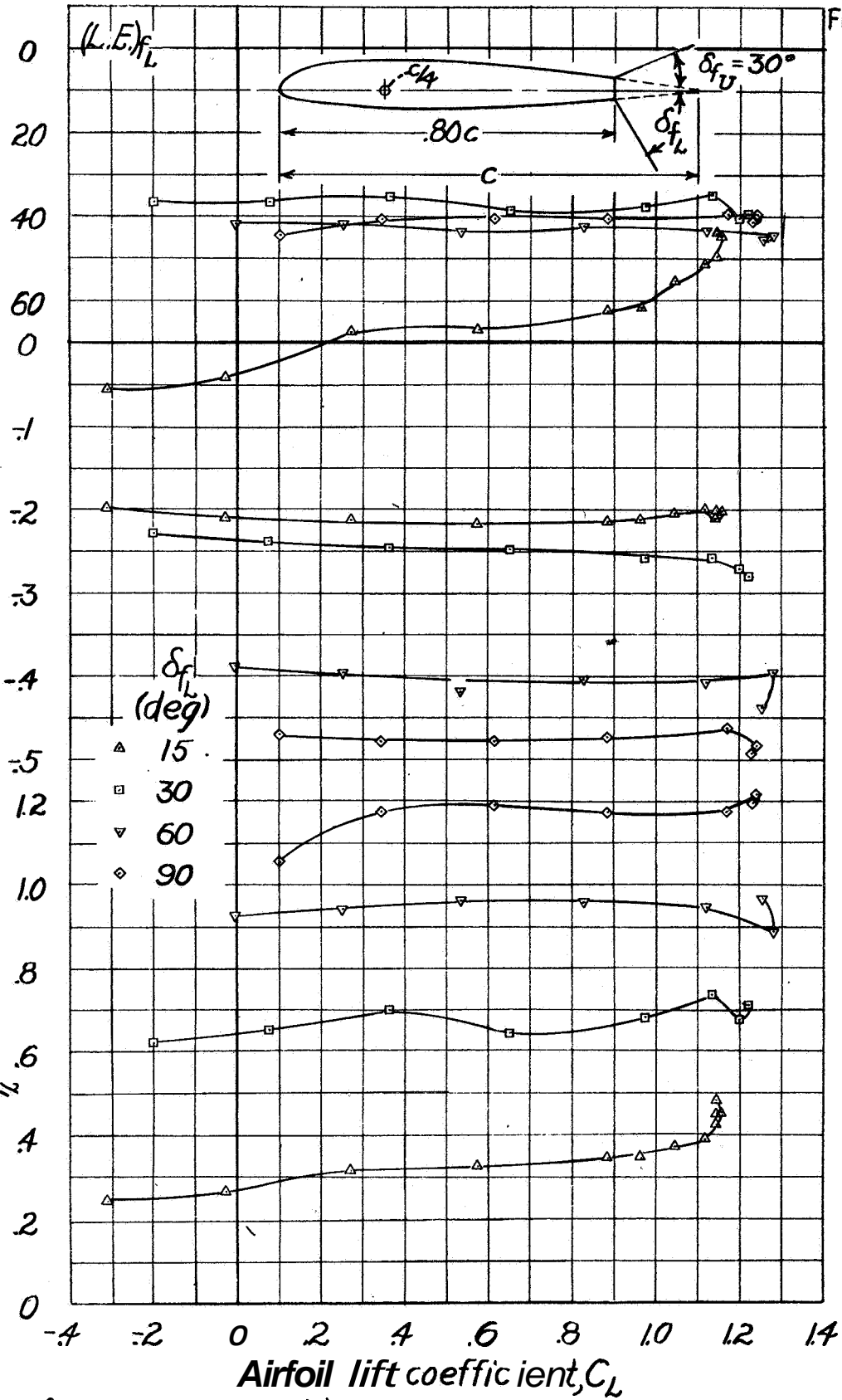
NACA

Fig. 12c

Flap center of pressure, $(C.P.)_{f_L}$, percent flap chord

Flap hinge-moment coefficient, $C_{h_{f_L}}$

Flap normal-force coefficient, $C_{N_{f_L}}$



measure with $1/40''$

(c) Lower flap.

figure 12.-Concluded.

2-415

NACA
Airfoil
pitching-mo-
ment coefficient,
 $C_{m,c/4}$

Fig. 13a

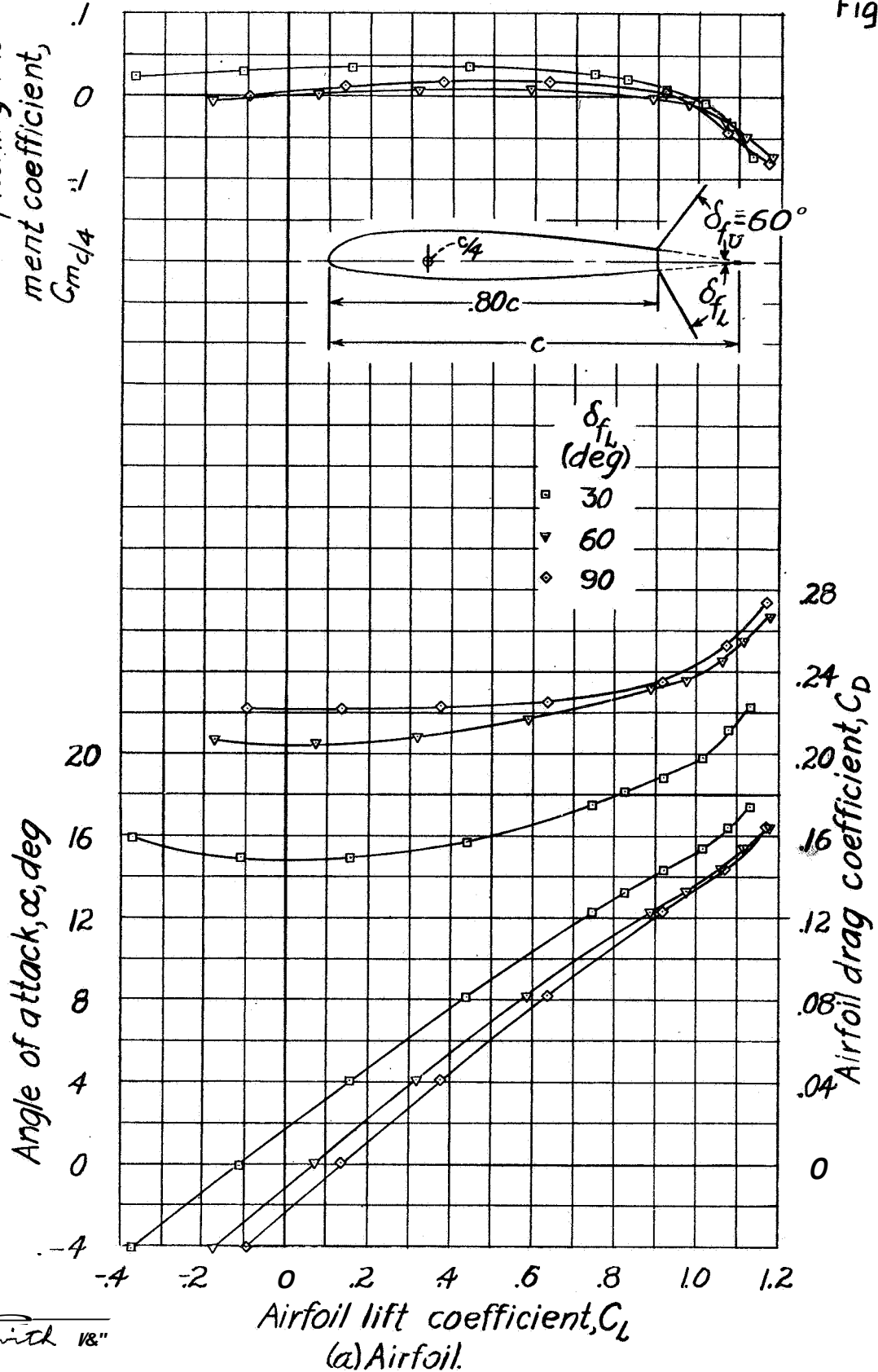


Figure 13: Characteristics of the rectangular NACA 23012 airfoil with 0.20c by 0.60b perforated double split flaps. Circular perforations remove 33.1 percent of original flap area. Flap loads on segment 2. δ_{fU} , 60° .

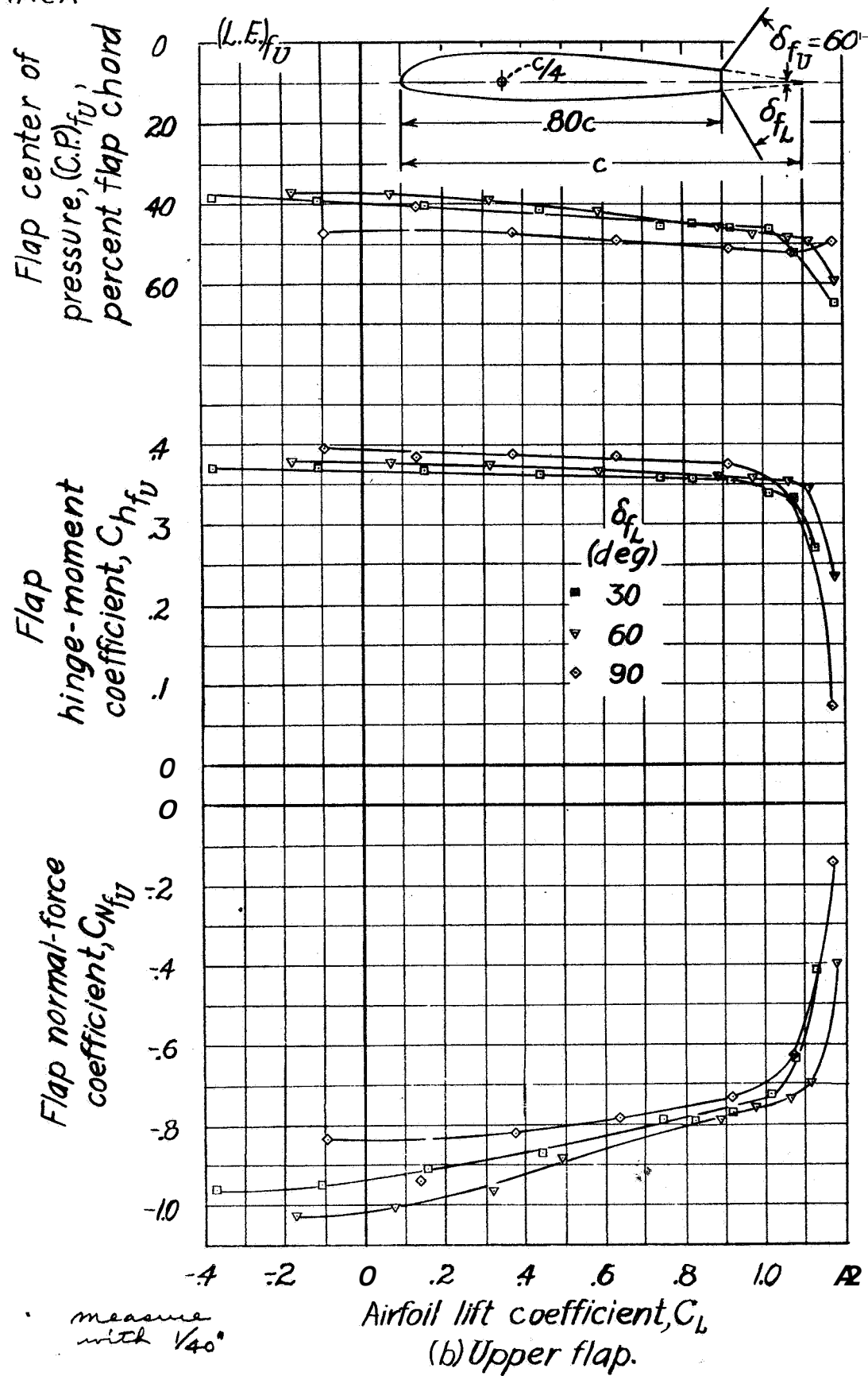


Figure 13.-Continued.

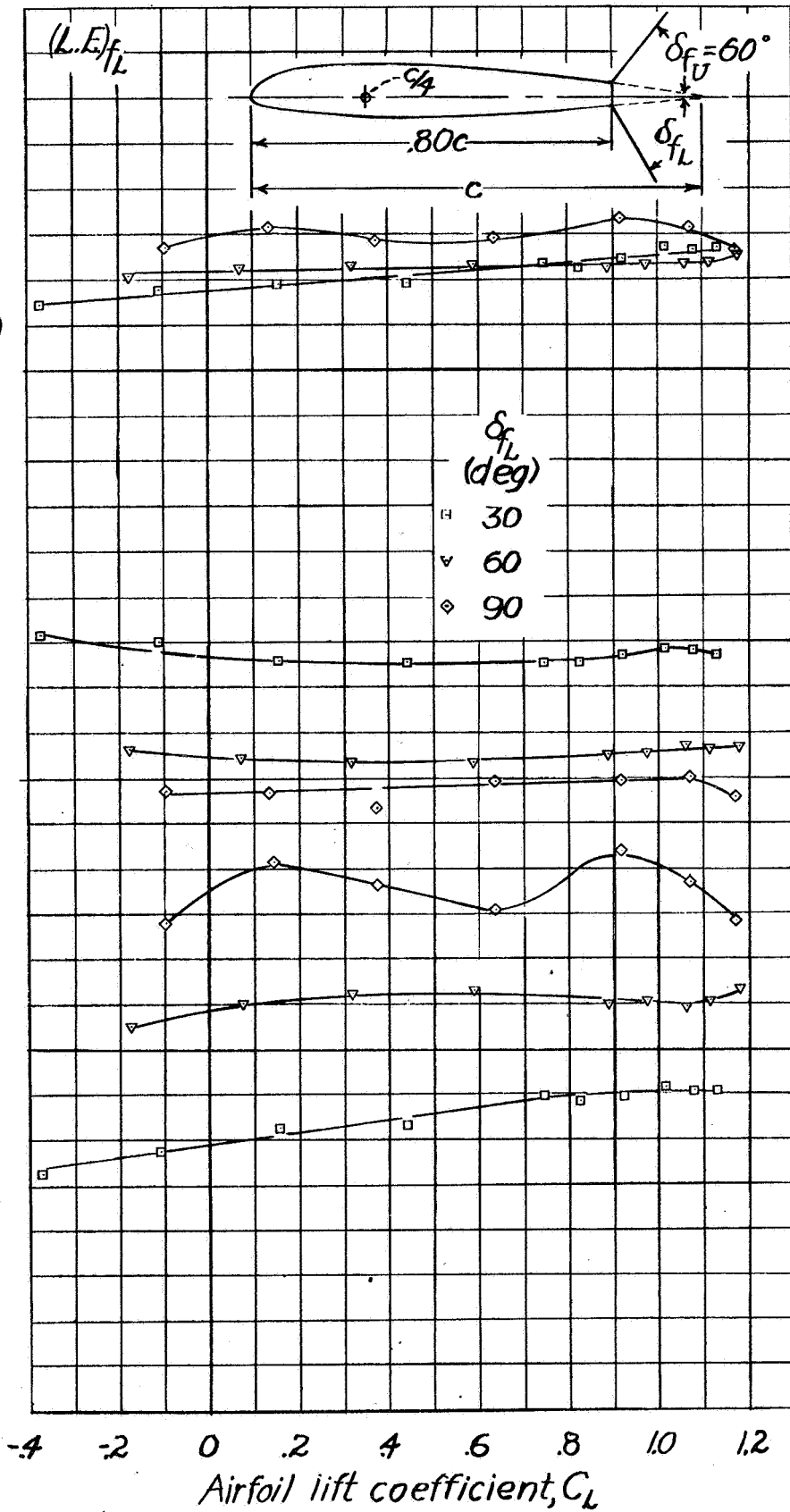
NACA

Fig. 13c

Flap center of pressure, $(C.P.)_{f_L}$, percent flap chord

Flap hinge-moment coefficient, $C_{h_{f_L}}$

Flap normal-force coefficient, $C_{N_{f_L}}$



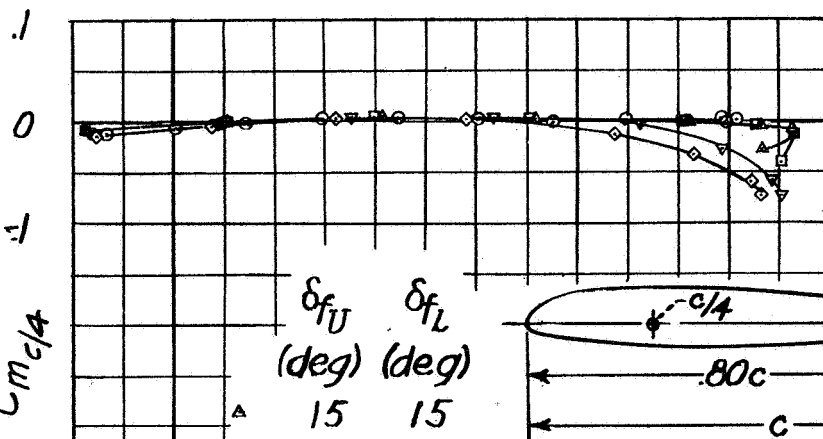
(measure with $1/40$)

(c) Lower flap.

Figure 13.-Concluded

NACA

Fig. 14a

Airfoil
pitching-moment
coefficient,
 $C_{m_{c/4}}$ 
 δ_{fU} δ_{fL}
(deg) (deg)

\triangle 15 15
 \square 30 30
 ∇ 60 60
 \diamond 90 90
 \circ Plain airfoil

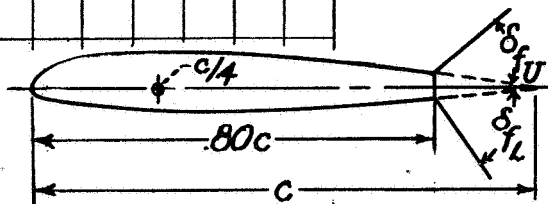
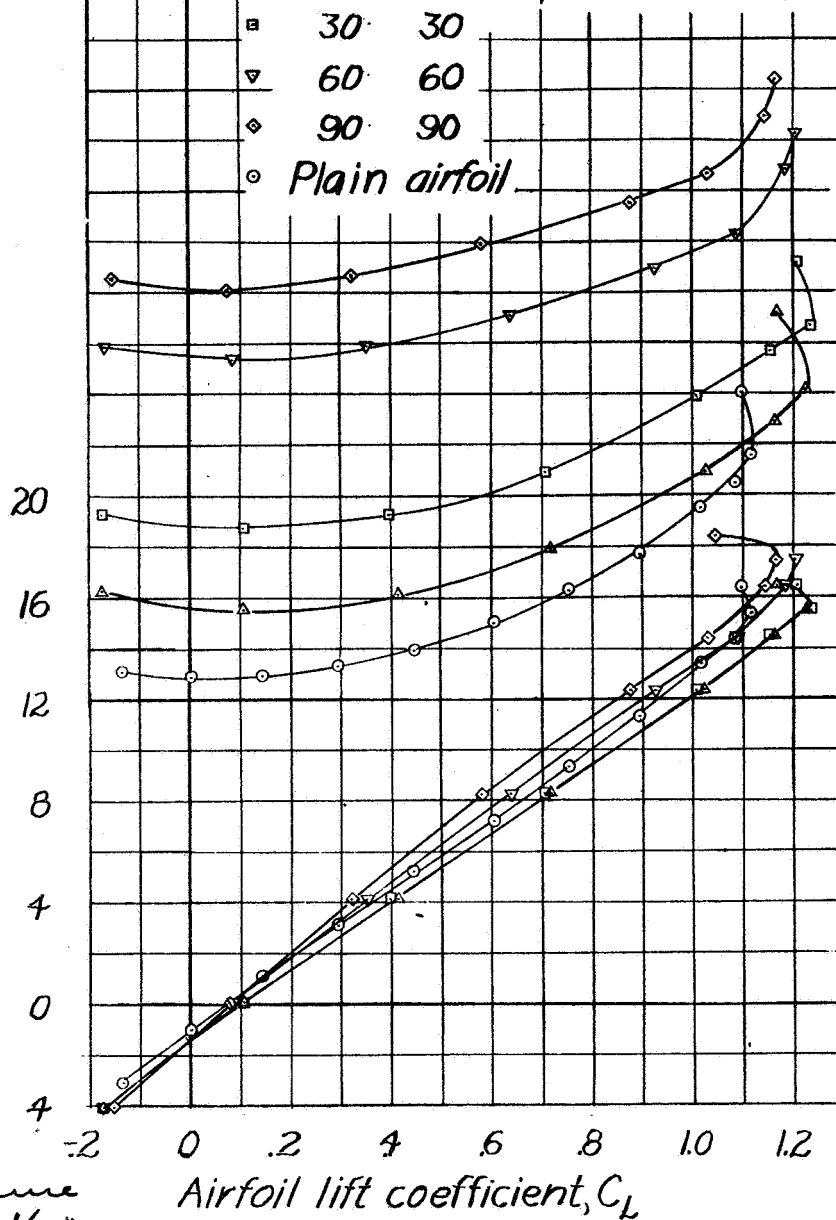
Angle of attack, α , degAirfoil drag coefficient, C_D measured
with $1/40"$ Airfoil lift coefficient, C_L
(a) Airfoil.

Figure 14 - Characteristics of the rectangular NACA 23012 airfoil with 0.20c by 0.40b perforated double split flaps. Circular perforations remove 33.1 percent of original flap area. Flap loads on segment 2. Equal upper and lower flap deflection.

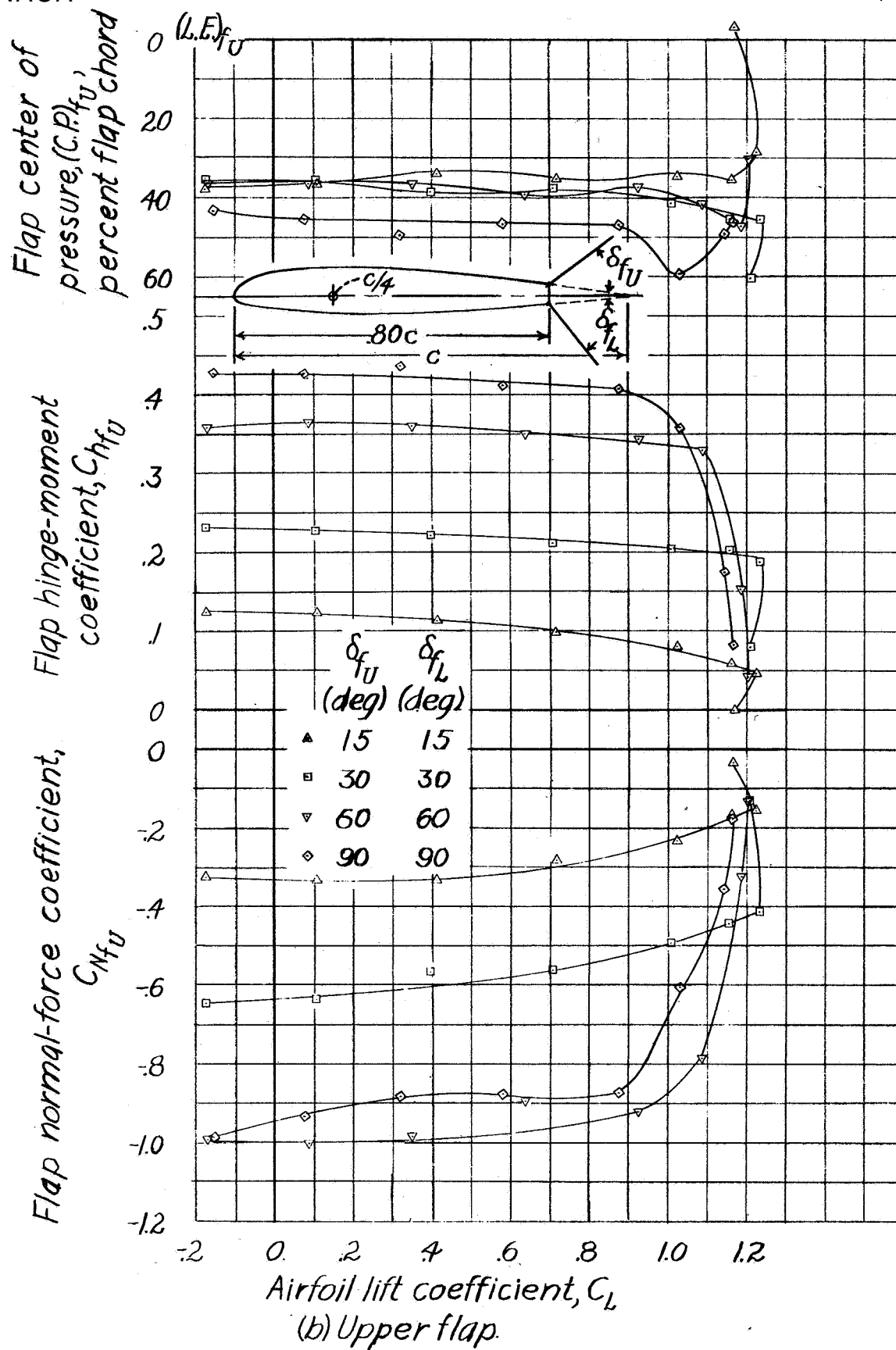


Figure 14.-Continued.

(measure with $\frac{1}{40}''$)

NACA

Fig. 14c

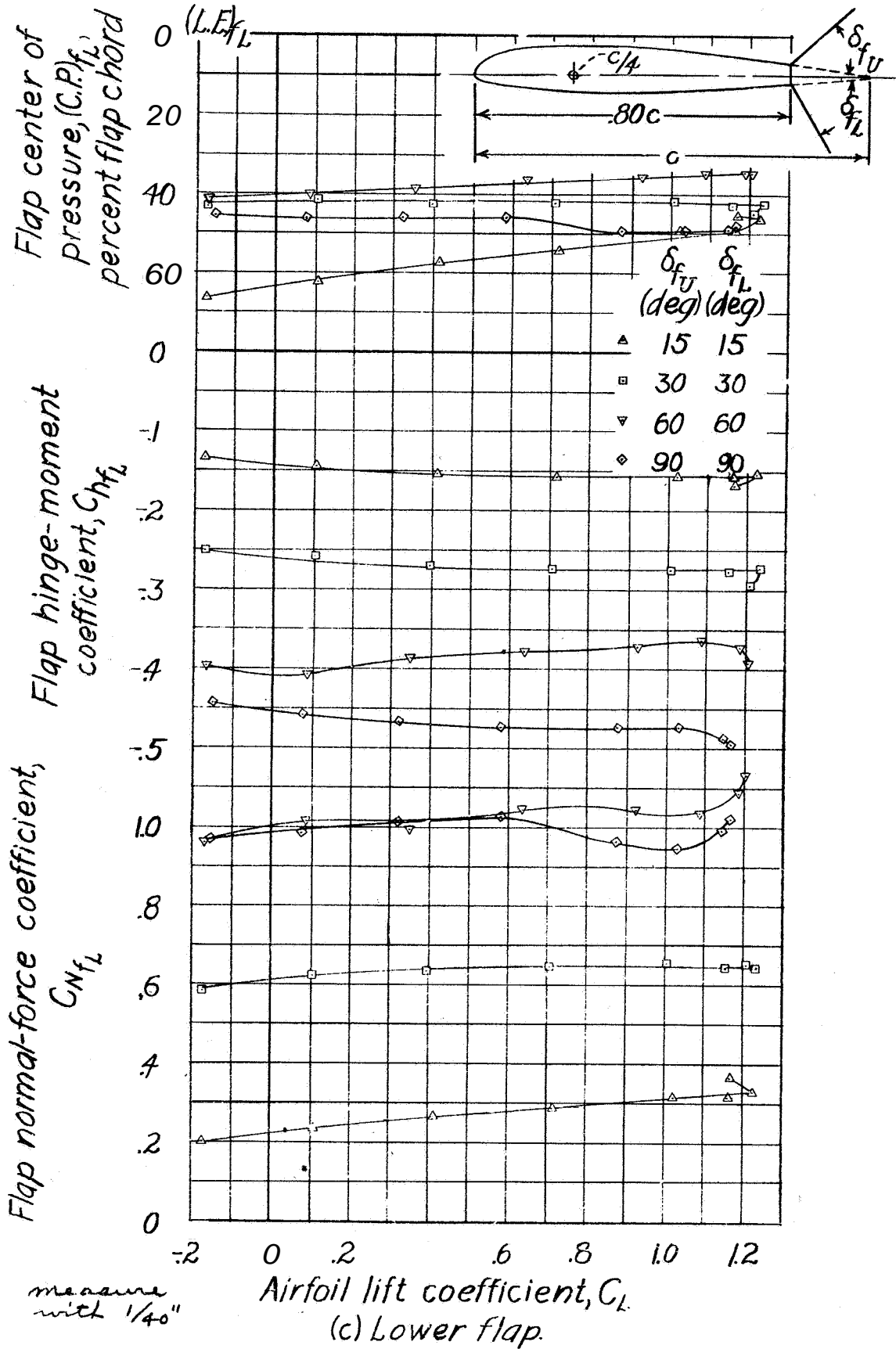


Figure 14.-Concluded.

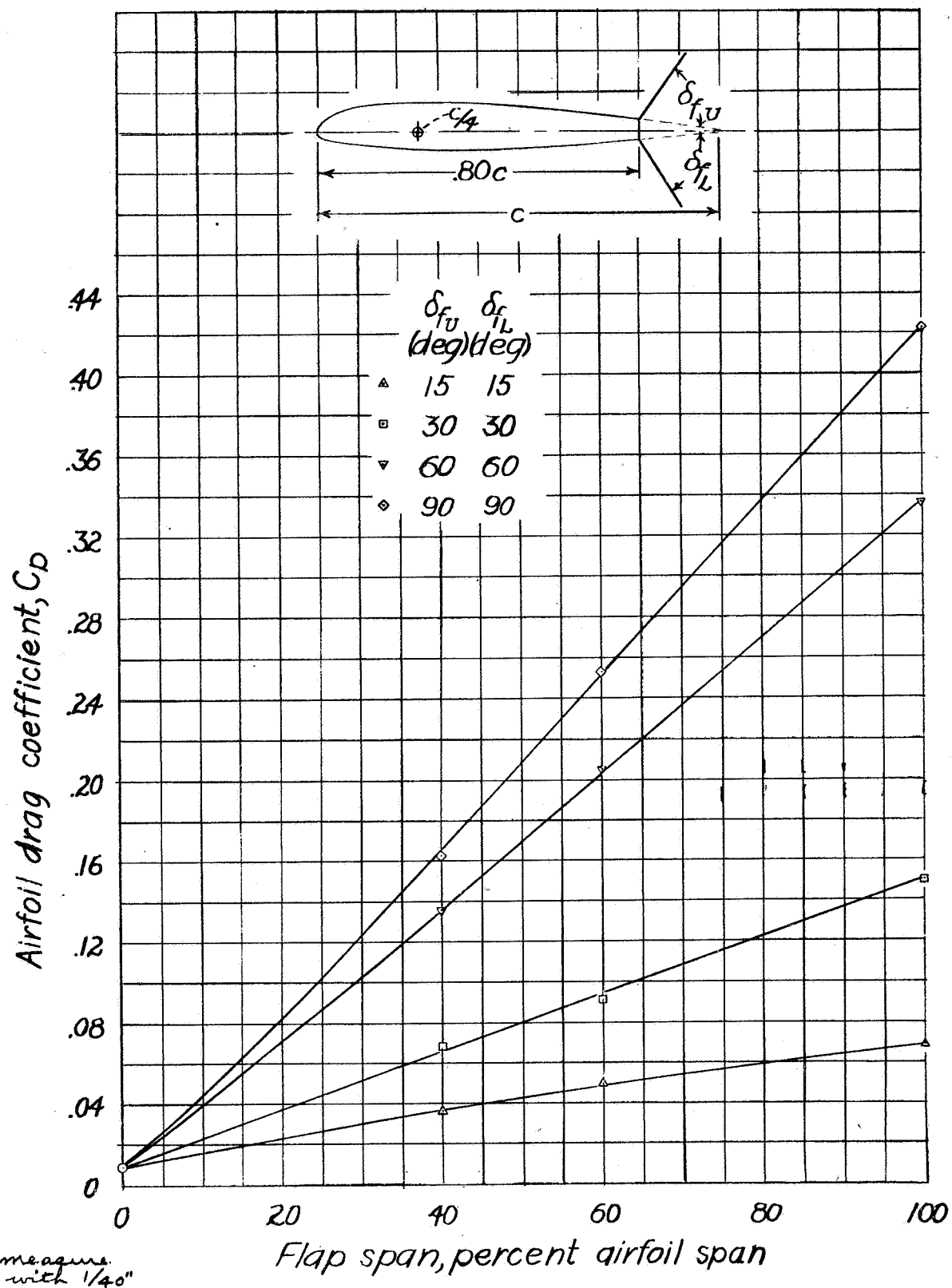


Figure 15.-Effect of flap span on the airfoil drag coefficient at zero lift. Rectangular NACA 23012 airfoil with 0.20c perforated double split flaps. Circular perforations remove 33.1 percent of original flap area. Equal upper and lower flap deflection.

NACA

Fig. 16a

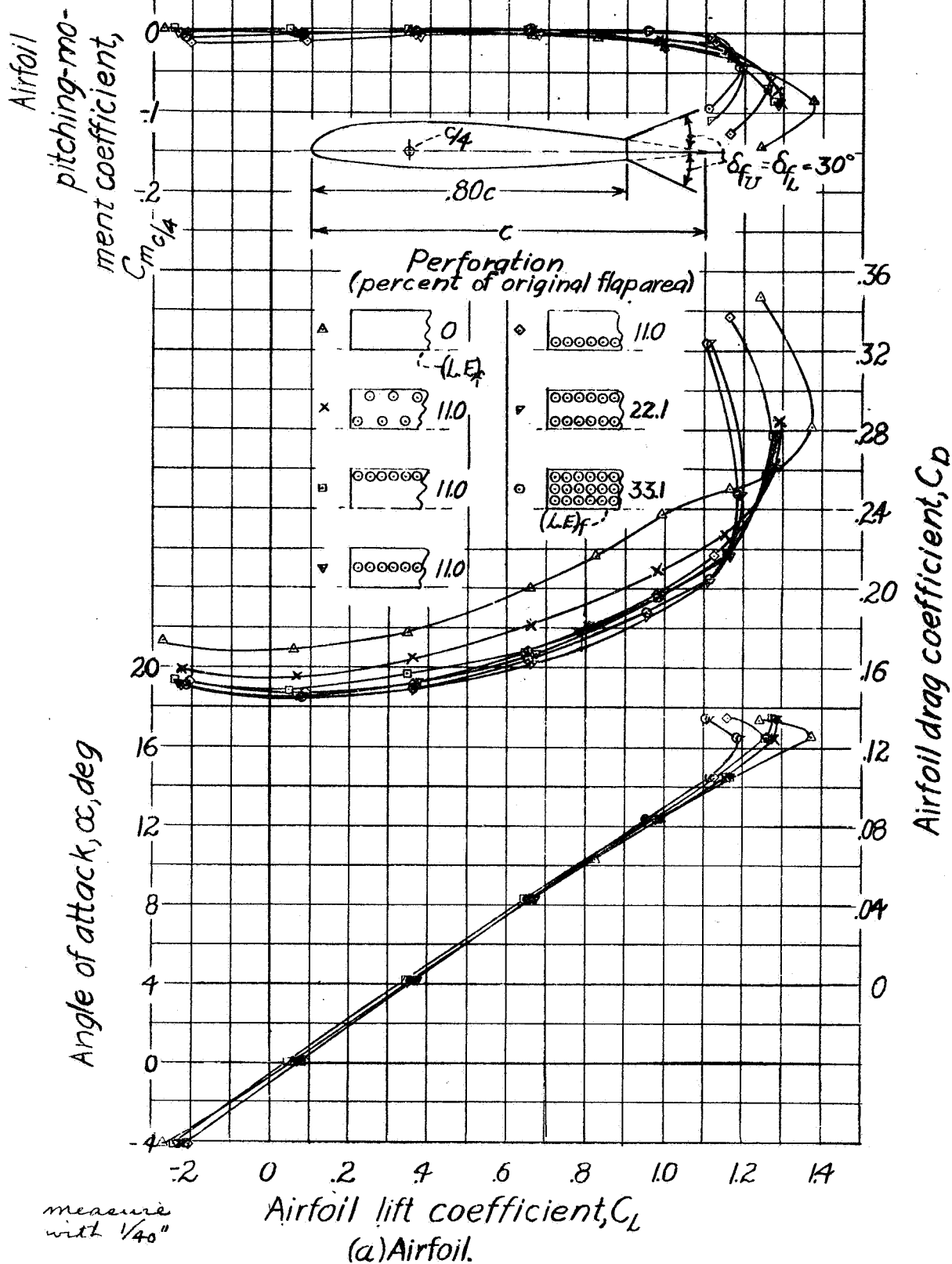


Figure 16.-Effect of circular perforations on the characteristics of the rectangular NACA 23012 airfoil with 0.20c full-span double split flaps. Flap loads on segment 2. $\delta_{fU}, \delta_{fL}, 30^\circ$

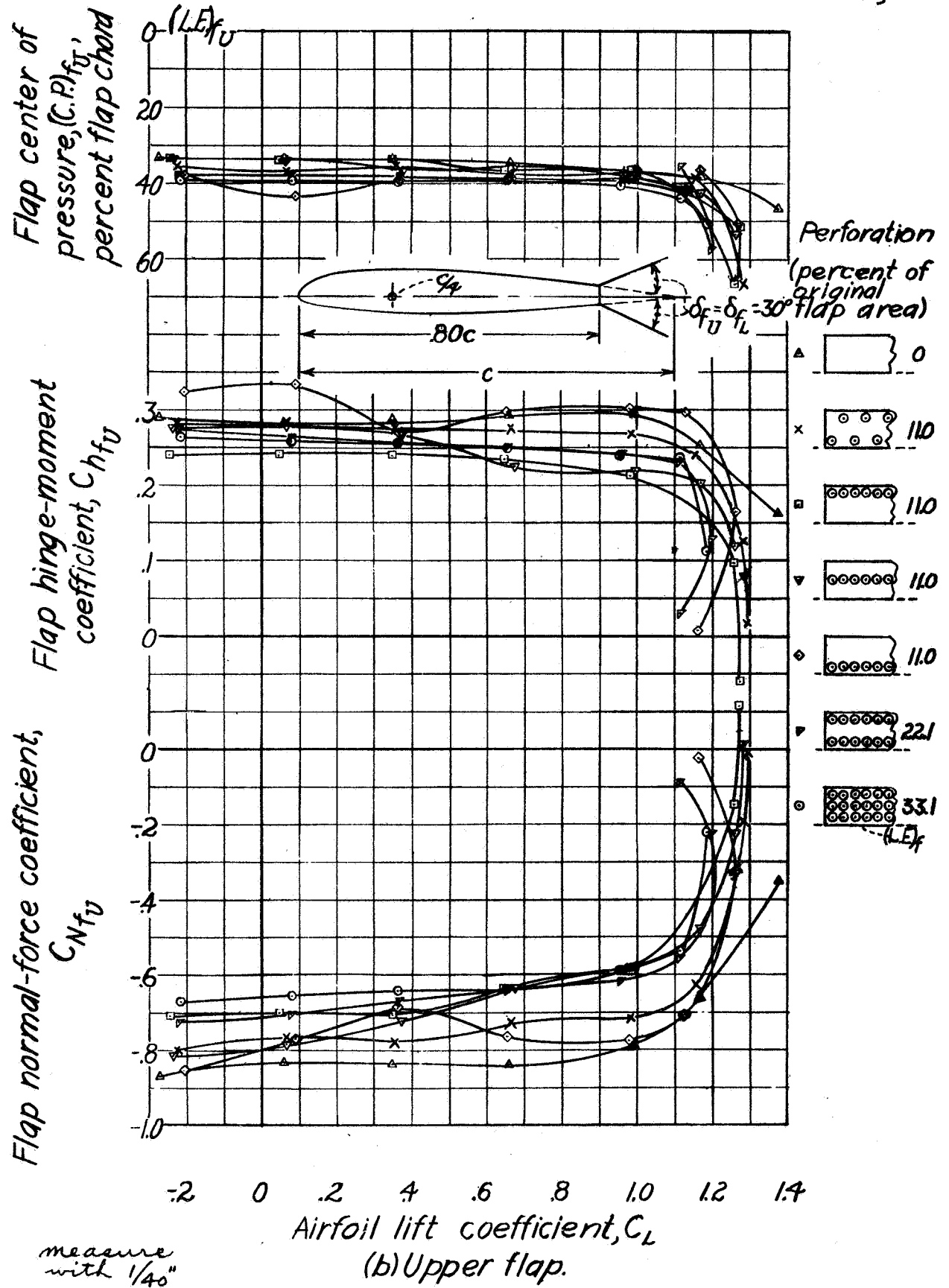


Figure 16.-Continued.

NACA

Fig. 16c

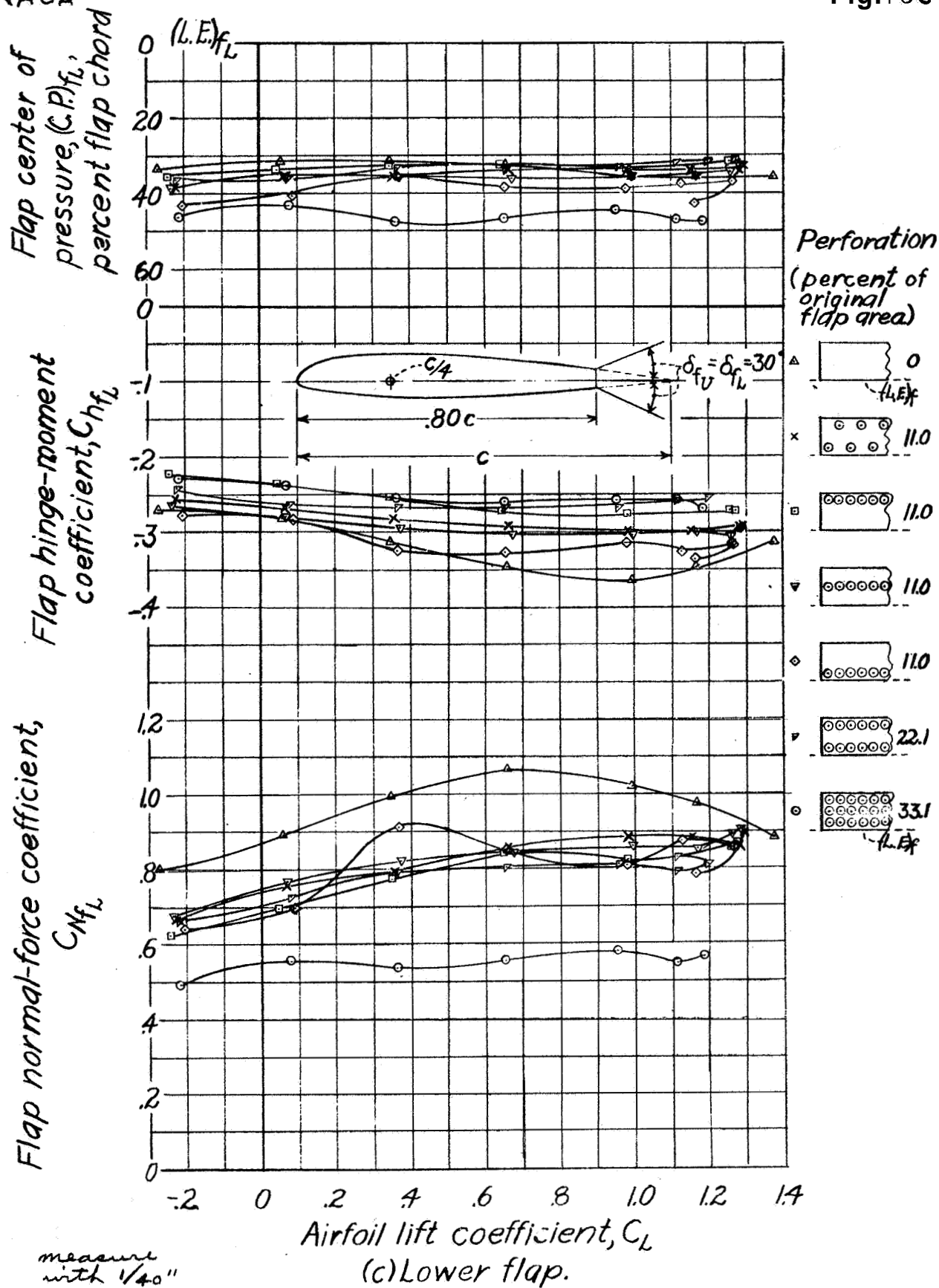


Figure 16.-Concluded.

NACA

Airfoil

pitching-moment
coefficient, $C_{m_{c/4}}$

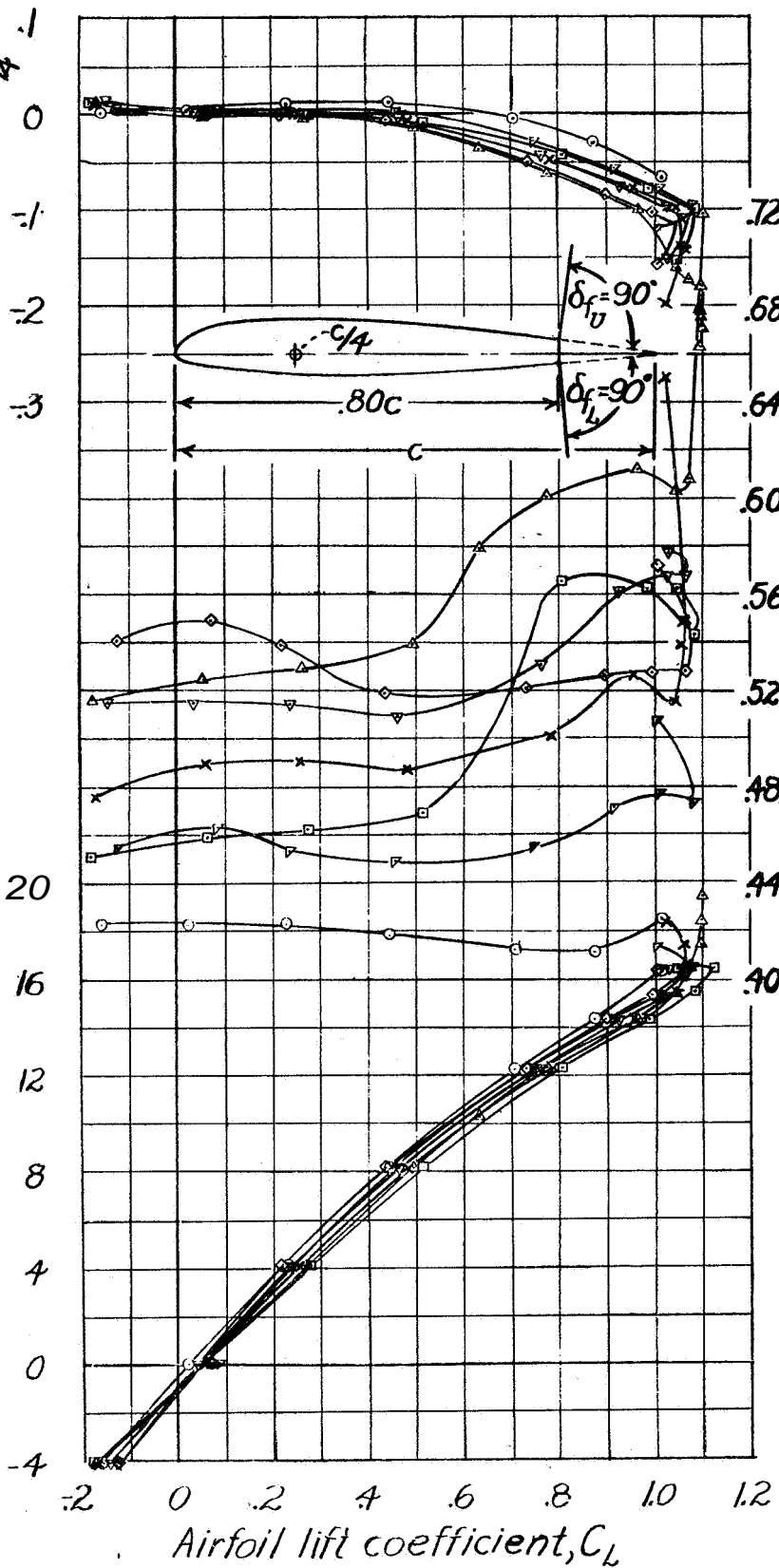
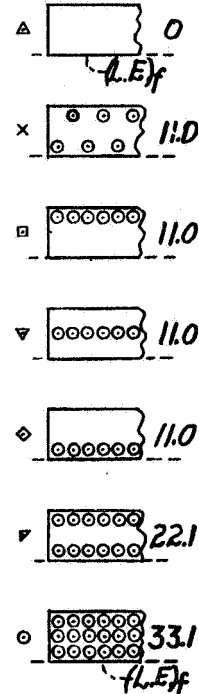


Fig. 17a
Perforation
(percent of
original
flap area)



measure
with
1/40"

(a) Airfoil.

Figure 17.-Effect of circular perforations on the characteristics of the rectangular NACA 23012 airfoil with 0.20c full-span double split flaps. Flap loads on segment 2. $\delta_{f_u}, \delta_{f_l}, 90^\circ$

Fig. 17b

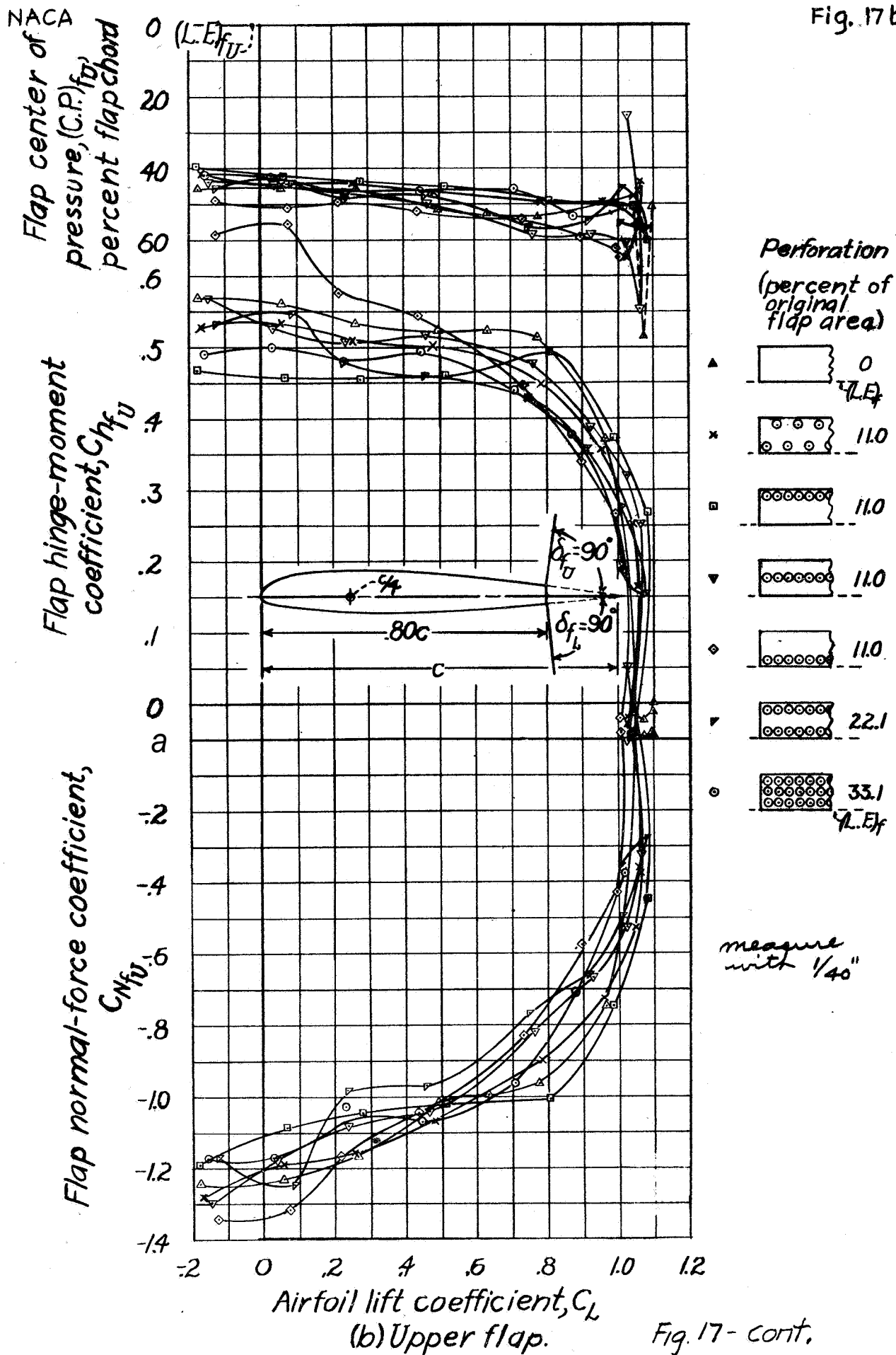
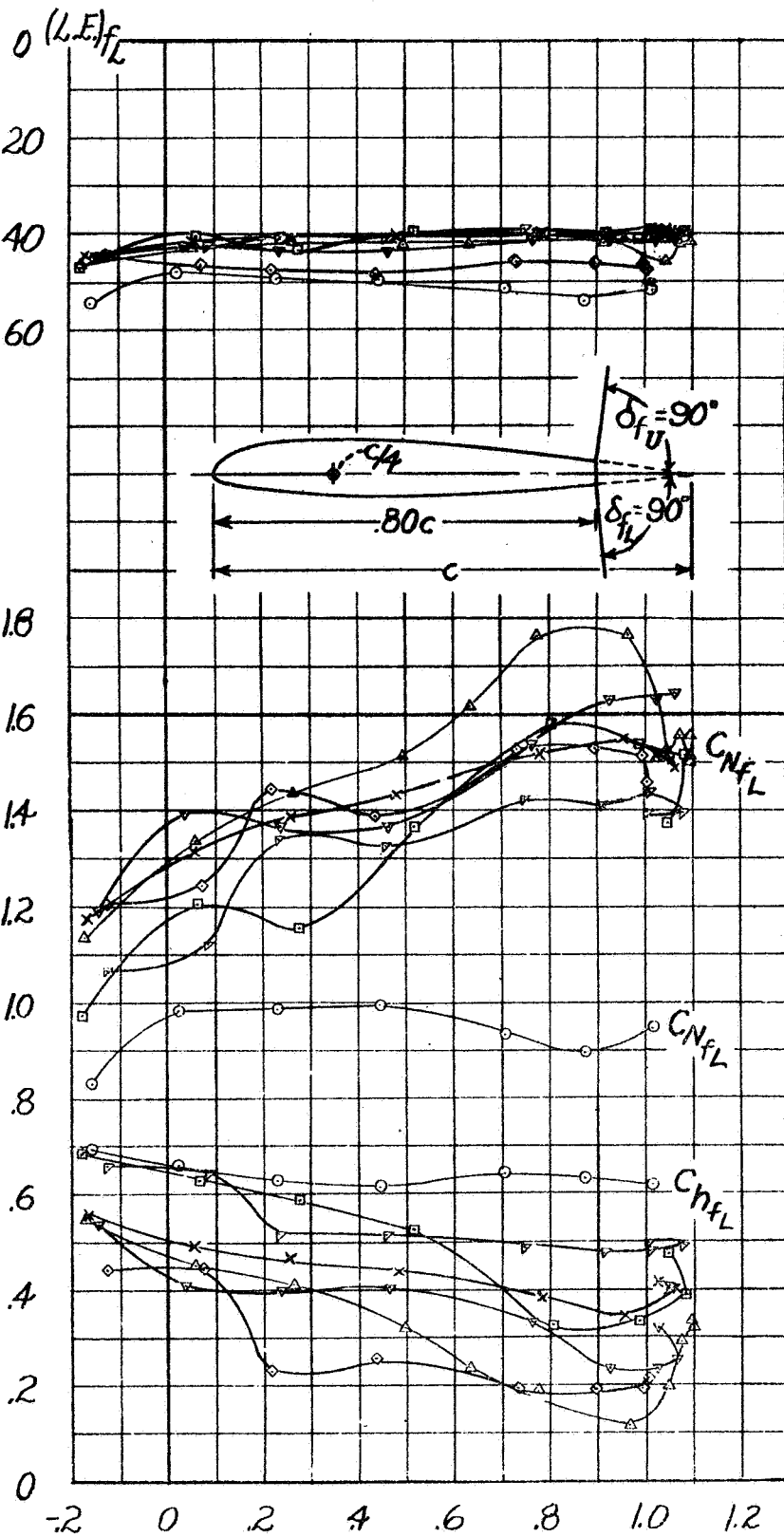


Fig. 17- cont.

NACA

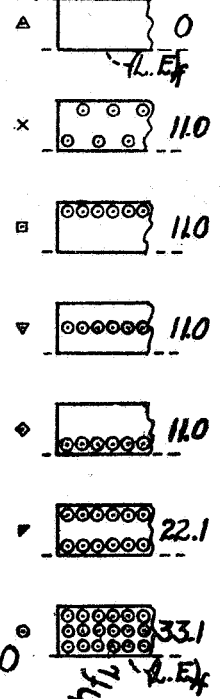
Flap center of pressure, $(C.P.)_{f_L}$, percent flap chord



measure with $1/40''$

(c) lower flap.

Fig. 17c
Perforation
(percent of
original flap
area)



Flap hinge-moment coefficient, C_{hfL}

0

-1

-2

-3

-4

-5

-6

-7

-8

Figure 17- Concluded.

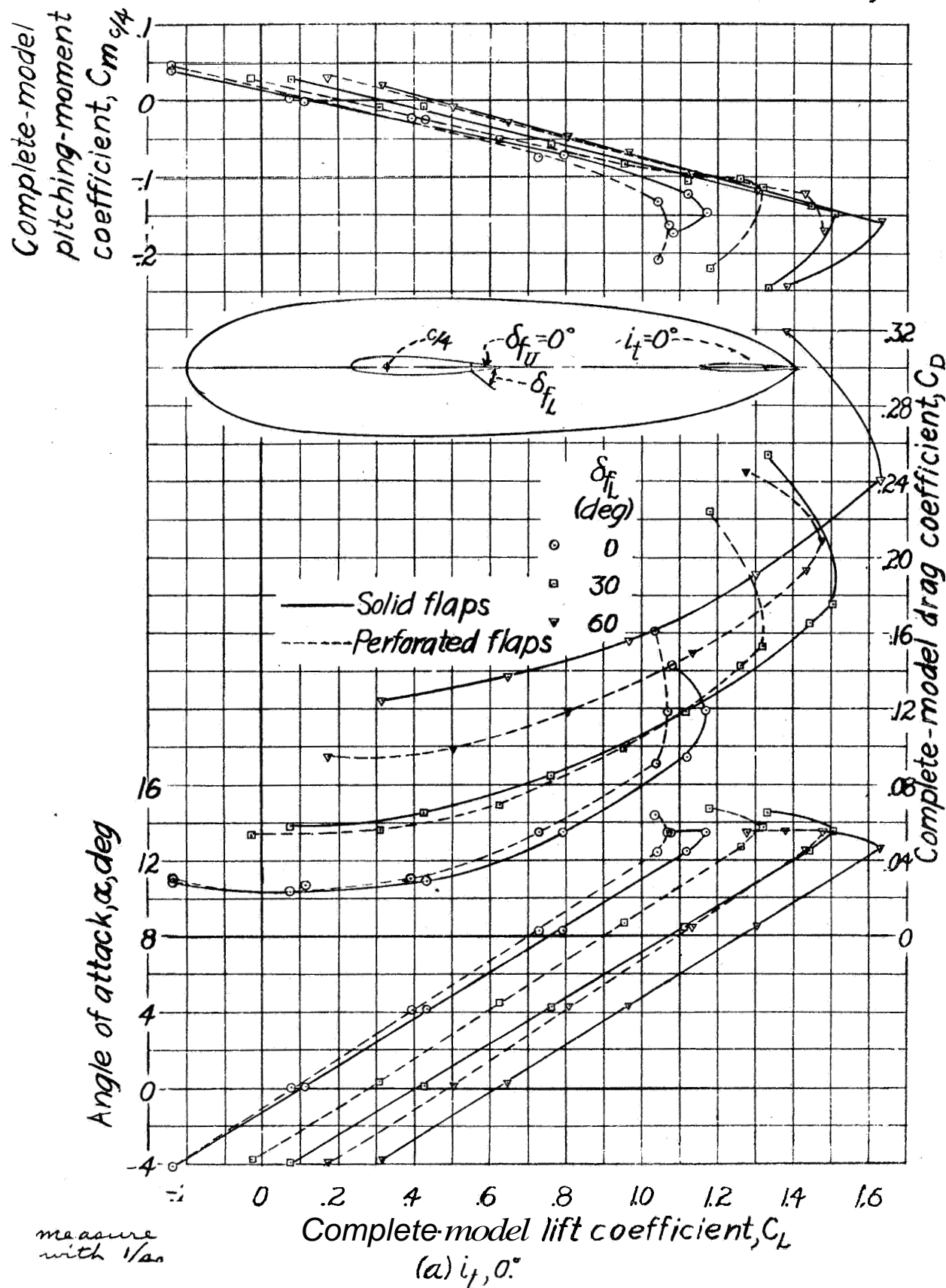


Figure 18 - Characteristics of the complete model with 0.20c by 0.60b solid and perforated double split flaps. Circular perforations remove 33.1 percent of original flap area. $\delta_{fU}, 0^\circ$.

NACA

Fig. 18b

Complete-model
pitching-moment
coefficient, $C_{m_{c/4}}$

Angle of attack, α , deg

Complete-model lift coefficient, C_L

(b) $i_t, -4.4^\circ$

measured
with $1/40"$

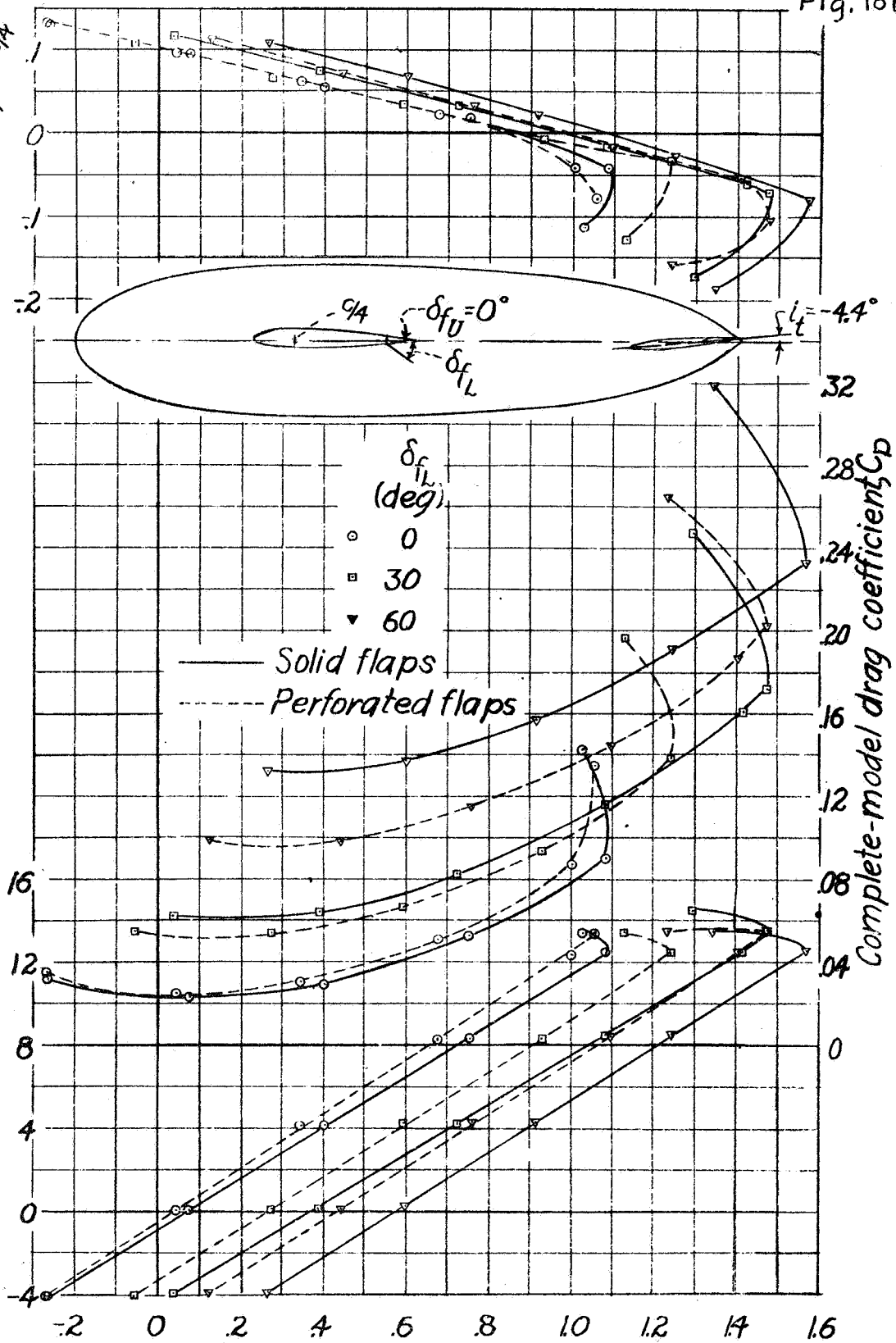


Figure 18 - Concluded.

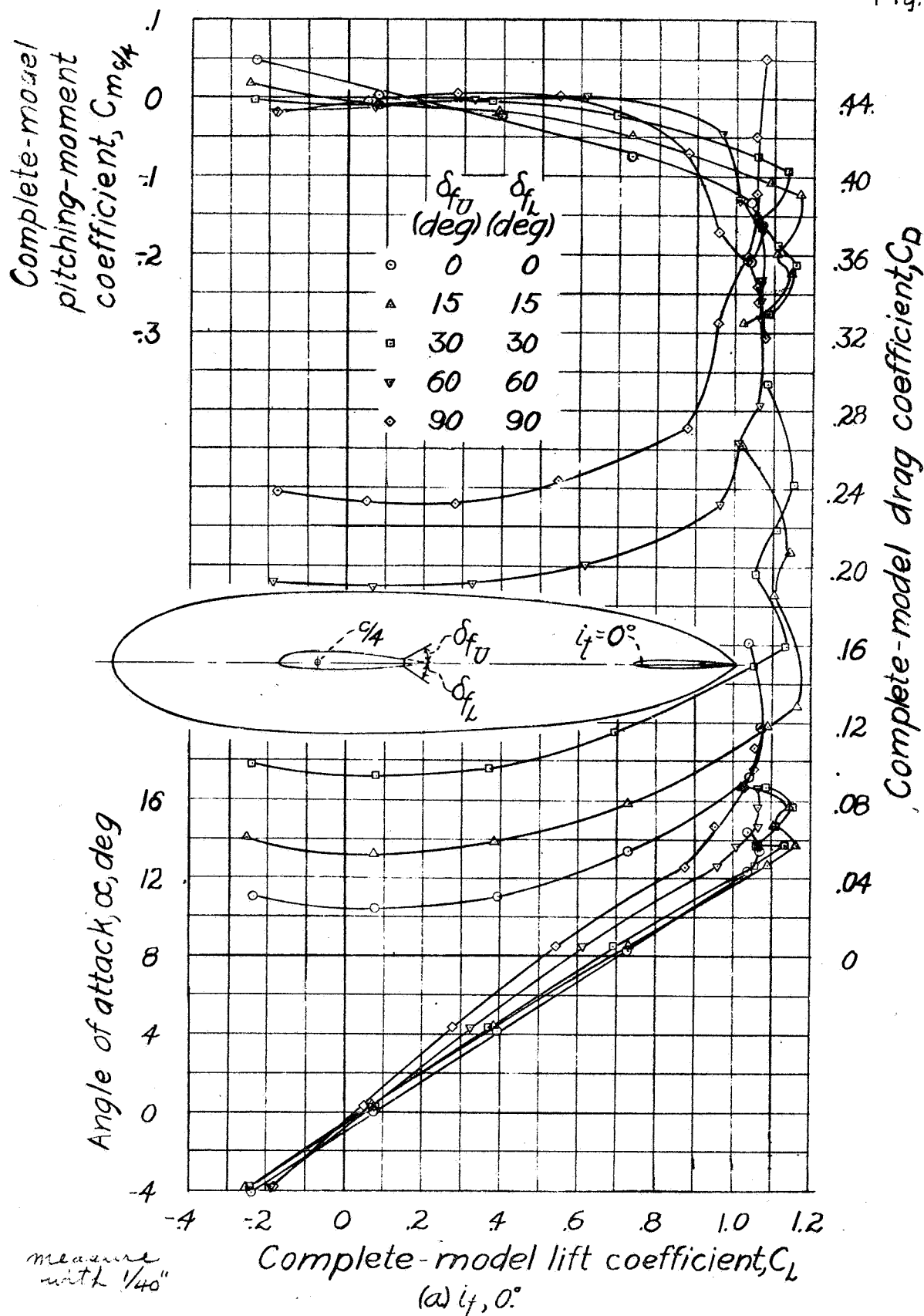


Figure 19.-Characteristics of the complete model with 0.20c by 0.60b perforated double split flaps. Circular perforations remove 33.1 percent of original flap area. Equal upper and lower flap deflection.

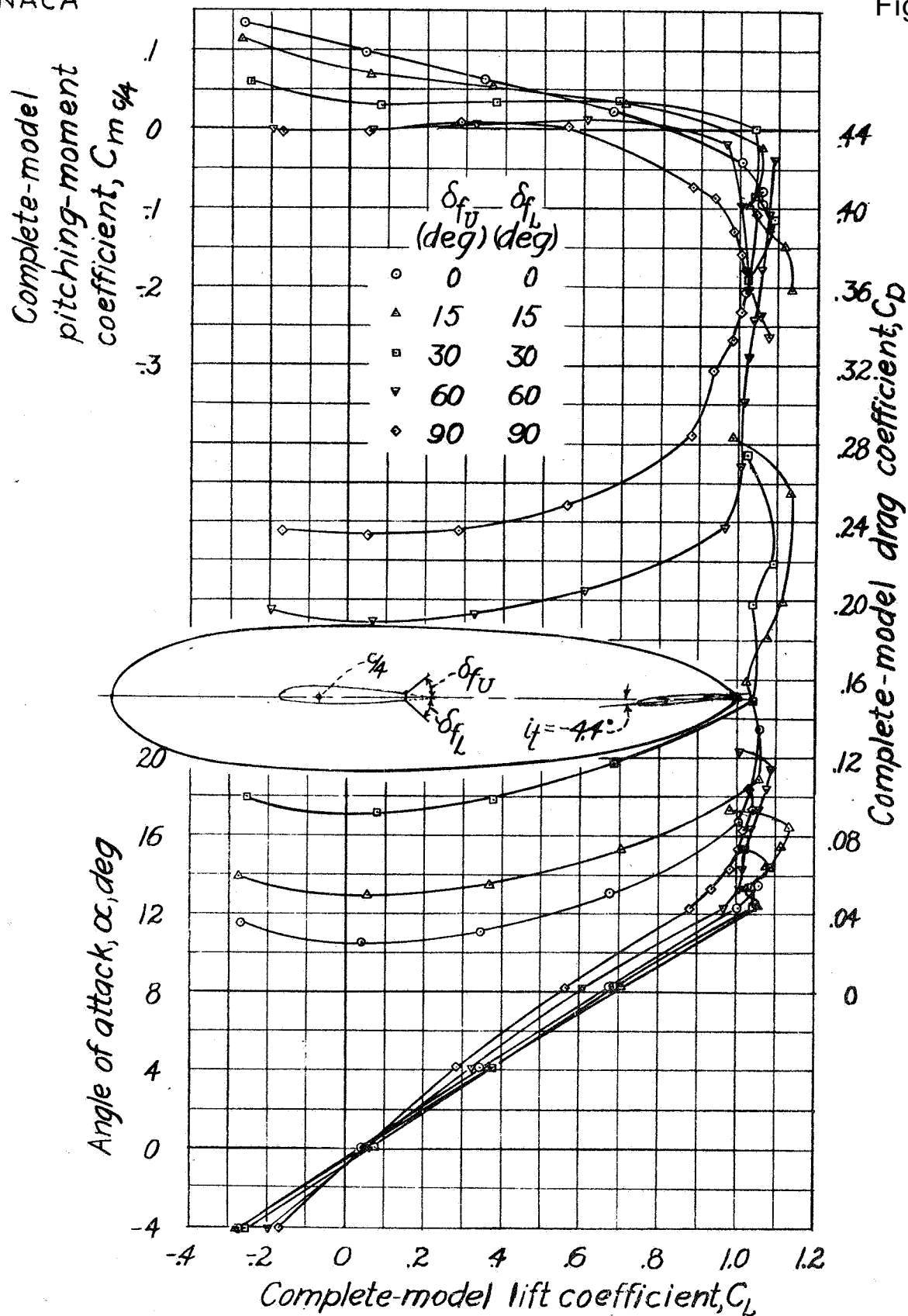


Figure 19 - Concluded.

Fig. 20

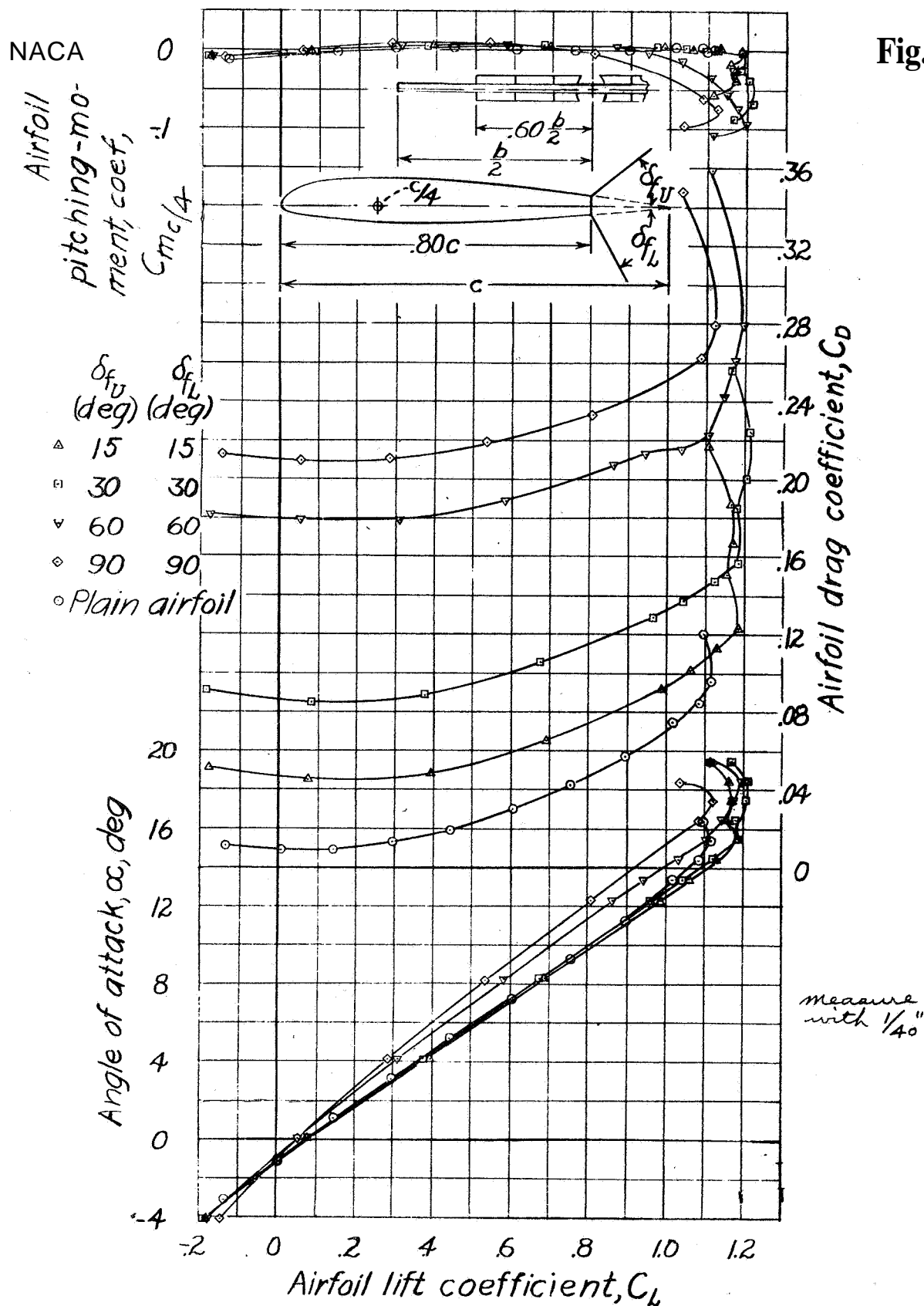


Figure 20.—Characteristics of the rectangular NACA 23012 airfoil with 0.20c by 0.60b perforated double split flaps. Mid-span portion of flaps removed over space equal to width of elliptical fuselage. Circular perforations remove 33.1 percent of original flap area. Equal upper and lower flap deflection.

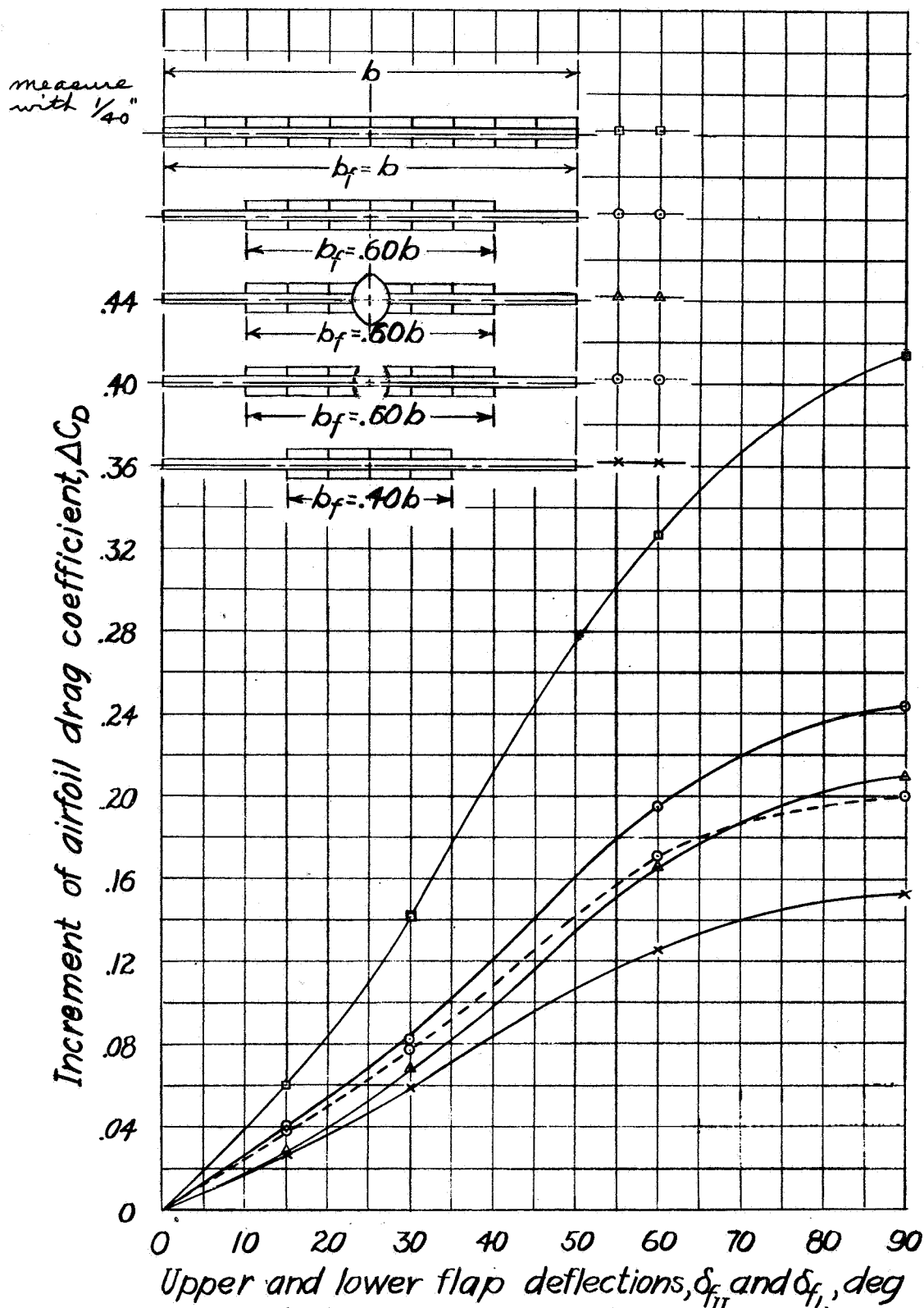


Figure 21 - Effect of flap span and fuselage on the increment of drag coefficient at zero lift. Rectangular NACA 23012 airfoil with 0.20c perforated double split flaps. Circular perforations remove 33.1 percent of original flap area. Equal upper and lower flap deflection.

NACA

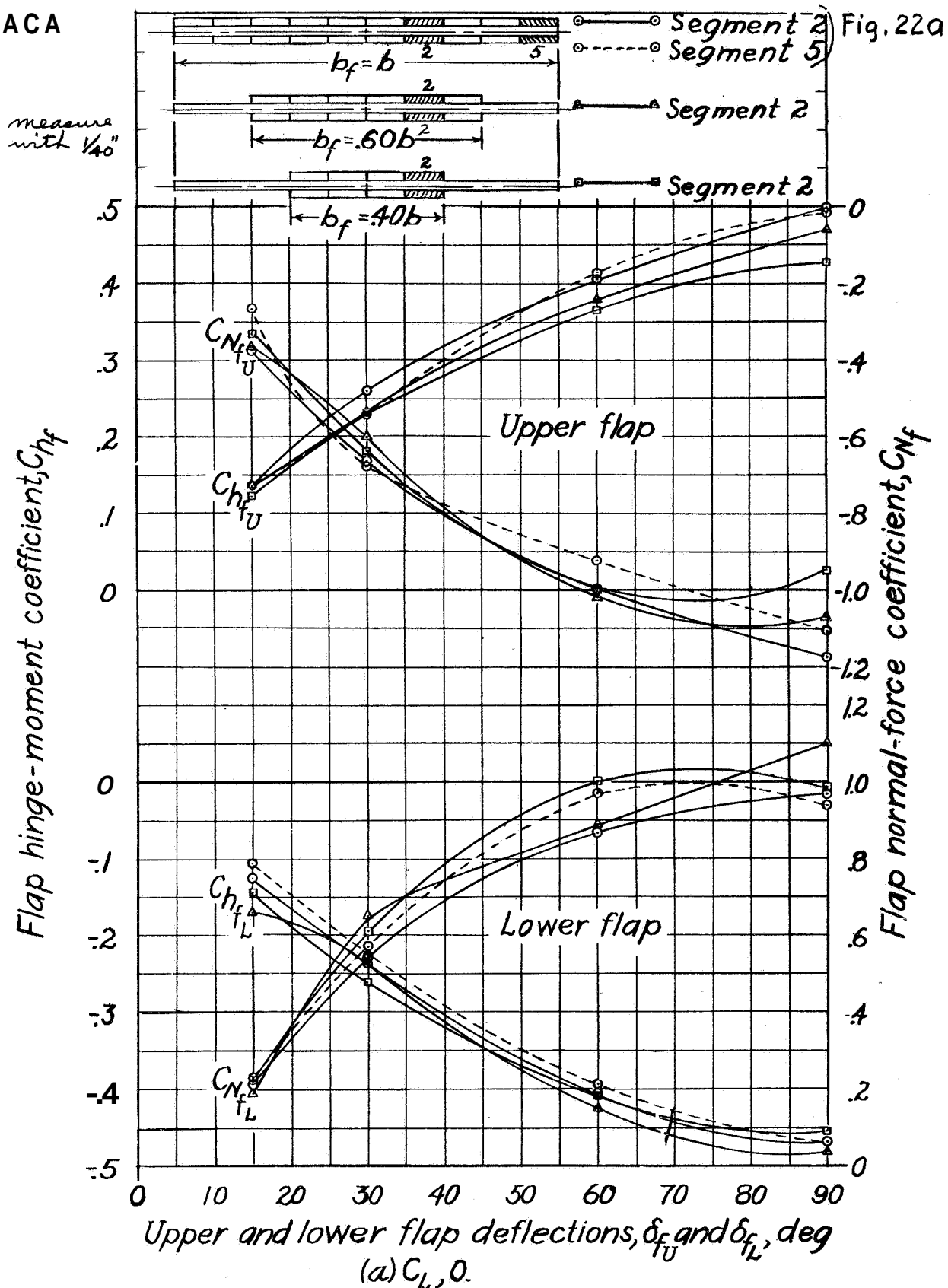


Figure 22.-Effect of flap span and location on flap loads. Rectangular NACA 23012 airfoil with 0.20c perforated double split flaps. Circular perforations remove 33.1 percent of original flap area. Equal upper and lower flap deflection.

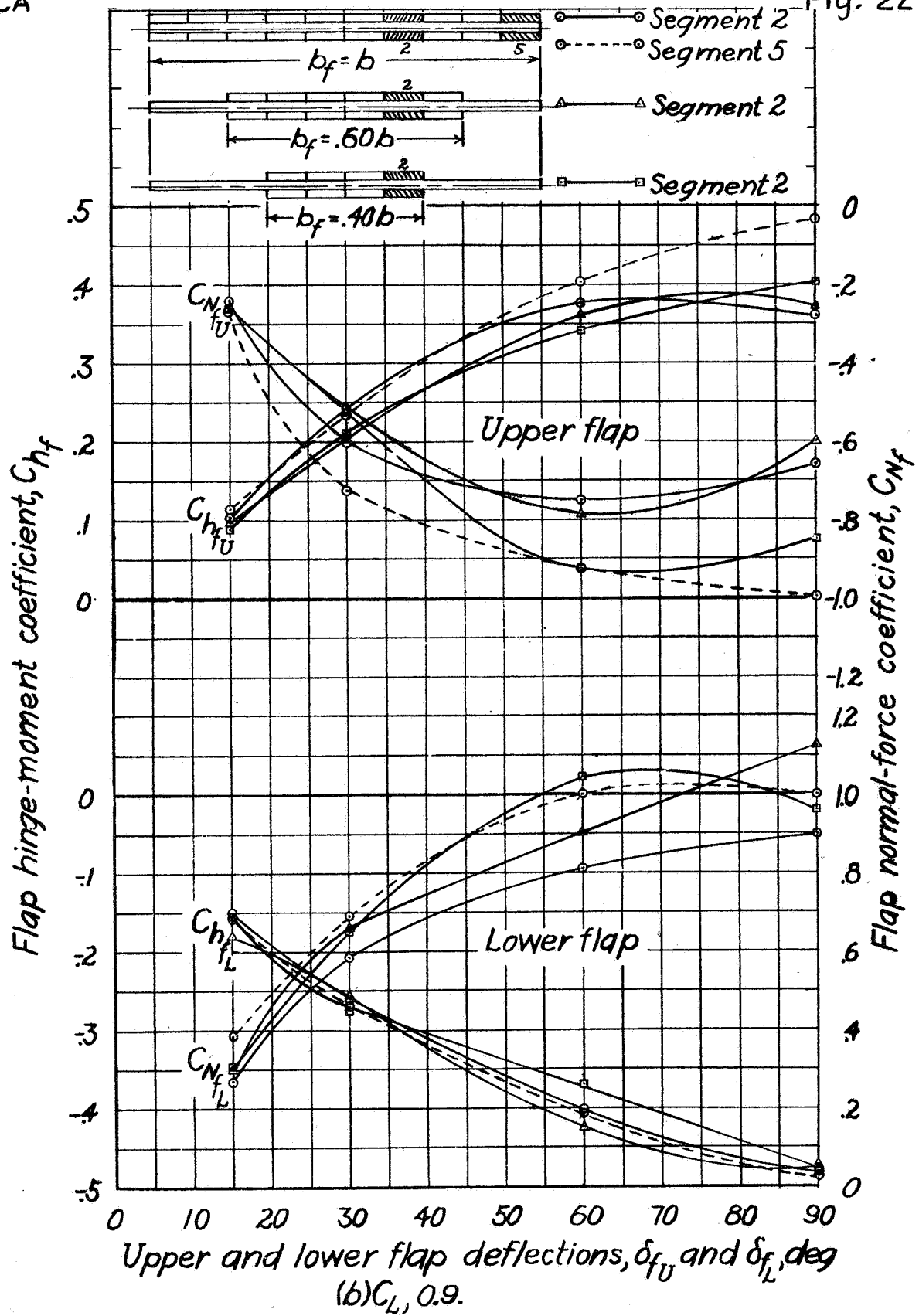
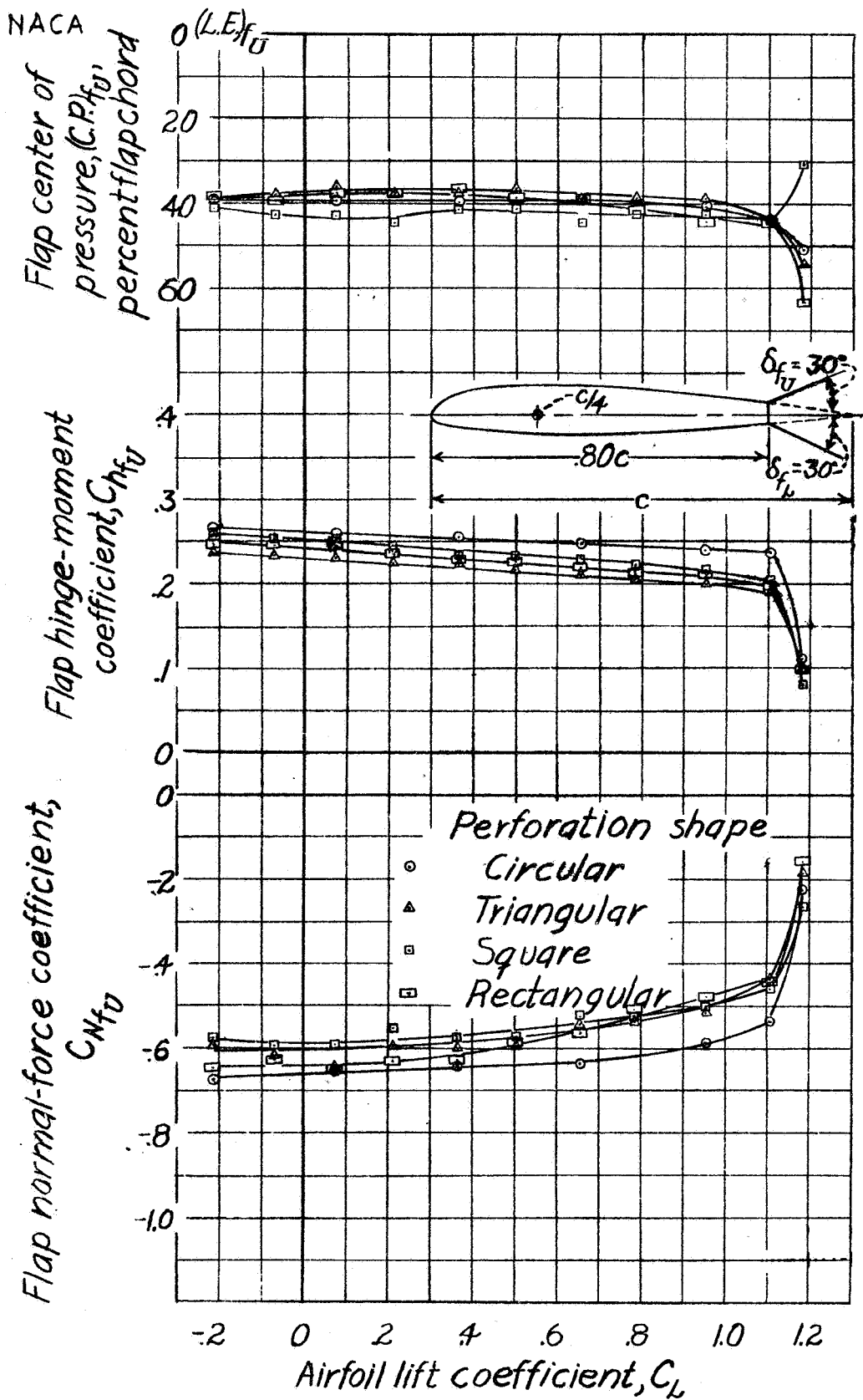


Figure 22.-Concluded.

measure with $\frac{1}{40}''$



measure with $\frac{1}{40}$ "

Figure 23.-Effect of perforation shape on the upper-flap loads. Rectangular NACA 23012 airfoil with 0.20c full-span perforated double split flaps. Perforations remove 33.1 percent of original flap area. Flap loads on segment 2.

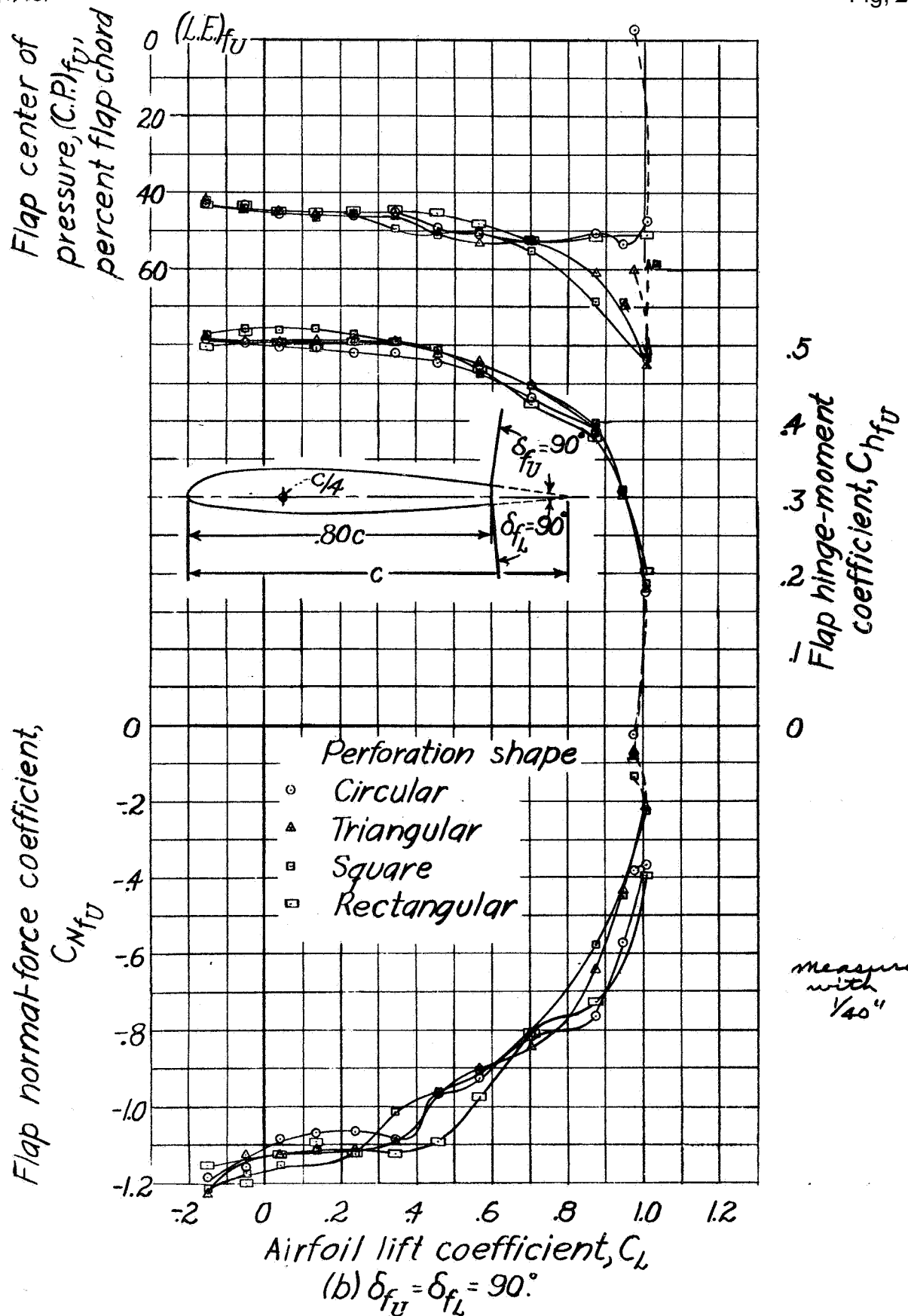


Figure 23 - Concluded.

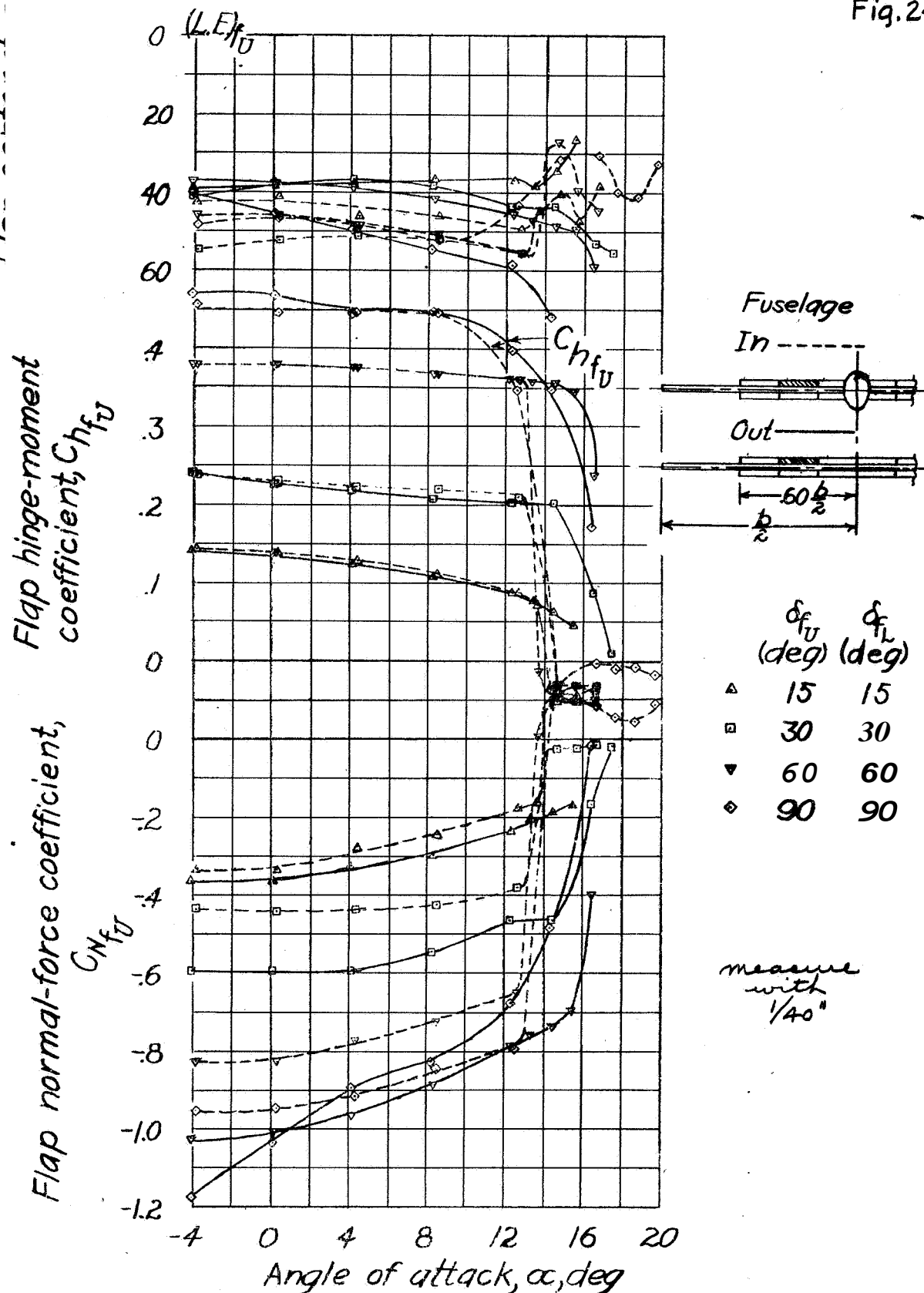
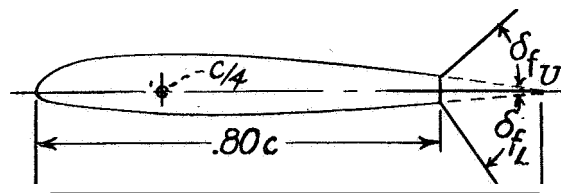
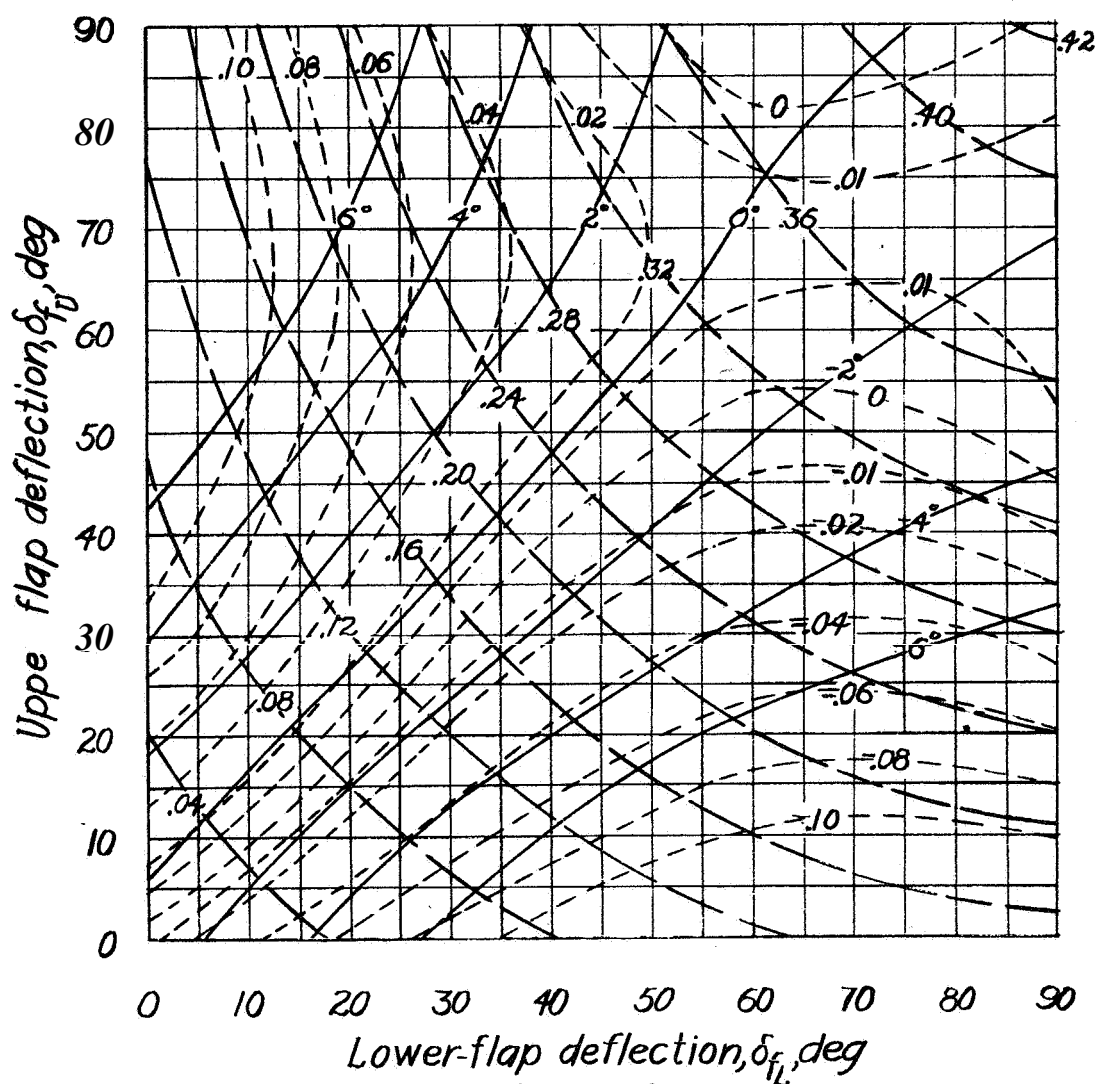


Figure 24.-Effect of fuselage on the upper-flap loads. Rectangular NACA 23012 airfoil with $0.20c$ by $0.60b$ perforated double split flaps. Circular perforations remove 33.1 percent of original flap area. Flap loads on segment 2. Equal upper and lower flap deflection.



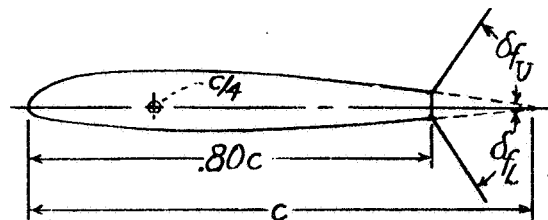
measure with $1/40''$

— α - - - C_D - - - $C_{m_{c/4}}$



(a) $b_f, 1.00b$.

Figure 25.-Contours of α , C_D , and $C_{m_{c/4}}$ at $C_L=0$ for the rectangular NACA 23012 airfoil with perforated double split flaps. Circular perforations remove 33.1 percent of original flap area.



measure with $\frac{1}{40}''$

— α — C_D - - - $C_{m_{c/4}}$

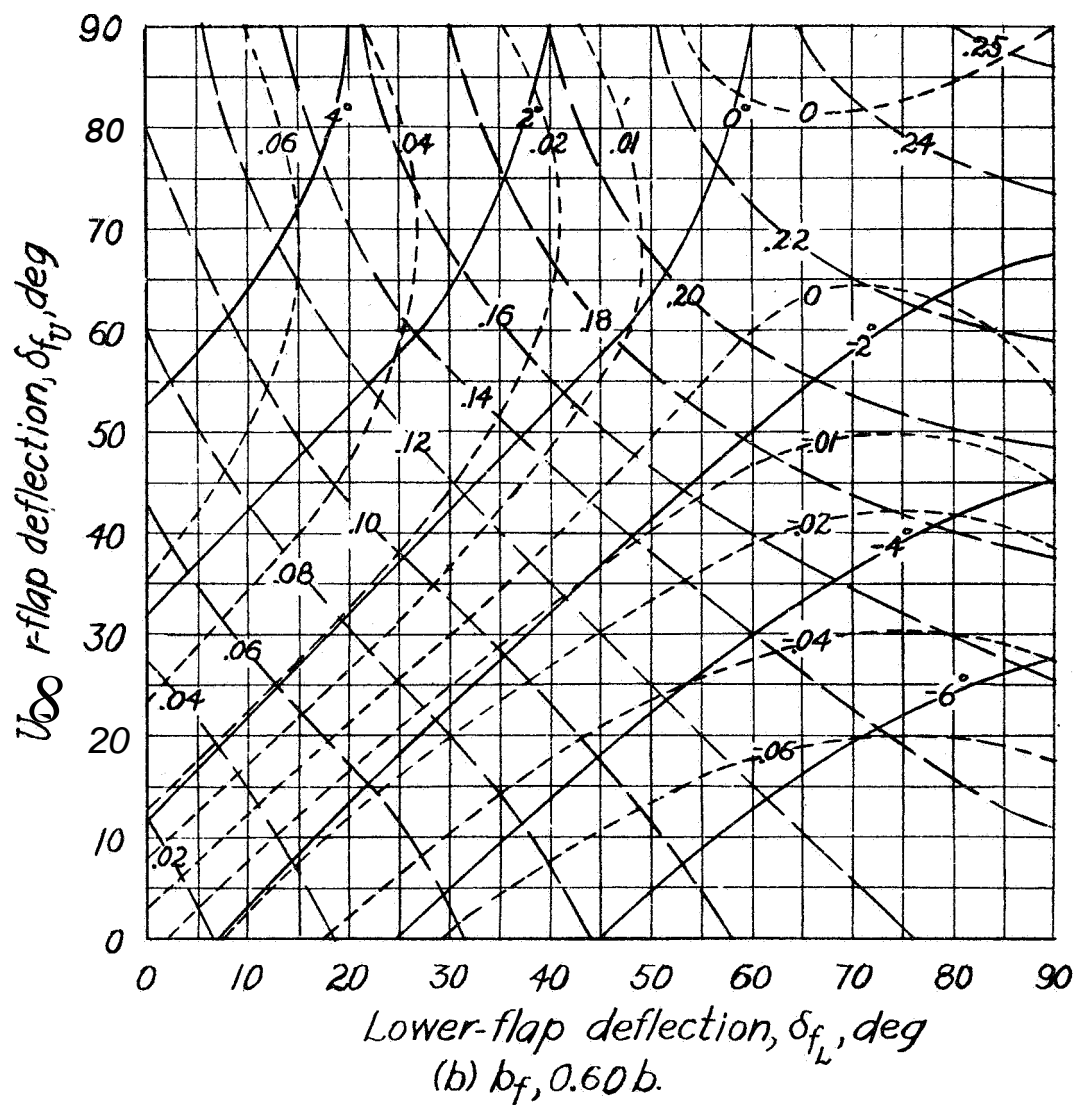
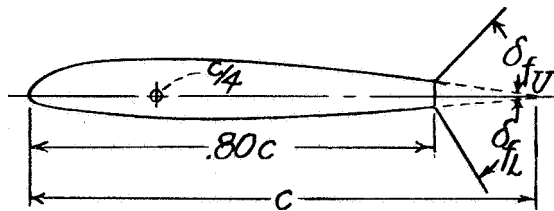
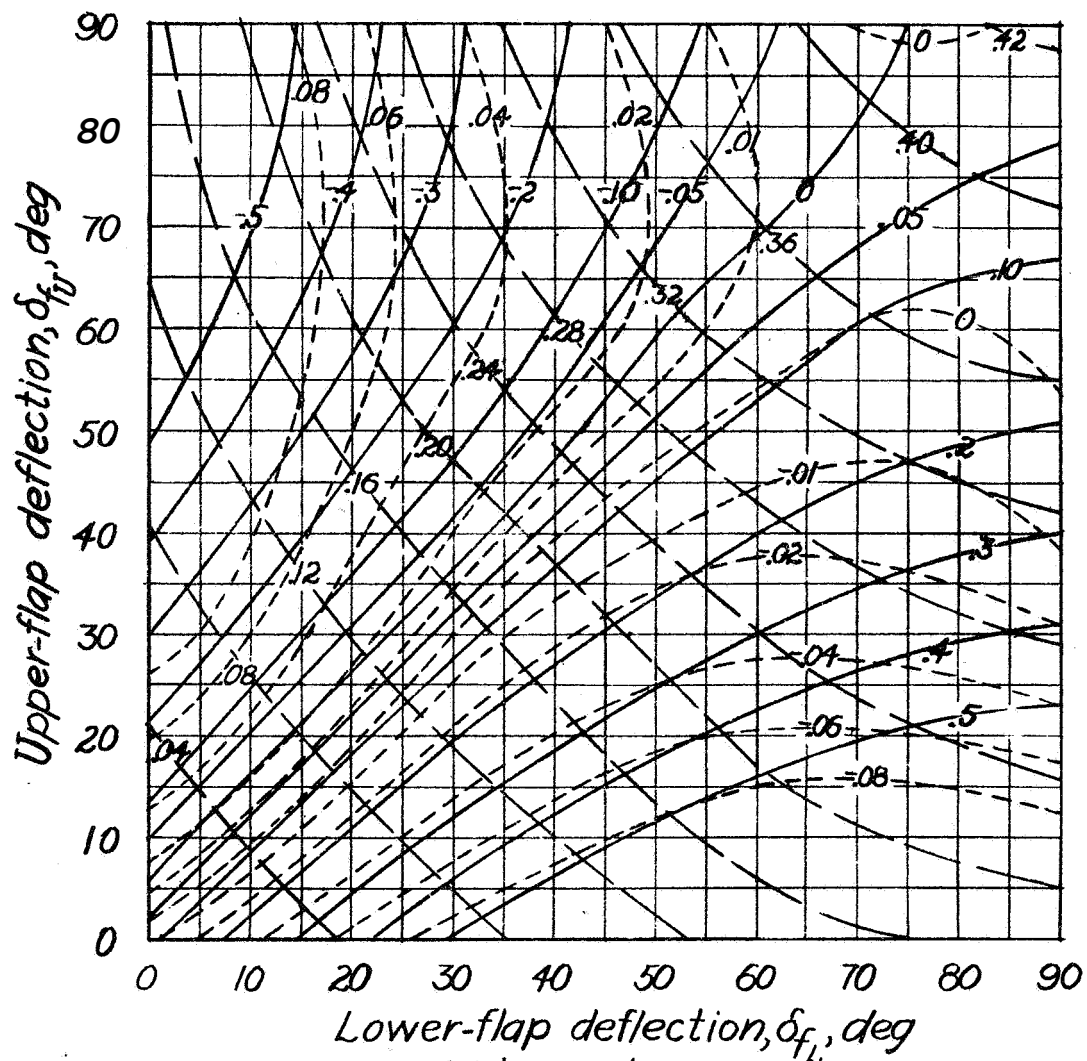


Figure 25-Concluded.



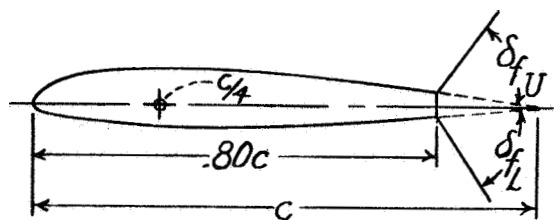
measure with 1/40"

— C_L — — C_D - - - $C_{m_{c/4}}$



(a) $b_f, 1.00b$.

Figure 26.-Contours of C_L , C_D , and $C_{m_{c/4}}$ at $\alpha=0^\circ$ for the rectangular NACA 23012 airfoil with perforated double split flaps. Circular perforations remove 33.1 percent of original flap area.



measure with $\frac{1}{40}''$

— C_L — C_D - - - $C_{mc/4}$

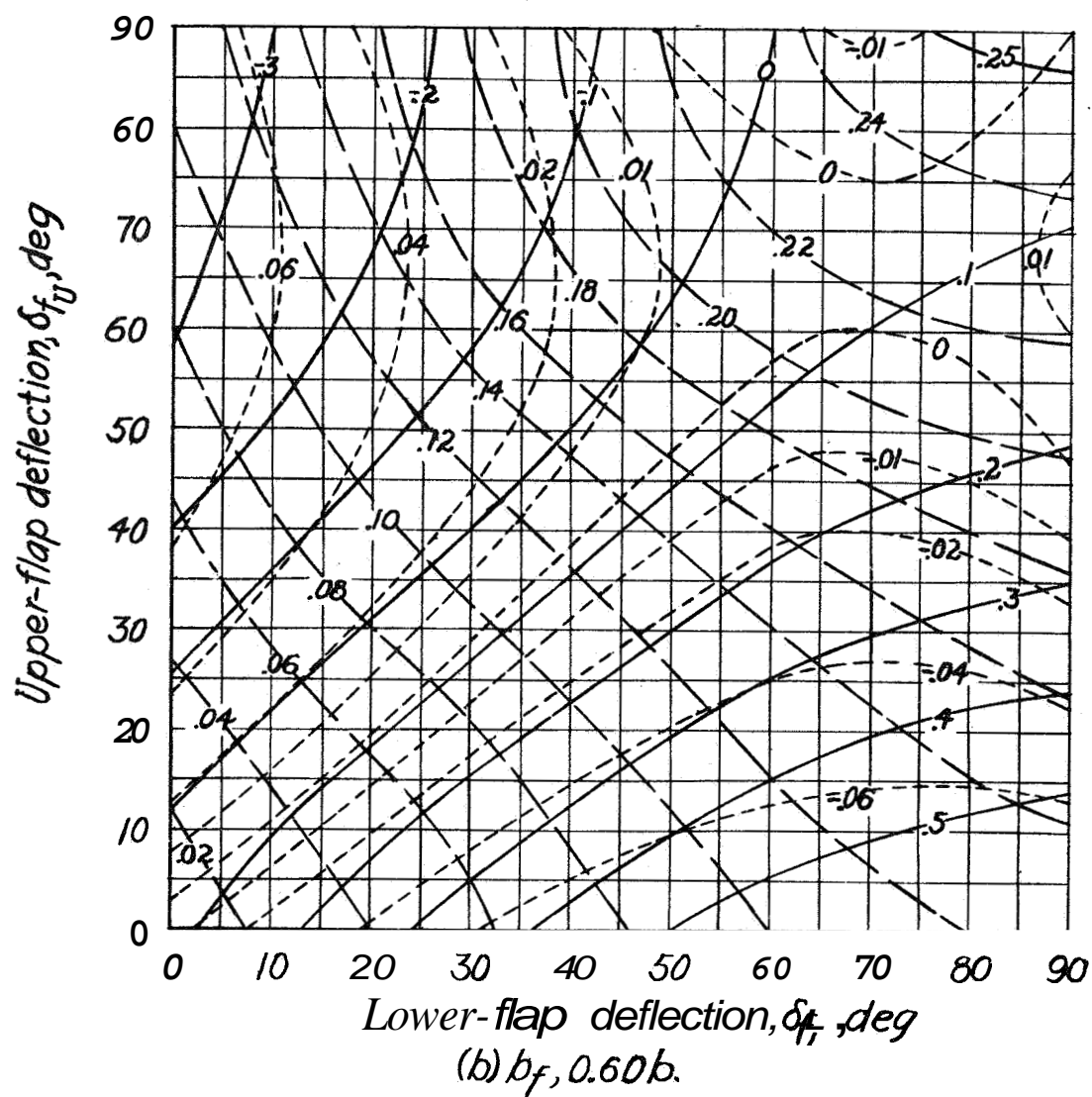


figure 26.-Concluded.